



UNIVERSIDADE ESTADUAL DE CAMPINAS
FACULDADE DE CIÊNCIAS APLICADAS

MATHEUS BRANDEMARTE SEVERINO

**A EDIÇÃO DO GENE *STK11* (LKB1) POR CRISPR/CAS9 EM CÉLULAS NÃO
PEQUENAS DE CÂNCER DE PULMÃO A549 E A RESPOSTA A METFORMINA E
CISPLATINA**

**THE *STK11* (LKB1) GENE EDITION BY CRISPR/CAS9 IN NON-SMALL CELLS LUNG
CANCER A549, AND THE RESPONSE TO METFORMIN AND CISPLATIN**

Limeira

2023

MATHEUS BRANDEMARTE SEVERINO

A EDIÇÃO DO GENE *STK11* (LKB1) POR CRISPR/CAS9 EM CÉLULAS NÃO PEQUENAS DE CÂNCER DE PULMÃO A549 E A RESPOSTA A METFORMINA E CISPLATINA

THE *STK11* (LKB1) GENE EDITION BY CRISPR/CAS9 IN NON-SMALL CELLS LUNG CANCER A549, AND THE RESPONSE TO METFORMIN AND CISPLATIN

Dissertação apresentada à Faculdade de Ciências Aplicadas da Universidade Estadual de Campinas como parte dos requisitos exigidos para obtenção do título de Mestre em Ciências da Nutrição e do Esporte e Metabolismo, na área de Ciências Nutricionais e Metabolismo.

Orientador Dr. Fernando Moreira Simabuco

Este trabalho corresponde à versão final da dissertação defendida pelo aluno MATHEUS BRANDEMARTE SEVERINO, e orientada pelo PROF. DR. FERNANDO MOREIRA SIMABUCO.

Limeira

2023

Ficha catalográfica
Universidade Estadual de Campinas
Biblioteca da Faculdade de Ciências Aplicadas
Ana Luiza Clemente de Abreu Valério - CRB 8/10669

Se83e Severino, Matheus Brandemarte, 1997-
A edição do gene *STK11* (LKB1) por CRISPR/Cas9 em células não pequenas de câncer de pulmão A549 e a resposta a metformina e cisplatina / Matheus Brandemarte Severino. – Limeira, SP : [s.n.], 2023.

Orientador: Fernando Moreira Simabuco.
Dissertação (mestrado) – Universidade Estadual de Campinas, Faculdade de Ciências Aplicadas.

1. Edição de genes. 2. Neoplasias pulmonares. 3. Autofagia. I. Simabuco, Fernando Moreira, 1982-. II. Universidade Estadual de Campinas. Faculdade de Ciências Aplicadas. III. Título.

Informações Complementares

Título em outro idioma: The *STK11* (LKB1) gene edition by CRISPR/Cas9 in non-small cells lung cancer A549, and the response to metformina and cisplatin

Palavras-chave em inglês:

Gene editing

Lung neoplasms

Autophagy

Área de concentração: Ciências Nutricionais e Metabolismo

Titulação: Mestre em Ciências da Nutrição e do Esporte e Metabolismo

Banca examinadora:

Fernando Moreira Simabuco [Orientador]

Clarissa Ribeiro Reily Rocha

Augusto Ducati Luchessi

Data de defesa: 15-12-2023

Programa de Pós-Graduação: Ciências da Nutrição e do Esporte e Metabolismo

Identificação e informações acadêmicas do(a) aluno(a)

- ORCID do autor: <https://orcid.org/0000-0003-2124-41>

- Currículo Lattes do autor: <http://lattes.cnpq.br/1121052068283115>



COMISSÃO EXAMINADORA

Profa. Dra. Clarissa Ribeiro Reily Rocha (UNIFESP)
(Membro titular)

Prof. Dr. Augusto Ducati Luchessi (UNICAMP)
(Membro titular)

Prof. Dr. Fernando Moreira Simabuco (UNIFESP)
(Presidente)

“A Ata da defesa com as respectivas assinaturas dos membros encontra-se no SIGA/Sistema de Fluxo de Dissertação/Tese e na Secretaria do Programa da Unidade.”

“A tarefa é um tanto ver aquilo que ninguém viu,
mas pensar o que ninguém ainda pensou sobre
aquilo que todo mundo vê”.

- Arthur Schopenhauer

AGRADECIMENTOS

Agradeço em primeiro lugar ao apoio essencial que a minha família me proporcionou no percorrer do programa de pós graduação, sempre me incentivando a realizar os meus sonhos.

Agradeço imensamente ao meu companheiro Danilo Augusto Machado que me deu forças para estudar e realizar os experimentos propostos, sempre me encorajando.

Agradeço ao programa ao programa de pós graduação de Ciências da Nutrição, Esporte e Metabolismo (CNEM) e a Faculdade de Ciências Aplicadas da (FCA) da Universidade Estadual de Campinas (UNICAMP), pela oportunidade de cursar um programa de pós graduação tão completo e com tanta estrutura para a continuação da formação com excelência.

Agradeço ao Laboratório Multidisciplinar em Alimentos e Saúde e à equipe que me auxiliou na execução do projeto, em especial ao meu orientador, Fernando Moreira Simabuco, que desde o início esteve presente e exerceu um papel fundamental na qualidade dos experimentos e na garantia de toda estrutura necessária para a execução exímia de cada passo proposto.

Por fim, agradeço a agência de fomento Fundação de Amparo à Pesquisa do Estado de São Paulo (FAPESP), pelo financiamento do projeto Jovem Pesquisador em fase 2 concedido ao Prof. Dr. Fernando Moreira Simabuco: Estudo de alvos moleculares importantes para o controle do metabolismo em câncer – a via da mTOR/S6K com papel central sob número – 2018/14818-9, além da concessão orçamentaria da Bolsa de Mestrado sob número – 2020/13660-2 e Bolsa de Estágio de Pesquisa no Exterior (BEPE) – 2022/09195-8.



RESUMO

INTRODUÇÃO: O câncer é uma doença complexa que se origina de mutações celulares. Entre os cânceres, os pulmonares têm as maiores taxas de mortalidade. O câncer de pulmão de células não pequenas (NSCLC), especialmente o adenocarcinoma, é o mais comum. As células A549, com uma mutação no gene *STK11*, são frequentemente resistentes ao tratamento com cisplatina, exigindo tratamentos sinérgicos. **OBJETIVOS:** O objetivo do trabalho foi gerar células A549 com expressão de LKB1 e avaliar sua resposta à cisplatina e à combinação com metformina, comparando-as com as células não editadas (selvagens). **METODOLOGIA:** O sistema CRISPR/Cas9 foi usado com uma Cas9 recombinante e um RNA guia sintetizado *in vitro* para editar o gene *STK11*. Foram realizados ensaios para avaliar a expressão de proteínas por Western Blotting e imunofluorescência, bem como análises do metabolismo glicolítico/aeróbico e do sistema redox, através de NRF2, enzimas antioxidantes e espécies reativas. **RESULTADOS:** Por meio do reparo NHEJ (*non-homologous end joining*), uma nova isoforma de LKB1 chamada "Super LKB1" de maior peso molecular foi gerada. Linhagens com essa isoforma mostraram uma maior ativação de AMPK e regulações em mTORC, autofagia e metabolismo. Os clones editados também responderam melhor à cisplatina, possivelmente devido ao acúmulo de H₂O₂. **CONCLUSÃO:** A nova isoforma de LKB1 gerada pelo CRISPR/Cas9 foi eficaz na ativação de AMPK, levando a várias regulações celulares e intensificando a atividade apoptótica nas células editadas. Além disso, a metformina intensificou a apoptose induzida pela cisplatina em células selvagens, mas não teve efeitos adicionais nas células editadas.

ABSTRACT

INTRODUCTION: Cancer is a complex disease originating from the accumulation of mutations in cells. Among cancers, lung cancer has the highest mortality rates, with non-small cell lung cancer, particularly adenocarcinoma, being the most common subtype. A549 cells, bearing a significant mutation in the *STK11* gene, often become resistant to cisplatin treatment, necessitating synergistic treatments. **OBJECTIVES:** The aim is to generate A549 cells with LKB1 expression and assess their response to cisplatin and the combination with metformin, comparing them to non-edited cells. **METHODOLOGY:** The CRISPR/Cas9 system was employed using a recombinant Cas9 and *in vitro*-synthesized guide RNA to edit the *STK11* gene. Assays were performed to evaluate protein expression through Western Blotting and immunofluorescence, as well as analyses of glycolytic/aerobic metabolism and the redox system, including NRF2, antioxidant enzymes, and reactive species. **RESULTS:** Through non-homologous end joining (NHEJ), a new isoform of LKB1, referred to as "CRISPR-LKB1 (Super LKB1)" with a higher molecular weight, was generated. Cell lines expressing this isoform showed AMPK activation and regulations in mTORC, autophagy, and metabolism. Edited clones also exhibited better responses to cisplatin due to the accumulation of H₂O₂. **CONCLUSION:** The novel LKB1 isoform generated through the CRISPR/Cas9 system proved effective in activating the downstream target AMPK, leading to various cellular regulations and intensified apoptotic activity in the edited cells. Additionally, metformin enhanced cisplatin-induced apoptosis in non-edited cells, but it did not have additional effects on the edited cells.

LISTA DE FIGURAS

Figura 1 As dez capacidades adquiridas pelas células de câncer maligno.

Figura 2 As 8 principais causas de óbito no mundo desde os anos 2000 até os anos 2020.

Figura 3 Taxa de incidência e mortalidade por câncer estratificado por tecido em todo o mundo.

Figura 4 Taxa de mortalidade por câncer no Brasil.

Figura 5 A via de LKB1.

Figura 6 Análise de bioinformática a respeito da expressão do gene *STK11*.

Figura 7 O tratamento com cisplatina.

Figura 8 Mecanismo de ação farmacológica da metformina nas células.

Figura 9 Esquema de ação do sistema CRISPR/Cas9.

LISTA DE ABREVIATURAS E SIGLAS

STK11	Serine/Threonine kinase 11
LKB1	Liver Kinase B1
CRISPR	<i>Clustered Regularly Interspaced Short Palindromic Repeats</i>
Cas9	<i>CRISPR-associated protein 9</i>
NSCLC	<i>Non Small Cell Lung Cancer</i>
SCLC	<i>Small Cell Lung Cancer</i>
K.O	<i>Knockout</i>
Wt	<i>Wild Type</i>
Spy.	<i>Streptococcus pyogenes</i>
RNA	Ácido ribonucleic
DNA	Ácido desoxirribonucleico
O₂	Oxigênio
H₂O₂	Peróxido de hidrogênio
NHEJ	<i>Non-homologous end-joining</i>
AMPK	Proteína Kinase ativada por AMP
mTORC1	Complexo 1 de mTOR
PCR	<i>Polymerase Chain Reaction</i>
cDNA	DNA complementary
sgRNA	<i>Single Guide RNA</i>
UVA	Ultraviolet A
UVB	Ultraviolet B
OMS	Organização Mundial da Saúde
OPAS	Organização Pan-Americana da Saúde
INCA	Instituto Nacional do Câncer
KRAS	<i>Kirsten rat sarcoma viral oncogene homolog</i>
MAPK	<i>Mitogen-Activated Protein Kinase</i>
EGFR	Fator de Crescimento Epidérmico
ATP	Adenosina trifosfato
ADP	Adenosina difosfato
p53	Proteína de tumor 53
TSC1/2	<i>Tuberous sclerosis protein</i>
IGF-1	Fator de crescimento semelhante a insulina-1
Rag	<i>Recombination-activating gene</i>
REDD1	<i>Regulated in development and DNA damage response 1</i>
HDR	<i>Homologous DNA Repair</i>
T7E1	T7 Endonuclease 1
IC₅₀	Concentração inibitória média
KEAP1	<i>Kelch-like ECH-associated protein 1</i>
3-MA	3-Metiladenina
p62	<i>Sequestome 1</i>
HAM-F12K	<i>Kaighn's Modification of Ham's F-12 Medium</i>
DMEM	<i>Dulbecco's Modified Eagle Medium</i>

SFB	Soro fetal bovine
P/S	Penicilina/Estreptomicina
DMSO	Dimetilsulfóxido
crRNA	<i>CRISPR-RNA</i>
TracrRNA	<i>Trans-activating CRISPR RNA</i>
DSB	<i>Double Strand Breaks</i>
PAM	<i>Protospacer adjacent motif</i>
Nt	Nucleotídeo
CO₂	Dióxido de carbono
DEPEC	Ultra pura livre de endonucleases
EDTA	Ácido etilenodiamínico
BCA	<i>Bicinchonic acid</i>
BSA	<i>Bovine Serum Albumin</i>
TBS-t	<i>Tris Buffered Saline – Tween20</i>
SDS-PAGE	Eletrforese em gel de poliacrilamida com dodecil sulfato de sódio
Lc3	<i>Microtubule-Associated Protein 1A/B Light Chain 3</i>
S6	<i>Ribosomal Protein</i>
S6K1	<i>Ribosomal Protein Kinase Beta-1</i>
S6K2	<i>Ribosomal Protein Kinase Beta-2</i>
mTOR	<i>Mammalian Target of Rapamycin</i>
GAPDH	<i>Glyceraldehyde-3-Phosphate Dehydrogenase</i>
NRF2	<i>NF-E2 Related factor 2</i>
NQO1	<i>NAD(P)H Quinone Dehydrogenase 1</i>
PRDX3	<i>Thioredoxin-Dependent Peroxidase Reductase, Mitochondrial</i>
BAK	<i>BCL2 Antagonist/Killer 1</i>
BAX	<i>BCL2 Associated X, Apoptosis Regulator</i>
FAS	<i>Apoptosis Antigen 1</i>
H2AX	<i>H2A Histone Family Member X</i>
LDHA	<i>Lactate dehydrogenase A</i>
H2X	<i>Hexoquinase-2</i>
H2B	<i>Histone 2B</i>
HCl	Ácido Clorídrico
PBS	<i>Phosphate-Buffered Saline</i>
KCl	Cloreto de Potássio
DTT	<i>DL-Dithiothreitol, Cleland's reagent</i>
MgCl₂	Cloreto de Magnésio
pH	Potencial Hidrogeniônico
GFP	<i>Green Fluorescent Protein</i>
RFP	Red Fluorescent Protein
CE	<i>Cytoplasmatic Extract Buffer</i>
NE	<i>Nuclear Extract Buffer</i>
NP40	Nonilfenol Etoxilado para surfactantes não iônicos
EGTA	Ácido Egtazico
KH₂PO₄	Fosfato Monopotássio
dNTP	Desoxirribonucleotídeos Fosfatados

CDS Coding DNA Sequence
RPM Rotações Por Minuto

SUMÁRIO

1 INTRODUÇÃO	15
1.1. Câncer e epidemiologia da doença	15
1.2. O cancer de pulmão	19
1.3. Estratégias de tratamento	23
1.4. Novas abordagens para geração de modelos experimentais	25
2. OBJETIVOS	29
2.1. Geral	29
2.2. Específico	29
3. CAPÍTULO 1 – The novel LKB1 isoform generated by CRISPR/Cas9 improves the response to cisplatin in A549 NSCLC through AMPK activation	31
3.1. INTRODUCTION	33
3.2. EXPERIMENTAL PROCEDURES	35
3.2.1 Cell culture	35
3.2.2 <i>STK11</i> (LKB1) edition by CRISPR/Cas9.....	36
3.2.3 Western blotting.....	37
3.2.4 Immunofluorescence	38
3.2.5 Autophagy flux detection	38
3.2.6 Wound healing – Scratch assay	38
3.2.7 Colony formation assay	39
3.2.8 Subcellular fractionation	39
3.2.9 DNA damage assay – detection of phosphorylated foci of H2AX.....	39
3.2.10 MTT and IC ₅₀	39
3.2.11 H ₂ O ₂ DETECTION ASSAY	40
3.2.12 OROBOROS mitochondrial respiration	40
3.2.13 PCR, RTqPCR, and LKB1 cloning.....	40
3.2.14 Bioinformatic analysis.....	42
3.2.15 Proliferation curve assay	42
3.2.16 Anti-FLAG immunoprecipitation	43
3.2.17 Pharmacological treatments (Cisplatin, Metformin, 3-MA, and Puromycin).....	43
3.2.18 Statistical analysis of data	43
3.3. RESULTS	43
3.3.1 The <i>STK11</i> gene edition in A549 cells by CRISPR/Cas9 generated a higher molecular weight LKB1, through the INDELS and alternative exon ..	43
3.3.2 LKB1 overexpression enhances AMPK phosphorylation at 173 Threonine residue	51
3.3.3 Super LKB1 affects the epithelium mesenchymal transition (EMT), survival, and migration of A549 cells.	56
3.3.4 Super LKB1 enhances oxidative metabolism in A549 edited cells	58

3.3.5	The expression of Super LKB1 in edited A549 cells led to the inhibition in mTORC1 and increase of autophagy signaling.....	60
3.3.6	The autophagy inhibition leads to p62/KEAP1 interaction, and its interaction can enhance the NRF2 cytoplasmatic localization and downregulation of the expression of antioxidant enzymes in A549 edited cells.	63
3.3.7	Edited cells accumulated more DNA Damage, and had a higher pro-apoptotic protein expression.	67
3.3.8	The A549 edited cells exhibited increased oxidative damage, rendering them more susceptible to cisplatin. The combined inhibition of autophagy by 3-MA and cisplatin resulted in reduced H2O2 generation and rescued cell viability	68
3.4.	DISCUSSION	71
3.5.	CONCLUSION	75
3.6.	ACKNOWLEDGMENTS	75
3.7.	FUNDING INFORMATION	76
3.8.	CONFLICT OF INTEREST	76
4.	CONCLUSÕES DO TRABALHO	77
5.	REFERÊNCIAS	78
6.	ANEXOS	84

1. INTRODUÇÃO

1.1 O câncer e epidemiologia da doença

O câncer é uma doença que se origina a partir do acúmulo de mutações no DNA das células de qualquer tecido do organismo (LEE et al., 2019). Essas mutações podem ocorrer por herança genética, onde filhos de pais portadores de câncer têm uma maior propensão ao desenvolvimento da doença (GÖTZE; BRÄHLER, 2012), ou devido ao estilo de vida a longo prazo. O acúmulo de mutações no organismo pode ser desencadeado, por exemplo, pela exposição à poluição, à luz solar (UVA/UVB) sem proteção, tabagismo, consumo excessivo de álcool e uma dieta rica em alimentos ultraprocessados e pobre em vitaminas e minerais (KOLAK et al., 2017). Além disso, a infecção por certos tipos de vírus, como o HPV ou o HIV, também representa um fator de risco para o desenvolvimento do câncer (WEISS, 1999).

Nesse contexto, o acúmulo de mutações nas células pode levar ao desenvolvimento de tumores. Dependendo das mutações presentes, um tumor pode ser classificado como benigno, mantendo algumas características do tecido de origem, como o processo de diferenciação celular (JÖGI et al., 2012). No entanto, muitas vezes, os tumores são classificados como malignos, perdendo a função do tecido de origem e adquirindo características específicas descritas na figura 1, como hallmarks of cancer (HANAHAAN; WEINBERG, 2011).

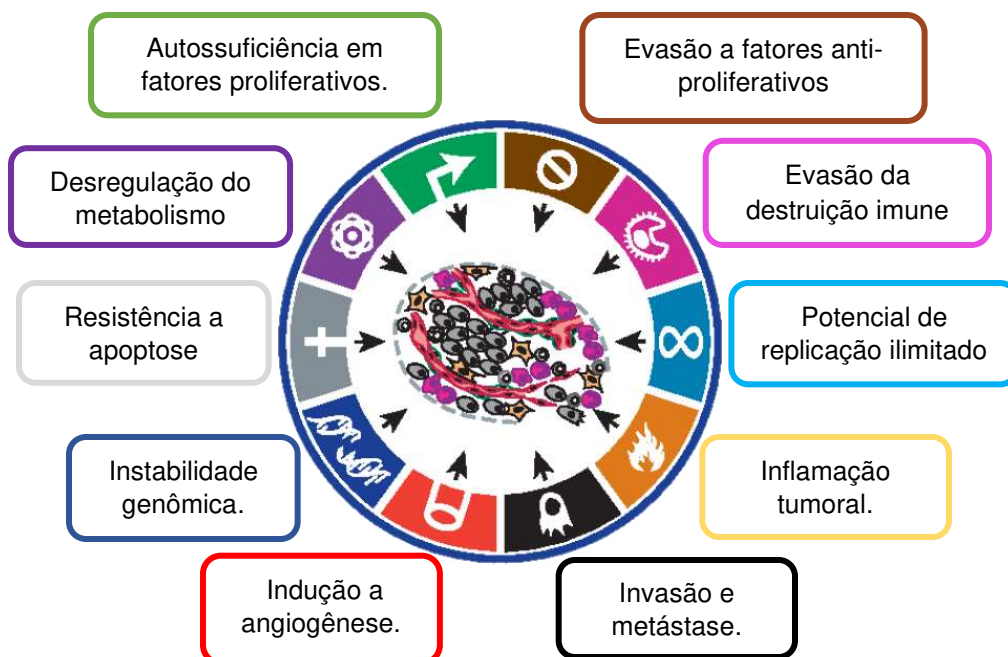


Figura 1. As dez capacidades adquiridas pelas células de câncer maligno. Durante o desenvolvimento de tumores malignos em humanos, as células tumorais adquirem algumas características que são comuns entre os tumores malignos. Sendo elas: Autossuficiência em fatores proliferativos; Evasão a fatores antiproliferativos; Evasão da destruição imune; Potencial de replicação ilimitado; Inflamação tumoral; Invasão e metástase; Indução a angiogênese; Instabilidade genômica; Resistência a apoptose e Desregulação do metabolismo.

Fonte: Hallmarks of câncer, 2011.

Assim, de acordo com as características expostas na figura 1, em geral, os tumores malignos apresentam: grande capacidade proliferativa e metástase, que é o processo de invasão de tecidos adjacentes e formação de novos nódulos tumorais em outras partes do organismo. Além disso, são resistentes a destruição via sistema imunológico, sendo necessário tratamentos específicos, como a quimioterapia ou radioterapia, o que torna o seu tratamento complexo. O câncer é portanto uma patologia desafiadora do ponto de vista clínico (MCLAUGHLIN et al., 2020).

Para compreender a complexidade do câncer, ao analisarmos estatísticas relacionadas às oito principais causas de óbito no mundo, apresentadas na figura 2, com base em dados atualizados publicados nos relatórios da OMS (Organização Mundial de Saúde) e da OPAS (Organização Pan-americana de Saúde), observamos que o câncer

figura como a segunda patologia que mais resulta em óbitos globalmente, representando 23,1% de todas as causas de morte desde os anos 2000 até 2020.

Entretanto, a sobrevivência após o diagnóstico varia significativamente, dependendo do tecido em que o câncer se desenvolve. Essa disparidade torna-se evidente ao analisarmos os dados apresentados na figura 3, que incluem incidência e mortalidade, conforme os registros da OMS e da OPAS. Ao estratificarmos os cânceres por tecido, abrangendo ambos os sexos, notamos que, embora os cânceres de mama e próstata tenham sido mais incidentes em 2023, a mortalidade foi mais elevada entre os portadores de câncer de pulmão em todo o mundo (BOTT et al., 2019; MOSS et al., 2021).

As 8 principais causas de óbitos no mundo no ano de 2020

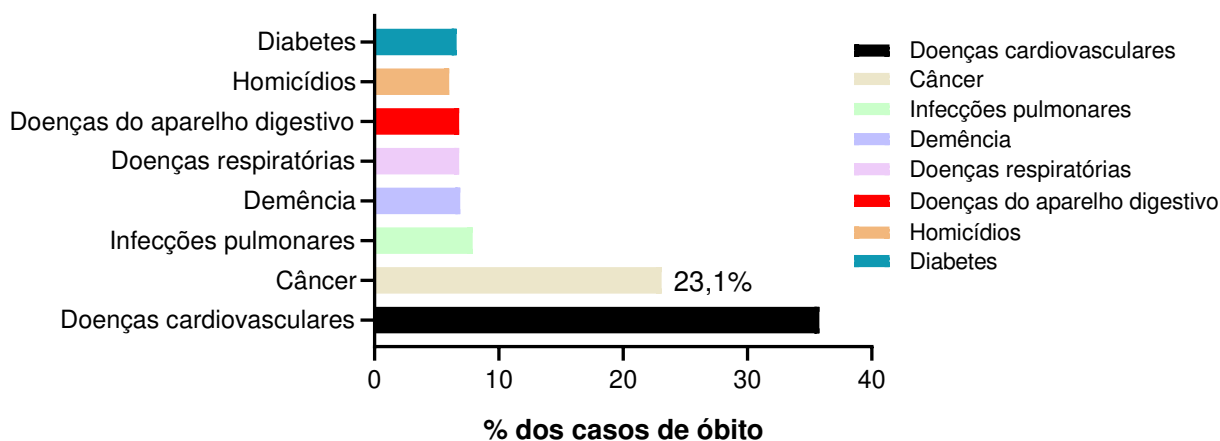


Figura 2. As 8 principais causas de óbito no mundo desde os anos 2000 até os anos 2020. Os dados agrupam as causas de óbitos, incluindo homens e mulheres desde neonatos até idosos (última atualização 2020).

Fonte: <https://www.who.int/data/gho/data/indicators/indicator-details/GHO/number-of-deaths-attributed-to-non-communicable-diseases-by-type-of-disease-and-sex>.

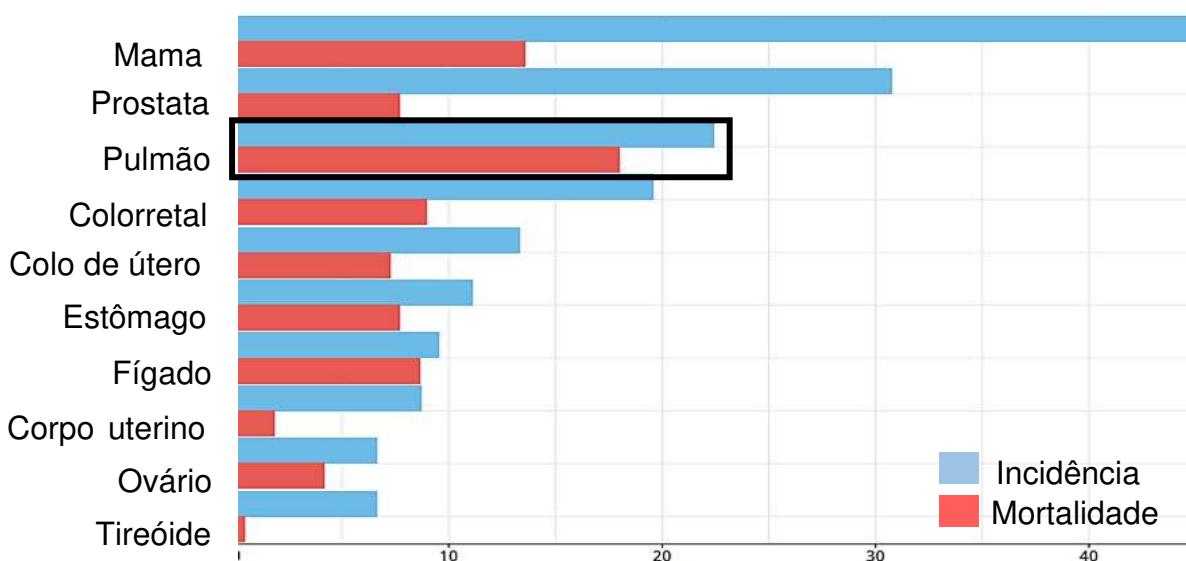


Figura 3. Taxa de incidência e mortalidade por câncer estratificado por tecido em todo o mundo. Os padronizadas estimadas em 2023 em todo mundo, incluindo ambos os sexos e todas as idades. A seta indica a taxa de mortalidade referente a câncer de pulmão.

Fonte: Global Câncer Observatory, Globocan, 2023.

No Brasil, em 2022, foi estimado um total de 66.280 novos casos de câncer entre homens e mulheres. Embora os tumores malignos pulmonares não tenham sido a forma mais incidente de câncer no país, ficando como a quarta na categoria de incidência, ela foi reponsável pela terceira maior taxa de mortalidade entre os homens e mulheres, representando 12,3 óbitos a cada 100.000 pessoas, segundo dados do INCA apresentados na figura 4.

Casos de óbito por câncer no Brasil a cada 100.000 pessoas, incluindo ambos os sexos e todas as idades

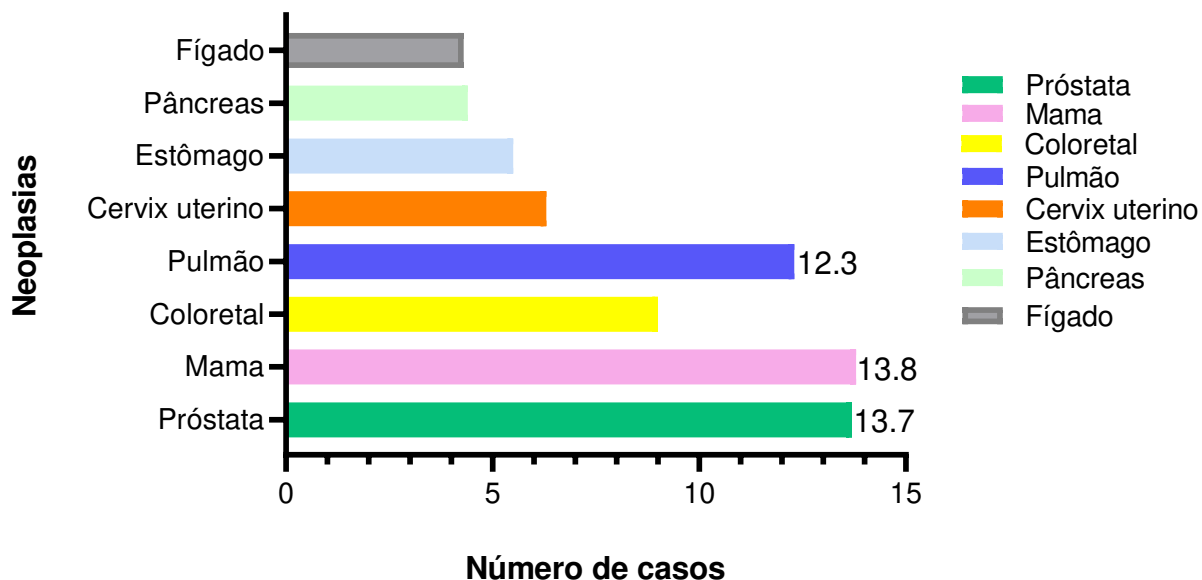


Figura 4. Taxa de mortalidade por câncer no Brasil. Os dados foram agrupados considerando o número de óbitos entre homens e mulheres de todas as idades, a cada 100.000 pessoas no ano de 2022, no Brasil.

Fonte: <https://www.who.int/data/gho/data/indicators/> / Global Câncer Observatory, Globocan, 2023.

1.2 O câncer de pulmão

Os cânceres de pulmão são subdivididos em 2 categorias: de células pequenas (*Small Cell Lung Cancer*; SCLC) que representam 15% dos casos e os de células não pequenas (*Non Small Cell Lung Cancer*; NSCLC) que são mais frequentes representando 85% dos casos. Entre os tumores pulmonares de células não pequenas, ocorrem o carcinoma espinonuclear, o carcinoma de grandes células e o adenocarcinoma, que é o mais comum (GU et al., 2003).

Como modelo de estudo, a linhagem de células A549 é amplamente utilizada, sendo derivada de adenocarcinoma pulmonar, apresentando diversas mutações, entre elas:

- 1) A mutação *KRAS* G12D que provoca uma alteração na conformação estrutural da proteína *KRAS*, impedindo a interação com a proteína GAP. Isso resulta em uma ativação constante da via MAPK, promovendo um crescimento celular intenso (SMITHEY et al., 1992).
- 2) O aumento na expressão do receptor de crescimento EGFR, que faz com o tumor cresça mais rapidamente.
- 3) Mutação em *STK11*, através da substituição de uma base, gerando um *stop códon* no primeiro éxon do gene (*Premature termination codon*, PTC), tornando a linhagem KO (*knockout*) para a proteína LKB1, que será objeto deste estudo e é um clássico supressor tumoral (WANG et al., 2021).

O potencial de supressor tumoral promovido pela proteína LKB1 é complexo, pois é associado à ativação da via de sinalização de AMPK e influencia diversas vias moleculares, como apresentado na figura 5 (CICCARESE; ZULATO; INDRACCOLO, 2019a). Entre elas podemos citar:

- 1) Polaridade celular e o processo de transição epitélio mesenquimal: as células perdem o fenótipo característico epitelial e adquirem o fenótipo mesenquimal que auxilia na infiltração dos tumores e geração de metástases adjacentes (SONG et al., 2021).
- 2) Alteração da atividade de síntese proteica e do crescimento celular: através da regulação do complexo de mTORC1 e seus efetores, como a família de quinases de proteínas ribossomais do tipo S6 (S6Ks) (ZHANG et al., 2019a).
- 3) Regulação da autofagia celular: promove o *turnover* de organelas citoplasmáticas, evitando o acúmulo de organelas disfuncionais nas células (KIM et al., 2011a).
- 4) Metabolismo celular: através da sinalização pela relação intracelular de ATP/AMP, a proteína AMPK pode regular a bioenergética celular, intensificando o metabolismo oxidativo em relação ao glicolítico (ZHANG et al., 2019b).

Além disso, a via de sinalização de LKB1/AMPK pode se relacionar com um fenômeno muito comum em células tumorais, chamado de efeito *Warburg*, onde as células, mesmo em condição aeróbia, intensificam o metabolismo anaeróbio, através da glicólise e fermentação láctica. Com isso as células geram intermediários

metabólicos para a via das pentoses fosfato, que produz NADPH, uma importante molécula para o balanço redox e proteção antioxidante das células, além de ribose-5-fosfato, uma molécula necessária para a síntese de nucleotídeos. O acúmulo de lactato produzido pela células pode ainda ser direcionado para o espaço extracelular, promovendo um microambiente tumoral ácido para auxiliar no processo metastático, através da degradação da matriz extracelular (NDEMBE et al., 2022).

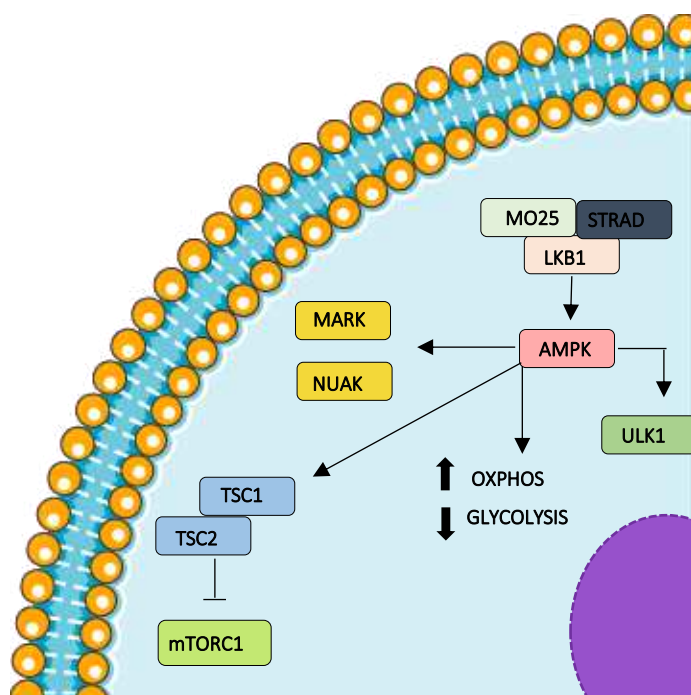


Figura 5. A via de LKB1. Na figura, está destacado na célula a ativação da proteína AMPK por LKB1 e os processos regulados por esse eixo: Polaridade celular, representado pela ativação de MARK e NUAK; síntese proteica e crescimento, através da regulação do complexo TSC1/2 que inibem mTORC1; autofagia, devido a ativação de ULK1; e controle metabólico, devido ao aumento na expressão de enzima da cadeia fosforilação (OXPHOS) e redução na expressão de enzimas da via glicolítica.

Fonte: (LI et al., 2015).

Assim, ao olharmos dados do portal GEPIA, apresentados na figura 6, a respeito da expressão de genes em tumores, percebemos que dos 31 tipos de cânceres humanos analisados, 18 apresentaram nas amostras uma menor expressão de LKB1, o que representa aproximadamente 58% dos tumores com menor expressão de LKB1 (Figura 6A).

Além disso, nos tumores com menor expressão de LKB1, a sobrevida é menor (Figura 6B). E especificamente em adenocarcinomas pulmonares humanos, a expressão do gene *STK11* é significativamente menor do que em amostras de pulmão saudáveis (Figura 6C), (GEPIA, 2021).

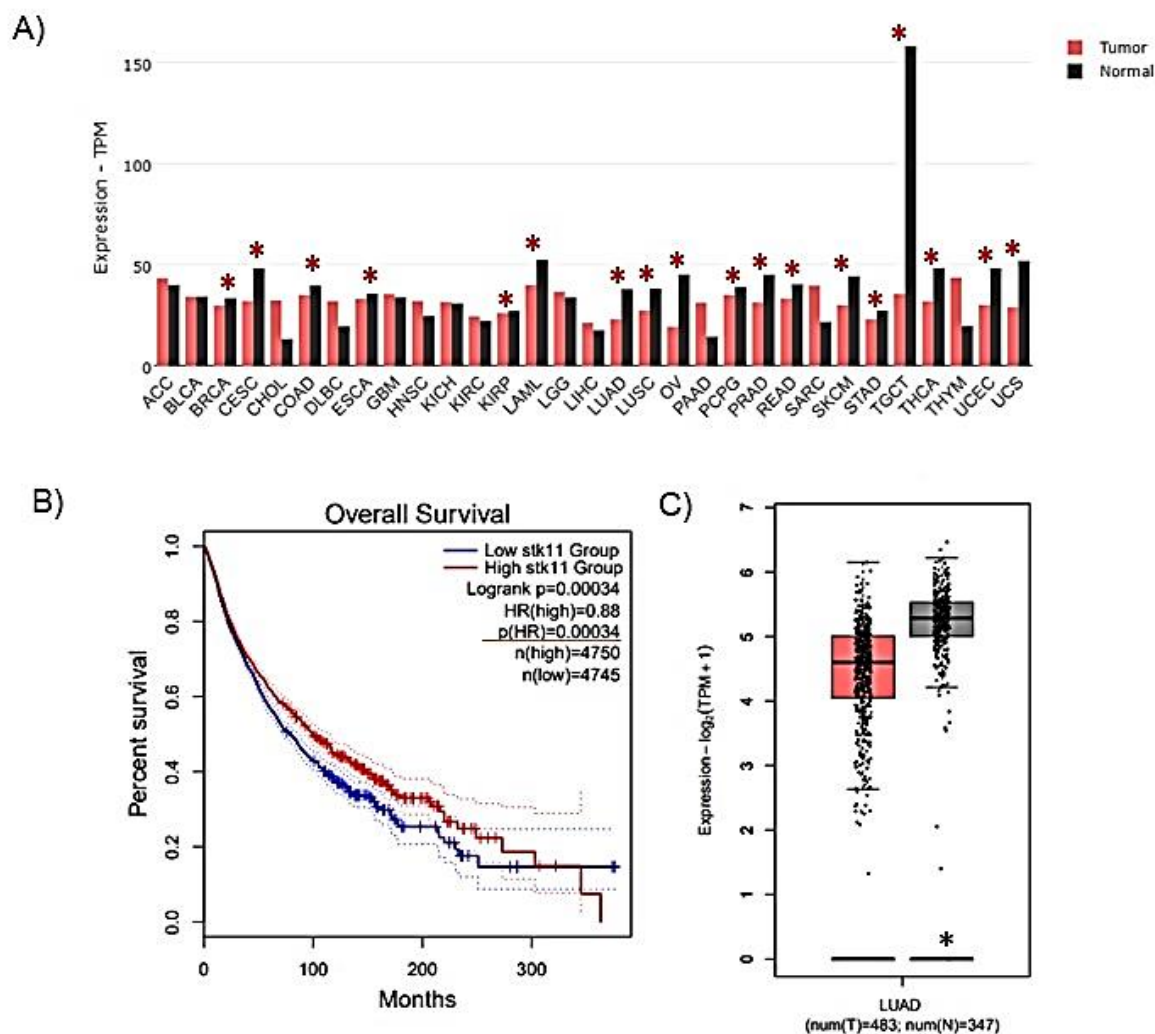


Figura 6. Análises de bioinformática a respeito da expressão do gene *STK11*. (A) Expressão de LKB1 em tumores humanos, as barras vermelhas simbolizam tumores. (B) Sobrevida de portadores de tumores com alta e baixa expressão de LKB1, a linha azul representa tumores com baixa expressão de *STK11*. (C) Expressão de LKB1 em adenocarcinoma pulmonar, o grupo vermelho representa amostras tumorais e o cinza amostras controle de biópsia humana.

Fonte: GEPIA, 2021.

1.3 Estratégias de tratamento do câncer de pulmão

A partir do diagnóstico de câncer de pulmão, existem diversas estratégias para o tratamento, entre elas as mais comuns: a ressecção cirúrgica, principalmente em fases mais iniciais; o tratamento quimioterápico com derivados de platina; e radioterapia, principalmente para estadiamentos mais avançados da doença (BOTT et al., 2019).

O tratamento com cisplatina tem sido amplamente utilizado. Como mostrado na figura 7, o fármaco é administrado via intravenosa e é transportado ligado a proteínas plasmáticas (Figura 7A). Ao acessar as células, a molécula de cisplatina passa por hidrólise, dando origem a metabólitos reativos capazes de alquilar ácidos nucleicos (Figura 7B), (GHOSH, 2019). Uma vez que a cisplatina interage com o DNA, preferencialmente em bases de adenina e guanina, promove distorção da dupla-hélice de DNA, impedindo, assim, a sua replicação e levando a célula ao processo de apoptose (BOLDINOVA et al., 2021).

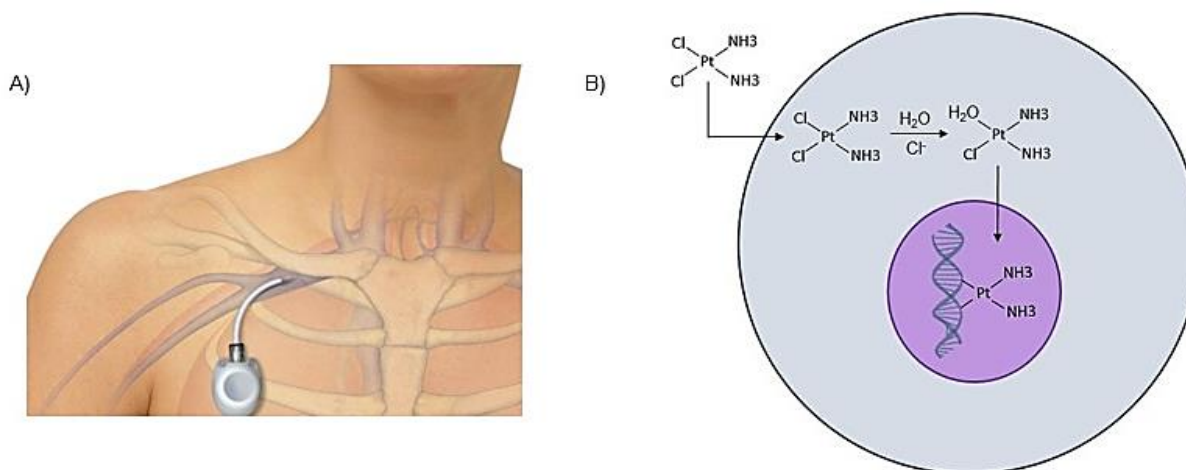


Figura 7. O tratamento com cisplatina. (A) Esquema de administração da cisplatina via intra venosa de acesso central por cateter Port-a-Cath. (B) Mecanismo de ação da molécula de cisplatina nas células, onde

ao acessar a células, a molécula passa por hidrólise, após esse processo a molécula pode intercalar com o DNA em bases de adenina e guanina, inibindo a replicação do DNA.

Fonte: (MILLER, 2000).

Contudo, sabe-se que o tratamento isolado de cisplatina muitas vezes não é capaz de eliminar toda a massa tumoral, isso porque, o tecido pulmonar frequentemente adquire resistência à cisplatina. Assim, tem sido cada vez mais desenvolvidas estratégias coadjuvantes à quimioterapia com cisplatina, para promover o aumento da eficácia do tratamento do adenocarcinoma pulmonar. Entre as estratégias, podemos citar: a utilização de anticorpos monoclonais para fatores de crescimento e vascularização, inibidores seletivos de vias moleculares importantes para a progressão tumoral e a combinação farmacológica para potencializar o efeito do quimioterápico (GALLUZZI et al., 2012).

A metformina tem sido amplamente estudada como um agente farmacológico para combinações com quimioterápicos, uma vez que seu efeito na redução do crescimento de várias linhagens de câncer maligno já foi documentado no tratamento *in vitro* de células (MORELLI et al., 2021). Isso ocorre devido à sua capacidade de promover ações sinérgicas nas células, tanto por meio da ativação de AMPK, como mostrado na figura 8, através da interação direta com receptores celulares como o receptor para fator de crescimento 1 (FGF1) e receptor de insulina (IGF-1R/IR) (PODHORECKA; IBANEZ; DMOSZYŃSKA, 2017).

As seguintes ações farmacológicas celulares da metformina via ativação de AMPK são conhecidas:

- 1) Aumento da autofagia e apoptose via regulação de p53 (HSIEH LI et al., 2018a).
- 2) Inibição do ciclo celular via ciclina D1 (YUDHANI et al., 2019).
- 3) Inibição da síntese proteica através da ativação do complexo TSC1/2, que inibe a proteína Rheb GTPase. A proteína Rheb é importante para a ativação do complexo mTORC1 e conseqüentemente a síntese proteica (AMIN; LUX; O'CALLAGHAN, 2019).

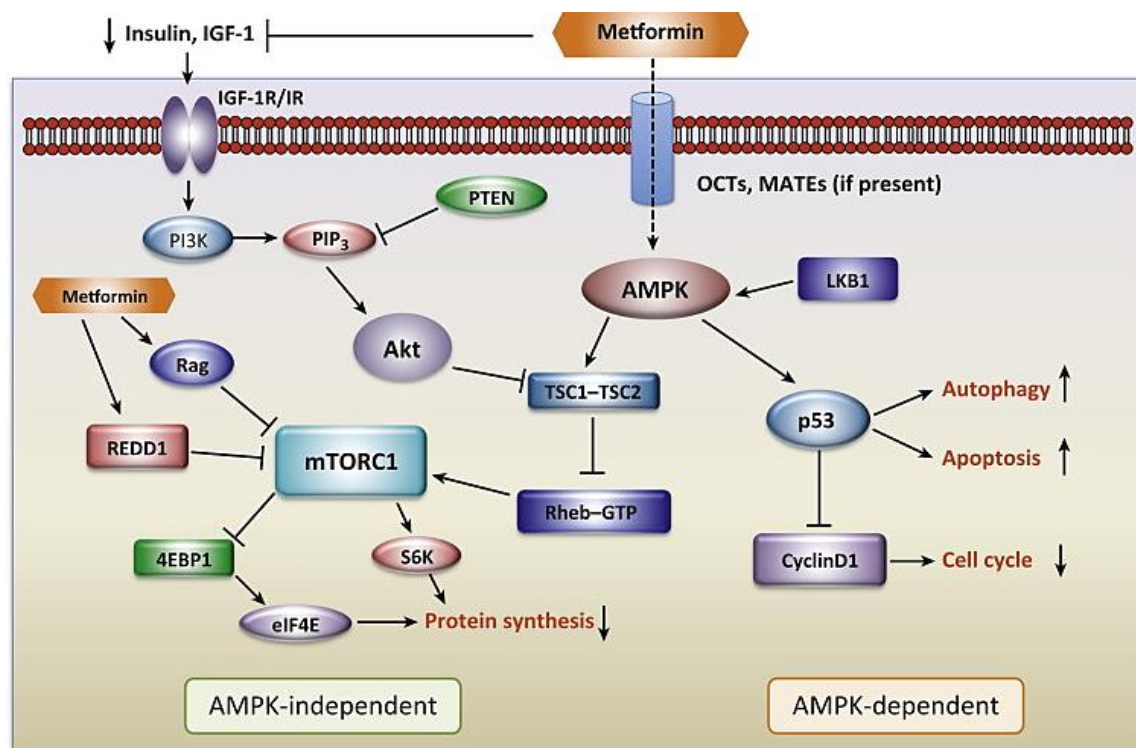


Figura 8. Mecanismo de ação farmacológica da metformina nas células. O esquema ressalta a atividade de ativação de AMPK pelo fármaco regulando as vias da autofagia, apoptose, ciclo celular e síntese proteica, além disso é destacado o papel da metformina na inibição de receptores celulares, como o FGF-1R e IR.

Fonte: (QUINN et al., 2013)

Dado que muitos dos efeitos da metformina dependem da ativação de AMPK, que é diretamente regulado por LKB1, surge a questão de como os efeitos sinérgicos da metformina, quando combinada com cisplatina, podem variar de acordo com o status de LKB1 nas células.

1.4 Novas abordagens para a geração de modelos experimentais

Afim de expandir o *background* de modelos para elucidações de respostas farmacológicas, relacionado a expressão de proteínas e garantindo uma maior individualização e personalização do tratamento farmacológico, novas tecnologias de construção de linhagens editadas têm estado em foco. A edição através do sistema

CRISPR/Cas9 é uma das técnicas mais utilizadas atualmente (ZHANG; WEN; GUO, 2014).

Este sistema, apresentado na figura 9, é composto pela proteína bacteriana Cas9, que é uma endonuclease que pode clivar a dupla fita de DNA. Quando a Cas9 está associada a uma sequência guia de RNA de fita simples, conhecida como *guideRNA* (sgRNA), ela pode ser utilizada para orientar a localização específica e intensional da clivagem do DNA (SHIVRAM et al., 2021).

A partir da clivagem do DNA, as células tentaram reparar a dupla quebra, e nesse processo poderá ocorrer por duas vias de reparo. A primeira é a via não homóloga (*Non-Homologous End Joining*; NHEJ) através de INDELS que são inserções ou deleções na região da dupla quebra do DNA. Neste processo poderá ocorrer a alteração do quadro de leitura do gene alvo, podendo ocasionar a inserção de um *stop* códon prematuro, gerando assim, uma linhagem *knockout* para o gene de interesse (LENTSCH et al., 2019).

Além disso, existe a via de reparo homóloga (*Homologous DNA Repair*; HDR), onde pode-se utilizar um molde para o reparo de dupla quebra na fita de DNA. O molde, também chamado de DNA doador, orientará o reparo homólogo da dupla quebra na fita de DNA. Esta via é muito utilizada para o estudo de variantes genéticas, biologia sintética, polimorfismos e para o reparo de mutações específicas em linhagens tumorais. Os construtos desenvolvidos com inserções homólogas são chamados de *knock-ins* (LIN et al., 2014).

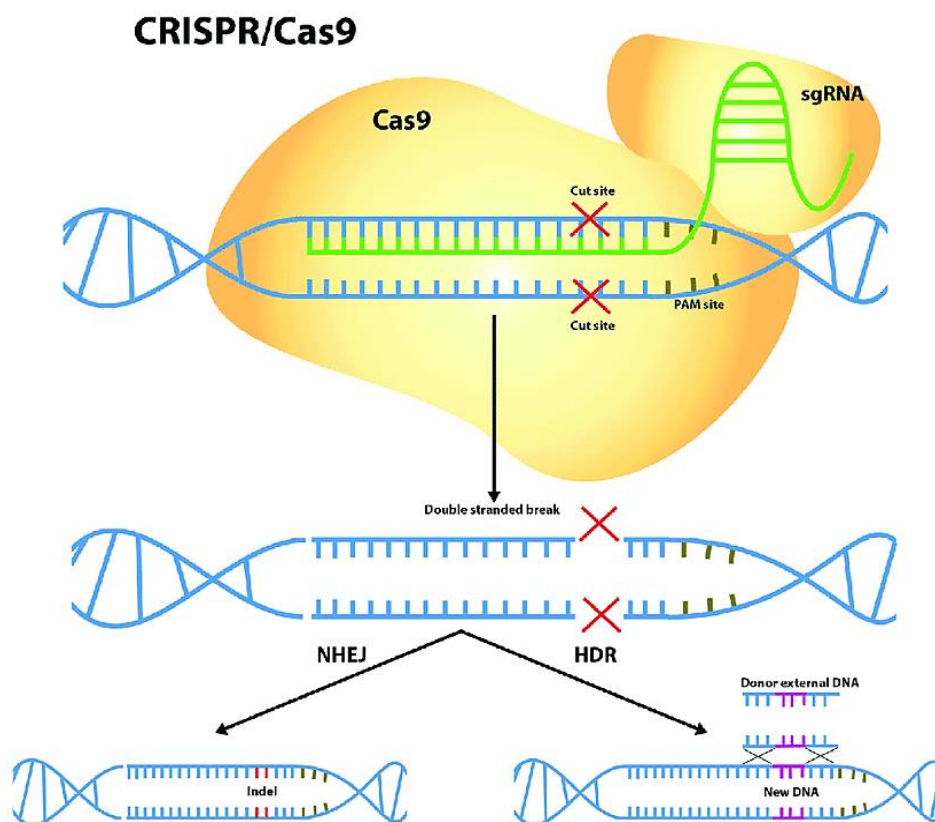


Figura 9. Esquema de ação do sistema CRISPR/Cas9. O sistema tem sido utilizado para edição em uma célula eucariota. Pode-se observar a dupla quebra na fita de DNA e dois mecanismos de reparo posteriores o não homólogo através de INDELS (NHEJ) e o homólogo através de um molde de DNA (HDR).

Fonte: (CRIBBS; PERERA, 2017).

A tecnologia de CRISPR/Cas9 pode ser utilizada nas células de diversas formas entre elas: plasmídeos ou proteínas recombinantes associadas a sgRNAs sintetizados *in vitro*. Contudo, independente do formato, esta tecnologia se mostrou muito efetiva e específica, gerando resultados satisfatórios (SIVA et al., 2021).

Nesse contexto, utilizando o sistema CRISPR/Cas9, buscamos resgatar a expressão de LKB1 por meio da edição do gene *STK11* na linhagem celular de adenocarcinoma pulmonar A549. Essa abordagem visa gerar um impacto significativo tanto no âmbito social quanto na prática clínica. Dada a complexidade no tratamento de tumores malignos, especialmente aqueles com baixa expressão de LKB1 que apresentam menores taxas de sobrevivência, a relevância desse estudo é enfatizada. Além disso, considerando a importância de LKB1 nas regulações celulares de supressão tumoral e

ativação de AMPK, a elucidação do tratamento combinado de cisplatina e metformina em células de câncer de pulmão torna-se crucial. A metformina, como um dos fármacos mais amplamente utilizados no Brasil devido ao seu baixo custo e mínimos efeitos colaterais, tem o potencial de reduzir os custos associados ao tratamento de tumores pulmonares pelo SUS, contribuindo assim para melhorias na expectativa e qualidade de vida dos pacientes.

2. OBJETIVOS

2.1 Geral

O objetivo do trabalho é a edição, através do sistema CRISPR/Cas9, do gene *STK11* em células não pequenas de câncer de pulmão A549, para resgatar a expressão da proteína LKB1, comparando os efeitos do tratamento combinado dos fármacos cisplatina e metformina em linhagens editadas e não editadas.

2.2 Específicos

a) Construção do sistema CRISPR/Cas9;

Desenho dos primers com a sequência do sgRNA no software de bioinformática Benchling, do oligo molde para a síntese *in vitro* do sgRNA e também aquisição da Cas9 recombinante para geração do sistema completo de CRISPR.

b) Geração e validação das linhagens editadas;

Transfecção do sistema CRISPR/Cas9, detecção de heteroduplex através da enzima T7EI, seleção clonal das células e posterior sequenciamento das linhagens, caracterização dos clones por sequenciamento de DNA tipo Sanger.

c) Caracterização de vias moleculares envolvidas com LKB1 nas linhagens editadas.

Ensaio funcionais a fim de avaliar as vias moleculares envolvidas com LKB1 - autofagia, síntese proteica, transição epitélio mesenquimal, metabolismo e respiração entre eles: *Western blotting* e imunofluorescência. Além dos ensaios de migração - *Scratch*, formação de colônias e dano no DNA.

d) Avaliação da cisplatina nas linhagens;

Determinação do IC₅₀ (concentração inibitória média) em 72h. Avaliação dos níveis de H₂O₂ nas linhagens com o tratamento quimioterápico.

e) Co-tratamento de cisplatina e metformina nas linhagens;

Co-tratamento com cisplatina e metformina durante 72h, para avaliação da viabilidade e geração de H_2O_2 nas linhagens.

f) Avaliação da interação da autofagia com o sistema redox (NRF2) na resposta a cisplatina das linhagens;

Investigação da interação da proteína autofágica p62 com KEAP1 e utilização do inibidor 3-MA para avaliar o efeito da autofagia associado ao tratamento com cisplatina.

Os resultados gerados serão apresentados na dissertação como um capítulo, uma vez que estão estruturados no formato de um artigo destinado à publicação

3. CAPÍTULO 1 – A novel LKB1 isoform generated by CRISPR/Cas9 improves the response to cisplatin in A549 lung cancer cells through AMPK activation.

Severino, M.B.¹, Morelli, A.P.¹, Pavan, I.C.B.^{1,2}, Mancini, M.C.S.¹, Gois, M.M.¹, Borges, R.J.⁴, Braga R.R.³, Ropelle E.R.³, Silva, L.G.S.¹, Ruiz, N.Q.¹, Costa, M.M.¹, Oliveira, W.de L.¹ Simabuco, F.M.^{1,5*}

¹ Multidisciplinary Laboratory of Food and Health, School of Applied Sciences, University of Campinas, Limeira, Brazil.

² Laboratory of Signal Mechanisms, School of Pharmaceutical Sciences (FCF), University of Campinas (UNICAMP), Campinas, São Paulo, Brazil.

⁴ Department of Physics and Biophysics, Biosciences Institute, State University of São Paulo, Botucatu, Brazil.

³ Laboratory of Molecular Biology of Exercise (LaBMEx), School of Applied Sciences, University of Campinas, Limeira, Brazil.

⁵ Department of Biochemistry, Federal University of São Paulo 04044-020, São Paulo, Brazil.

ABSTRACT

Lung cancer has the highest mortality rate in the world compared to other cancer types, often presenting chemotherapy resistance to cisplatin. The A549 NSCLC (non-small cell lung cancer) is widely used as a model for lung adenocarcinoma studies, presenting high proliferative rates and a nonsense mutation in the *STK11* gene. The LKB1 protein, coded by the *STK11* gene, is one of the major regulators of cellular metabolism through AMPK activation under nutrient deprivation, and its mutation in A549 cells potentiates cancer hallmarks such as deregulation of cellular metabolism, besides the Warburg effect, mTOR activation, autophagy inhibition, and NRF2 and redox activation. Here, we investigated the integration of these pathways associated with the metabolism regulation by LKB1/AMPK, to improve cisplatin response in the A549 cell line. First, we used the CRISPR/Cas9 system to generate cell lines with a CRISPR-edited LKB1 isoform (called Super LKB1) by the generation of a +1 adenine insertion on the first *STK11* exon. This INDEL led to the expression of higher molecular weight protein containing an alternative exon that was described in the PJS (Petuz-Jeghers Syndrome). Through metabolic regulation by LKB1 expression and AMPK activation, we found in edited cells an increase in autophagy flux (LC3 GFP/RFP $p < 0.05$), and a reduction in mTORC1 downstream targets through the reduction in the Serine 423 phospho-S6K2 ($p < 0.05$) and Serine 240/244 phospho-S6 ($p < 0.03$). The A549 WT (wild-type) cells exhibited higher levels of NRF2 ($p < 0.01$), and nuclear localization of this protein compared to the edited cells ($p < 0.01$). These findings suggest more NRF2 activation in the WT A549 cells may contribute to lower levels of H_2O_2 ($p < 0.01$), and a higher requirement of cisplatin to achieve the IC_{50} (WT $10 \mu M$ x $\pm 5.5 \mu M$ edited cells). The data presented here suggests that the regulation of molecular pathways by the novel CRISPR-edited LKB1 isoform (Super LKB1) in A549 cells related to metabolism, mTORC1, and autophagy, promoting a better response of cisplatin in lung cancer.

Keywords: *STK11*(LKB1), CRISPR/Cas9, metabolism, autophagy, cisplatin.

3.1 INTRODUCTION

Lung cancer has the highest cancer mortality rate (THANDRA et al., 2021). NSCLC represents 85% of cancer cases in men and women, with lung adenocarcinoma being the most frequent type (GREENLEE et al., [s.d.]). From lung cancer diagnosis, the standard treatment is chemotherapy with cisplatin. However, NSCLC often presents resistance to chemotherapy, causing most lung cancer patients to progress to death (CRUZ-BERMÚDEZ et al., 2019).

Lung cancer adenocarcinomas are predominantly associated with: Kirsten Rat Sarcoma Viral Oncogene Homolog (*KRAS* - 32%); Epidermal Grow Factor Receptor (*EGFR* - 11%), and V-Raf Murine Sarcoma Viral Oncogene Homologue B (*BRAF* - 7%) driver mutations. Additionally, molecular profiling of lung adenocarcinoma has identified a significant frequency of mutations in the tumor suppressors Serine Threonine Kinase 11 (*STK11* - 17%) and Kelch Like ECH associated protein 1 (*KEAP1* - 17%) based on the analysis of 230 samples from the TCGA database (CANCER GENOME ATLAS RESEARCH NETWORK, 2014). A cohort study has demonstrated that mutations in tumor suppressors, such as *STK11*, are correlated with a poor prognosis for malignant tumors. These mutations can also contribute to increased chemoresistance to platinum-based chemotherapy and reduced efficacy of immunotherapies, including immune checkpoint blockade such as anti-PDL1 treatment (PAPILLON-CAVANAGH et al., 2020).

The *STK11* is the gene coding for Liver Kinase B1 (LKB1) protein. The LKB1 is an upstream activator of AMP-Activated Protein Kinase (AMPK). The LKB1/AMPK is activated by increase in intracellular AMP, and ATP depletion (KE et al., 2018). AMPK is a well-studied protein, that presents a central role in cellular metabolism, regulating several molecular pathways, among them: glycolytic and oxidative metabolism, mammalian target of rapamycin (mTOR), cell cycle, autophagy, and apoptosis (MIHAYLOVA; SHAW, 2011). The related tumoral suppressor activity of LKB1/AMPK consists of a cascade of signaling that influences important pathways and the interplays between these pathways is related to cancer hallmarks acquisition (CICCARESE; ZULATO; INDRACCOLO, 2019b).

A549 cells have a mutation on the first *STK11* exon, turning this cell line knockout for the canonical LKB1 by a premature terminal codon (PTC) insertion (LYKKE-ANDERSEN; JENSEN, 2015). A non-translated LKB1 transcript, containing the insertion of 131 nucleotides as a new exon between exons 1 and 2, was described in PJS (Peutz-Jeghers) syndrome patients (MASUDA et al., 2016). Recently, it was reported that the A549 cells present this transcript, and this alternative exon could function as an alternative start codon for a novel mitochondria-localized LKB1 variant (TAN et al., 2023). This new variant presents different functions in comparison with the canonical LKB1, while the mitochondria-localized LKB1 seems to regulate the redox balance in A549 cells, the canonical LKB1 through the AMPK activation regulates pathways related to metabolism and tumor suppression (ZHAO; XU, 2014).

Using the CRISPR/Cas9 system, we targeted *STK11* to generate cell lines with mutated LKB1, obtaining functional mRNA similar to the canonical isoform. Recently, was demonstrated by Tuladhar and collaborators that the insertion or deletion mutations (INDELs) by *Non-Homologous DNA Repair* (NHEJ) can produce mutated mRNAs, and proteins. Specifically, in the *STK11* gene edition, they generated after CRISPR a higher molecular weight isoform of LKB1 named Super LKB1, due to the +1/-2 INDELs, and the presence of alternative exon, however the functions of this isoform remain unclear (TULADHAR et al., 2019).

Thus, we aimed to edit the previous region of nonsense mutation (Q37*, also known as c.109C>T) in A549 cells, present in the canonical exon 1 (1a). The insertion of 1 nucleotide in the edition locus, generated a re-framed transcript with the alternative exon (1b), generating a higher molecular weight LKB1 isoform, akin to the approach employed by Tuladhar and collaborators. Comparing the A549 wild types to A549 LKB1 edited cells we explored some of the molecular pathways associated with LKB1/AMPK and highlight regulations in mTORC1, autophagy, and redox.

We found that A549 wild-type cells present low activation of AMPK due to the lack of LKB1, thus we observed a higher activation of ribosomal proteins kinases (S6K1 and S6K2) of the mTORC1 pathway. Furthermore, we observed autophagy dysfunction through sequestosomo-1 (p62) accumulation and low autophagy flux. This cellular

signaling profile is compatible with non-canonical activation of nuclear factor erythroid 2-related factor 2 (NRF2), once the accumulated p62 could interact with KEAP1, sequestering this protein in positive p62 autophagosomes, that is unable to fuse with lysosomes, leading to robust activation of NRF2 (SILVA-ISLAS; MALDONADO, 2018).

Hence, the regulation of metabolism through LKB1/AMPK appears to contribute significantly to an upsurge in autophagy flux and the inhibition of NRF2. Under these conditions, A549 LKB1 edited cells exhibited an enhanced response to cisplatin. We used metformin as a pharmacological stimulus of autophagy promoted by AMPK activation (BHARATH et al., 2020), and 3-Methyladenine (3-MA) as an autophagy inhibitor (DONG et al., 2019). This allowed us to assess the impact of autophagy in conjunction with cisplatin treatment. Consequently, we characterized the Super LKB1 isoform generated through CRISPR/Cas9, elucidating its influence on cellular metabolism and non-canonical NRF2 activation in A549 cells. Our findings position the Super LKB1 generated by CRISPR as a potential candidate for the development of anticancer treatments.

3.2 EXPERIMENTAL PROCEDURES

3.2.1 Cell culture.

A549 (human lung adenocarcinoma cell line) was cultivated in Ham's F12K (Sigma-Aldrich, #N3520) medium supplemented with 10% fetal bovine serum (FBS; Gibco, #12657029) and 1% penicillin/streptomycin (Gibco, #15140-122). HEK293T (human embryonic kidney cell line that expresses a mutant version of the SV40 large T antigen) was cultivated in Dulbecco's Modified Eagle Medium (Sigma-Aldrich, #D7777) supplemented with 10% fetal bovine serum and 1% penicillin/streptomycin. Cells were maintained at 37 °C in a humidified atmosphere containing 5% carbon dioxide.

3.2.2 *STK11* (LKB1) edition by CRISPR/Cas9

First, in Benchling software we imported the human *STK11* sequence and we added the Q37*, c.109C>T, that generate a premature termination codon (PTC) that is

present in A549, which was validated by Sanger sequencing. CRISPOR software was used to select a sequence for sgRNA adjacent to a PAM sequence (NGG) necessary for Cas9 activity (the sgRNA sequence is CCACCGCATCGACTCCACCG). The sgRNA was *in vitro* transcribed by EnGen sgRNA Synthesis Kit, *S. pyogenes* Kit (NEB #E3322V) following the manufacturer's instructions. The A549 cells were plated into a 6-well plate and, when a confluence of 70% was reached the cells were transfected with Lipofectamine CRISPRMAX (Invitrogen #CMAX00003), and EnGen Spy Cas9 NLS (Neb # M0646T), following the manufacturer's instruction. A group of cells transfected without sgRNA was used as a control of transfection. To analyze the editing efficiency of the system, we perform the T7 endonuclease (T7E1) assay in the cell populations. After 48h, cells were then isolated into 96-well plates by seeding cells at low density using serial dilutions. The resulting monoclonal cultures were screened by Western blotting for the LKB1 expression using an LKB1 antibody (Cell signaling #3050). To evaluate the INDELS generated by the CRISPR/Cas9 system, the targeted genomic region for LKB1 was amplified by PCR, the primer sequence is in Table 1, from genomic DNA and sequenced by Sanger sequencing.

Primer	Sequence
LKB1_genomic_F	TAGAACAATCGTTTCTGTTGAAGAAGGG
LKB1_genomic_R	CAGGGCATTTTAACTGGAGTCCAAGAG

- **Table1.** Primers used in PCR to amplify the genomic locus of edition by CRISPR/Cas9.

3.2.3 Western Blotting.

Protein extracts from A549 cells were obtained using a cell lysis buffer (50 mM Tris-Cl pH 7.5, 150 mM NaCl, 1 mM EDTA, 1% Triton X-100, protease, and phosphatase inhibitor cocktail), and samples containing 40 µg were separated by SDS-PAGE and transferred into nitrocellulose membranes (Bio-Rad Laboratories, Inc.).

Membranes were blocked in a solution of TBS-T (50 mM Tris-Cl, pH 7.5; 150 mM NaCl; 0.1% Tween-20) containing 5% of nonfat dry milk for 1h with constant agitation. The membranes were incubated with primary antibodies overnight at 4°C, washed 5 times with TBS-T, and incubated for 1h with secondary antibodies at room temperature, followed by washing 5 times with TBS-T. The membranes were incubated with Pierce ECL Western Blotting Substrate (Thermo Scientific, #32106) to visualize the protein band in ChemiDoc Imaging System (Bio-Rad Laboratories, Inc.), and densitometry was performed using ImageJ software v1.53. Primary antibodies: LKB1 (Cell signaling, #3050), pLKB1 (Cell signaling, #3482), AMPK (Cell signaling #5831), pAMPK (Cell signaling #50081), p62 (Cell signaling #50081), LC3B I/II (Cell signaling #2775), S6 (Cell signaling, #2317), pS6 (Cell signaling #9234), S6K1 (Cell signaling #5707), pS6k1 (Cell signaling #9234), S6K2 (Cell signaling #14130), pS6K2 (Invitrogen # PA5-105036), mTOR (Cell signaling #2972), pmTOR (Cell signaling #2971), GAPDH (Cell signaling #2118), E-cadherin (Cell signaling #3195), N-cadherin (Cell signaling #13116), β -Actin (Cell signaling #4970), NRF2 (Cell signaling #12721), KEAP1 (Cell signaling #4678), NQO1 (Cell signaling #3187), PRDX3 (Abcam #ab73349), BAK (Cell signaling #12105), BAX (Cell signaling #5023), BCL2 (Cell signaling #15071), FLAG (Cell signaling #14793), LDHA (Abcam #ab 52488), HK2 (Abcam #ab209847), H2B (Cell signaling #12364), Puromycin (Sigma-Aldrich, 12D10). Secondary antibodies: HRP-conjugated goat anti-mouse IgG (Sigma-Aldrich, AP308P, 1:2,000), goat anti-rabbit IgG (Sigma-Aldrich, AP307P, 1:5,000), and goat (Sigma-Aldrich, A5420, 1:5,000).

3.2.4 Immunofluorescence

A549 cells were fixed with 4% formaldehyde for 15 minutes at room temperature, permeabilized with methanol for 10 minutes at 4°C, then treated with blocking solution with 3% of BSA, 0.1% tween 20 in PBS 1x for 30 minutes at room temperature. Primary antibodies were added: LKB1 (Cell signaling, #3050), pLKB1 (Cell signaling, #3482), NRF2 (Cell signaling #12721), and γ H2AX (Cell signaling #9718) overnight at 4°C, washed 5 times with PBS 1x, and incubated with the secondary antibody anti-rabbit Alexa Fluor 594 (Invitrogen, A-11012). The cells were incubated with Hoechst diluted 1:10,000

in PBS 1x for 10 minutes for nuclei staining. Coverslips were finally mounted using Prolong (Invitrogen, #P36980).

3.2.5 Autophagy flux detection

The cells were transfected with ptfLC3 (Addgene #21074) using Lipofectamine (Thermo Scientific, #18324012), and PLUS reagent (Thermo Scientific, #11514015) following the manufacturer's instruction. After 48h, cells were fixed with 4% formaldehyde for 15 minutes at room temperature and washed 2 times with PBS 1x. The cells were incubated with Hoechst diluted 1:10,000 in PBS 1x for 10 minutes for nuclei staining. Coverslips were finally mounted using Prolong (Invitrogen, #P36980). The autophagy flux was measured through the ratio between red dots (RFP⁺) by green dots (GFP⁺).

3.2.6 Wound healing – Scratch assay

A549 cells were seeded at a density of 1×10^5 cells/well in a 24-well plate, until confluence. Cells were treated with mitomycin-C at 60 μ M for 2h. Cell monolayers were scratched by a p200 sterile pipette, washed with PBS 1x and incubated with Ham's F12K supply with 10% SFB and 1% P/S. The images were captured at 0, and 24 hours. The scratch area was analyzed under a light microscope (Optika Italy) and using Optika Proview software.

3.2.7 Colony formation assay

A549 cells were seeded into 60 mm dishes at a density of 5×10^2 cells/plate, incubated for 10 days at 37°C and stained with violet crystal solution (0.05% violet crystal w/v, 1% formaldehyde, 1% PBS, 1% methanol, and deionized water) for 20 minutes at room temperature. The violet crystal was eluted with isopropyl alcohol and the absorbance was measured in a spectrophotometer at 560 nm. The number and size of colony cells were manually quantified. Demonstrative images of the colonies were obtained under an optical microscope (Optika Italy) and using Optika Proview software.

3.2.8 Subcellular fractionation

From a p100 plate, 8×10^6 cells were collected, centrifuged at $500 \times g$ for 5 minutes, then washed with PBS 1x and again centrifuged at $500 \times g$ for 5 minutes. The cell pellet was resuspended in 100 μ L of CE buffer (10 mM HEPES, 60 mM KCl, 1 mM EDTA, 0,075% de NP40, 1 mM DTT, and protease inhibitor cocktail at pH 7,6), and the sample was incubated on ice for 3 minutes and then cells were centrifuged at $1.300 \times g$ for 45 minutes at 4°C. The supernatant constituted the cytoplasmic extract of the cells and the pellet is the nuclear extract. The supernatant (cytoplasm) was collected and the pellet was washed with 100 μ L of CE buffer without NP40 the nuclear extract was centrifuged at $1.000 \times g$ for 5 minutes and the supernatant was discarded, this procedure was repeated 4 more times. The nuclear pellet was resuspended in 100 μ L of NE buffer (20 mM Tris-HCl, 420 mM NaCl, 1,5 mM $MgCl_2$, 0,2 mM EDTA, 25% glycerol, and protease inhibitor cocktail at pH 8), and the sample was homogenized in the vortex for 1 minute.

3.2.9 DNA damage assay – detection of phosphorylated foci of H2AX

The cells were seeded similarly to the immunofluorescence assay. After 48h, the cells were incubated with 10 μ M of cisplatin (Sigma-Aldrich, PHR1624) or vehicle for the control group for 4h. The cells were washed with PBS 1x and incubated with Ham's F12K supply with 10% SFB and 1% P/S for 16h for H2AX foci formation. After, immunofluorescence protocol was performed as described.

3.2.10 MTT and IC₅₀

A549 cells were plated at a density of 8×10^3 cells/well, in 96-well plates. After 24h, the cells were incubated with cisplatin at 0, 1,25, 2,5, 5, 10, 20, and 40 μ M (Sigma-Aldrich, PHR1624) for 72h. The viability was measured by adding 10 μ L of 12 mM MTT (Invitrogen, M6494) to each well and incubating for 2 hours at 37°C. The formazan crystals were solubilized in HCl and isopropanol solution for 20 minutes at 37 °C. The

optical density was measured in a spectrophotometer at 570 nm. The IC₅₀ was determined by a non-linear regression on PRISM software.

3.2.11 H₂O₂ detection assay

For H₂O₂ detection the Amplex™ Red Hydrogen Peroxide/Peroxidase kit was used (Invitrogen - A22188) following the manufacturer's instructions.

3.2.12 OROBOROS Mitochondrial respiration

The cells were seeded into a p100 plate, and, after 72h, 2×10^6 cells were collected, washed with PBS 1x, and centrifuged at $500 \times g$ for 5 minutes. The pellet was resuspended on miR05 buffer (EGTA 0.5 mM, MgCl₂ 3 mM, 60 mM lactobionic acid, 1mg/mL bovine serum albumin free fatty acid, taurine 20 mM, KH₂PO₄ 10 mM, HEPES 20 mM, sucrose 110 mM at pH 7.1). The oxygen consumption rate (OCR) measurement was taken at basal conditions, 1 mM oligomycin, 1 mM FCCP in OROBOROS equipment (NextGen O2k).

3.2.13 PCR, RTqPCR, and LKB1 cloning

Total RNA was extracted from A549 cells using TRIzol (Thermo Fisher Scientific, #15596026). The High-Capacity cDNA Reverse transcription kit (Thermo Fisher Scientific, #4368814) was used to synthesize the cDNA. iTaq Universal SYBR Green Super Mix (Bio-rad #10000068167) was used following the manufacturer's instruction to perform Real-time quantitative Polymerase Chain Reaction (RTqPCR). The Gene expression was analyzed by the formula: $2^{-\Delta\Delta C_t}$, described by Livak in 1997, using β -actin as a housekeeping gene. Samples, in triplicate, were arranged in a 96-well plate (MicroAmp, Applied Biosystems, #4306737) for amplification and were run in the Step One Plus Real-Time PCR System (Applied Biosystems). The primer sequences used for RT-qPCR are presented in Supporting Figure 7A – Table 1.

The Coding DNA Sequence (CDS) of canonical LKB1 was amplified with Platinum Taq DNA Polymerase (Invitrogen, #10966018) following the manufacturer's instruction. The PCR product was purified with the PureLink PCR Purification Kit (ThermoFisher Scientific, #K310001). The cDNA of HEK293T cells was used as a template for canonical LKB1 cloning, the primer sequences for LKB1 cloning are in Table 2. For PCR the High-Fidelity DNA Polymerase (NEB, #M0491S), was used following the manufacturer's instructions. PCR product was cloned into a pGEM T easy vector (Promega, A1360), digested with *EcoR1*, and *Xho1*, purified with the PureLink PCR Purification Kit and then ligated into a pcDNA-FLAG.

Primer	Sequence
β -Actin qPCR Human F	GCCGCCAGCTCACCAT
β -Actin qPCR Human R	CCACGATGGAGGGGAAGAC
NQO1	AGGACCCTTCCGGAGTAAGA
NQO1	TGGAGATGTGCCCAATGCTAT
SOD1	GTTTCCGTTGCAGTCCTCG
SOD1	GGTCCATTACTTTCCTTCTGCTC
SOD2	AAGGAACGGGGACACTTACAAA
SOD2	AGCAGTGGAATAAGGCCTGTTG
LKB1_cDNA_F_ <i>EcoR1</i>	AAAGAATTCAATGGAGGTGGTGGACCCGCA
LKB1_cDNA_R_ <i>Xho1</i>	AACTCGAGTCACTGCTGCTTGCAGGCCG

- **Table 2.** Primers used in the RTqPCR experiments, and the primers used to amplify the canonical LKB1 CDS, that was cloned to overexpression.

3.2.14 Bioinformatic analysis

The Benchling web server was used to align the DNA sequence, the DECODR web server was used to decompose the Sanger sequencing, the Expasy web server was used to translate the DNA sequence into an amino acid sequence, and the Clustal Omega was used to align the amino acid sequences of the A549 wild-type clones (cWT), and the clone 2 Super LKB1 + (c2SL+) cell line.

The AlphaFold Protein Structure Database was used to predict the protein structure of LKB1 CRISPR isoform, the RCSB Protein Data Bank was used to import the canonical LKB1 sequence, and the PyMOL software was used to visualize the proteins.

The TargetP2.0 and MULocDeep web servers were used to predict the localization of the isoforms. The String web server was used to generate the protein-protein interaction net of the LKB1, and the ClusPro protein-protein docking was used to demonstrate the interaction between AMPK and the LKB1 isoforms canonical, and CRISPR.

3.2.15 Proliferation curve assay

The A549 cells were plated into a 6-well plate at a density of 1×10^4 cells and manually counted with trypan blue exclusion for 72h.

3.2.16 Anti-FLAG immunoprecipitation

HEK293T cells seeded into a p100 after were transfected with pFLAG-GFP and pFLAG-KEAP1 with Lipofectamine following the manufacturer's instruction. After 48h, the cells were incubated with 10 mM metformin (D150959), 200 μ M 3-MA (914363), or a vehicle for the control group for 24h. Protein was collected, 40 μ g was used as input, and the remaining protein extract was incubated with 50 μ L of washed anti-FLAG resin (Millipore, #A4596), per group overnight. After the samples were centrifuged $8,200 \times g$ for 1 minute, the beads were washed 5 times with TBS (50 mM Tris-Cl, pH 7.5; 150 mM

NaCl). Finally, the beads were denatured with Laemmli buffer with 10% of β -Mercaptoethanol (Thermo Scientific, #21985023), followed by a Western Blotting assay.

3.2.17 Pharmacological treatments (Cisplatin, Metformin, 3-MA, and Puromycin)

For viability, anti-FLAG immunoprecipitation, and H₂O₂ A549 cells were treated with 10 μ M cisplatin, 10 mM metformin, and 200 μ M 3-MA for 72 hours. For SUnSET A549 cells were treated with 1 μ M puromycin for 30 minutes, and the protein was extracted from cells as described in the Western blotting section.

3.2.18 Statistical analysis of data

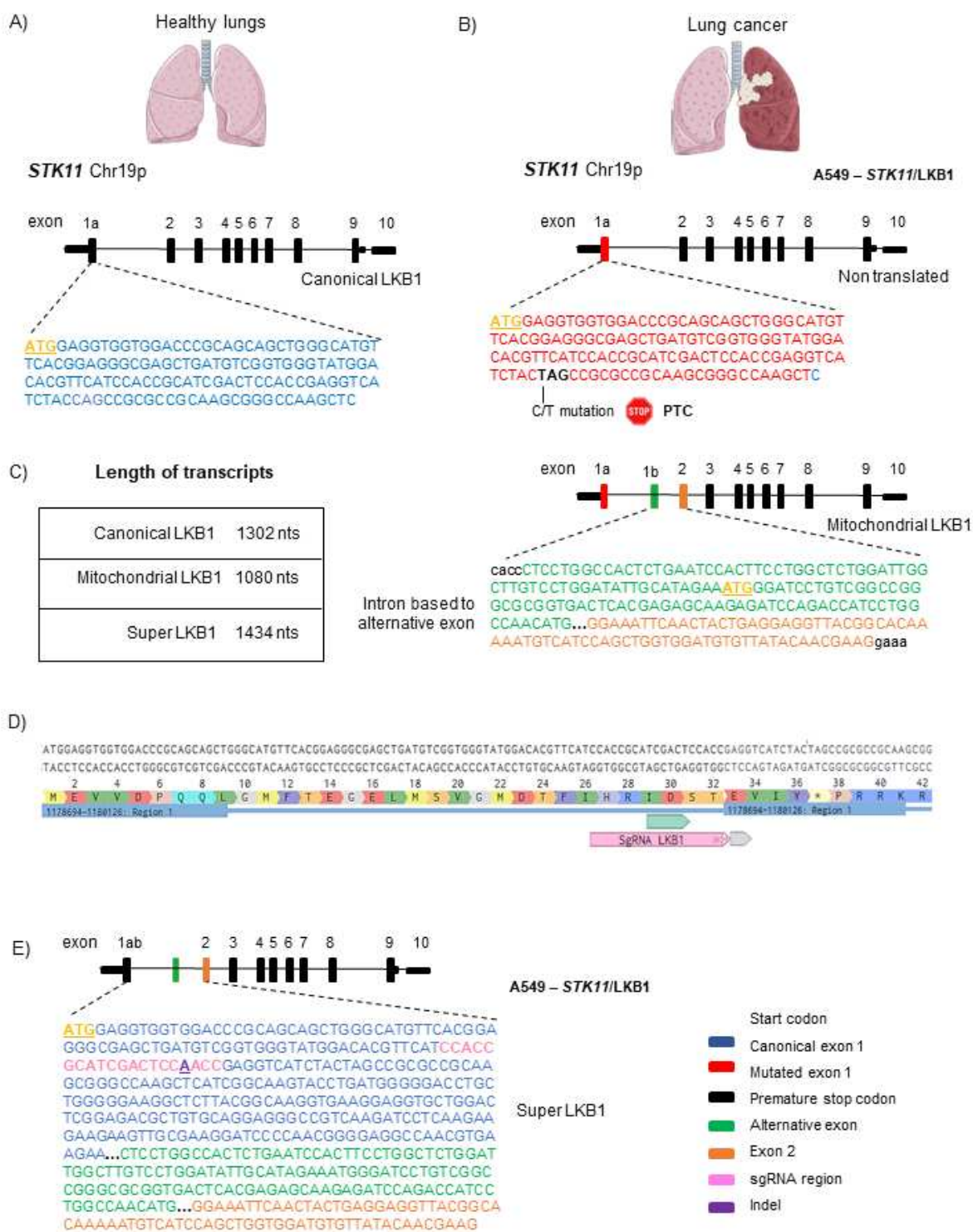
Statistical analysis was performed using GraphPad Prism 8.01 software (<https://www.graphpad.com/>) and all data were expressed as Mean and Standard Deviation. The difference between means was tested by Student's T-Test, One-way or Two-way ANOVA, followed by Post Hoc of Tukey and Dunnet, in which * $p < 0.05$, ** $p < 0.01$, *** $p < 0.001$, and **** $p < 0.0001$ was considered significant.

3.3 RESULTS

3.3.1 The *STK11* gene edition in A549 cells by CRISPR/Cas9 generated a higher molecular weight LKB1, through the INDELS and alternative exon.

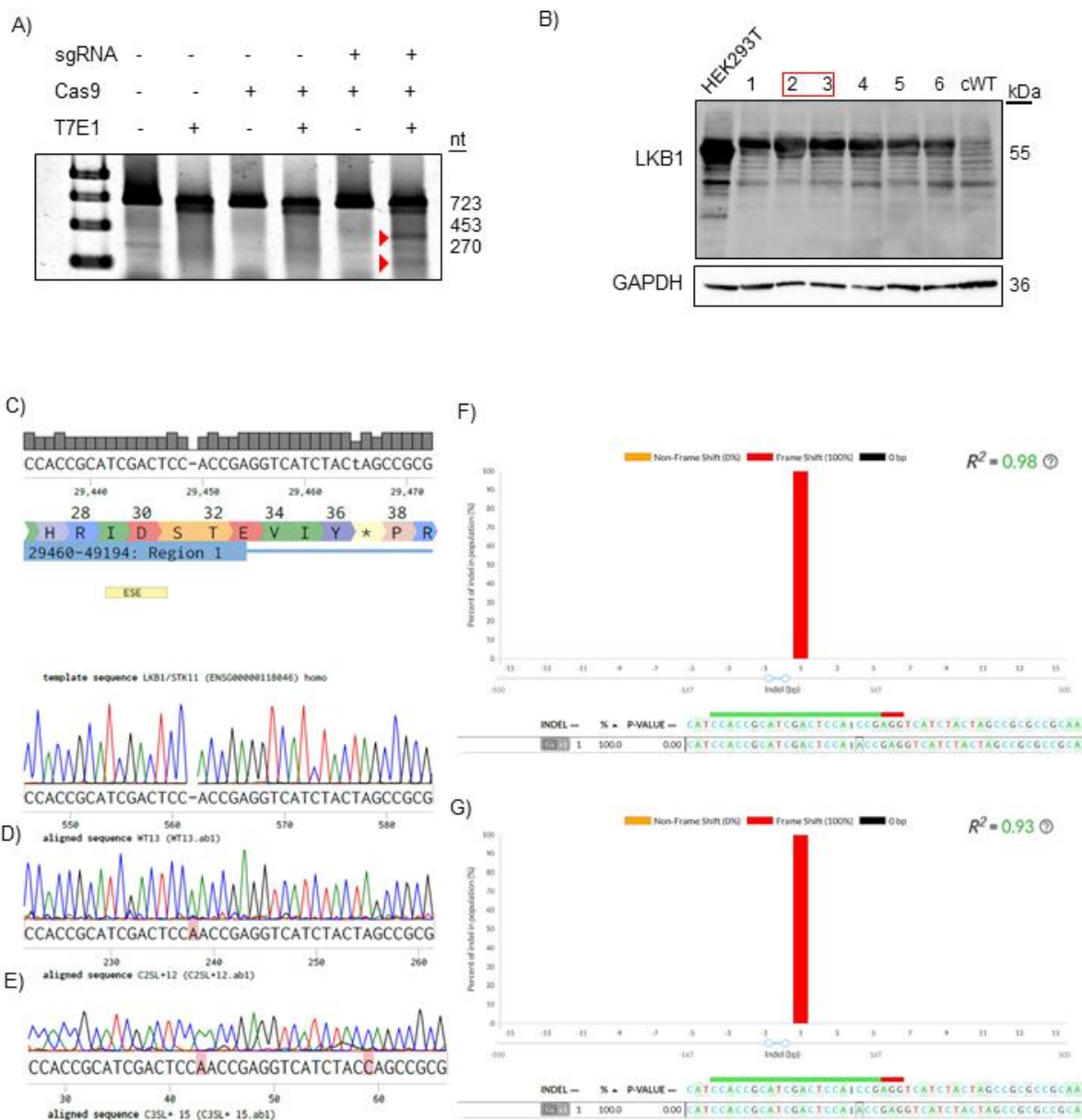
First, it was compared *STK11* variants expression in healthy lungs (Figure S1A) versus lung cancer represented by A549 cells (Figure S1B), indicating the mutation Q37*, c.109C>T in lung cancer and the presence of a mitochondrial LKB1 isoform generated by alternative splicing, as described by Tan et al. (2023). The length of the transcripts (Figure S1C), and a scheme of edition we designed for the first exon of *STK11* in A549 (Figure S1D) was also showed. At last, we present the scheme of the Super LKB1,

generated in our experiments by an INDEL and the alternative exon incorporation (Figure S1E).



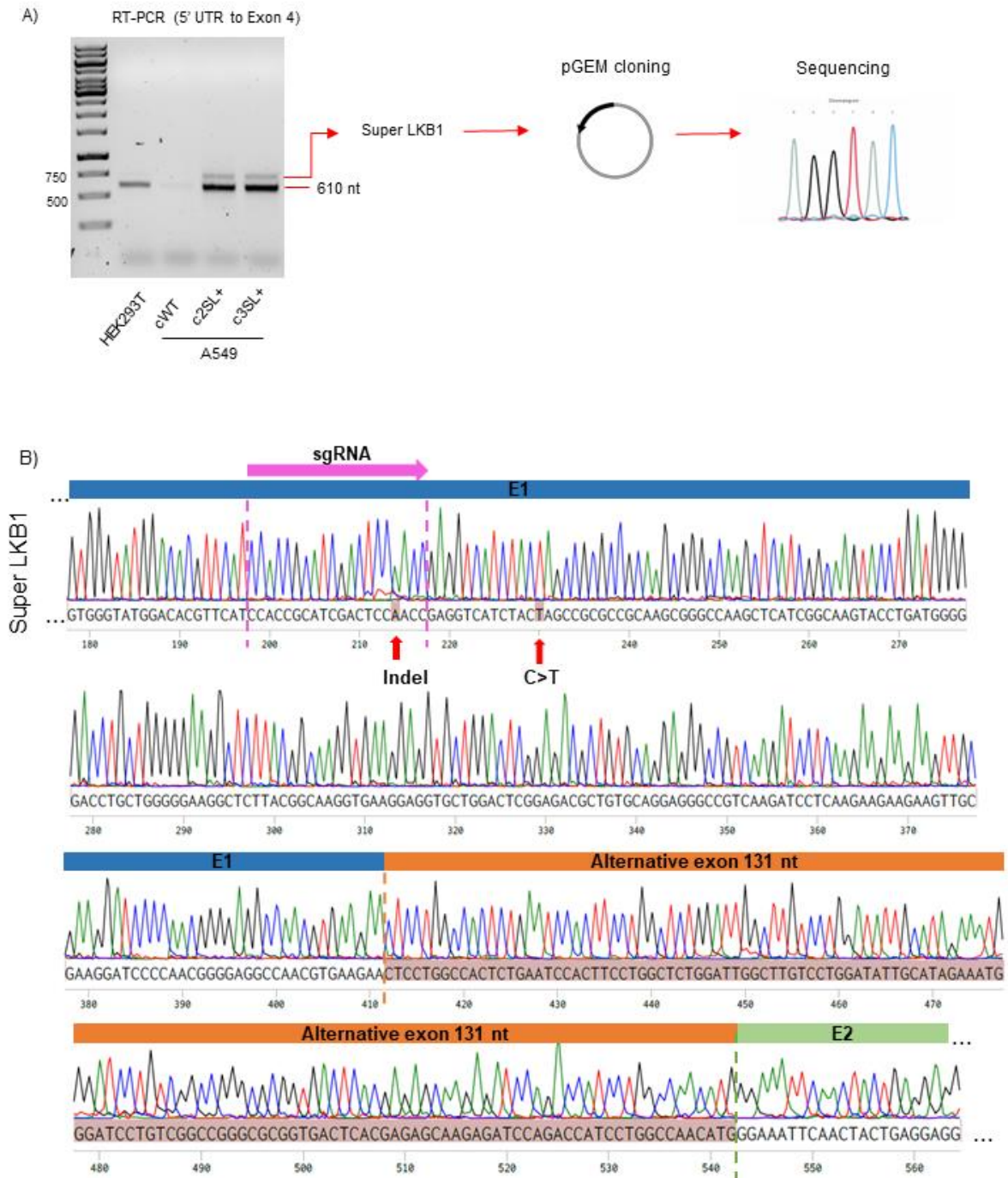
Support information Figure 1. Super LKB1 scheme, generated by CRISPR/Cas9 edition in A549 cells. (A) Scheme of the *STK11* gene in healthy lungs; (B) Scheme of the *STK11* gene in lung cancer represented by A549 NSCLC; (C) Table with the length of LKB1 transcripts: canonical, mitochondrial, and Super LKB1; (D) Scheme of CRISPR/Cas9 edition in the first exon of *STK11* gene, highlighting the sgRNA sequence; (E) Scheme of Super LKB1 generated in the A549 cells, and the color legend of the figure.

To evaluate the efficiency of the edition by CRISPR/Cas9, the PCR product of the *STK11* genomic locus of edition was digested with T7E1, it was demonstrated that the sgRNA/Cas9 group was positive for INDELS (Figure S2A). After clone selection, one wild type clone was named cWT, and two clones with LKB1 expression were named clone Super LKB1: c2SL+, and c3SL+, since these clones presented a higher molecular weight band compared to a positive control (HEK293T), (Figure S2B). The locus of the edition was sequenced from gDNA, and aligned against cWT (Figure S2C). Both clones c2SL+ and c3SL+ presented the same adenine (A) insertion (Figure S2D and S2E). Chromatograms were decomposed to evaluate the INDELS, confirming the adenine insertion in both edited clones (Figure S2F and S2G).



Support information Figure 2. The +1 adenine insertion, is part of higher molecular weight LKB1, the Super LKB1. (A) PCR of gRNA from A549 cells transfected with Cas9 or Cas9/sgRNA, followed by T7E1 digestion. Primers for LKB1 genomic DNA were used to amplify the Cas9 target locus of edition. **(B)** Western blotting of LKB1 and GAPDH in HEK293T cells was used as a positive control and A549 edited lineages were generated through isolated clones. **(C)** The sequence of Human STK11 imported in the Benching software **(D)** Sanger sequencing of the C2SL+ edited cell line aligned against the cWT sequence, with highlights in the INDEL. **(E)** Sanger sequencing of the C3SL+ edited cell line aligned against the cWT sequence, with highlights in the INDEL. **(F)** C2SL+ Chromatogram decomposition by DECODR software. **(G)** C3SL+ Chromatogram decomposition by DECODR software.

To evaluate if the higher molecular weight band of LKB1 detected in western blotting (Fig S2B) of the c2SL+, and c3SL+ clones presented the alternative exon (131 nts) already described by Tuladhar et al (2019), and Tan et al (2023) in frame with the INDEL, +1 adenine insertio, RNA extraction was performed followed by cDNA synthesis and PCR of 5'UTR region to the exon 4. A higher molecular weight transcript can be observed specifically in the edited clones (Figure S3A), this band was cloned into a pGEM-T easy vector and sequenced. The sequence showed the presence of the INDEL, +1 adenine insertion, followed by the A549 mutation (Q37*; 109C>T) highlighted in red, and the alternative exon between exons 1 and 2 (Figure S3B).



Support information Figure 3. The alternative exon re-frame with the INDEL in the Super LKB1. (A) Reverse transcription followed by PCR of HEK293T cells, cWT (A549), C2SL+ (A549), and C3SL+ (A549) RNA. 5' UTR to exon 4 primers were used. The upper band was cloned into pGEM-T easy vector (B) Sequencing of the upper band showing the +1 adenine insertion, and the alternative exon in frame with the exon 2.

After confirming the sequence of the edited transcript, it was designed the full amino acids sequence of the Super LKB1 that was submitted in the Clutal Omega. The Super LKB1 exhibits a comprehensive translation amino acid sequence devoid of premature termination codons (PTCs). In our alignment of amino acid sequences between WT LKB1 and Super LKB1 (Figure S4A), a resemblance in the N-terminal regions of the proteins was observed. Notably, from the INDEL regions onward, a distinct sequence emerged in Super LKB1 compared to WT, featuring an additional 44 amino acids. Subsequently, from exon 2 to the terminus of the C-terminal region, the amino acid sequences of the isoforms remained identical.

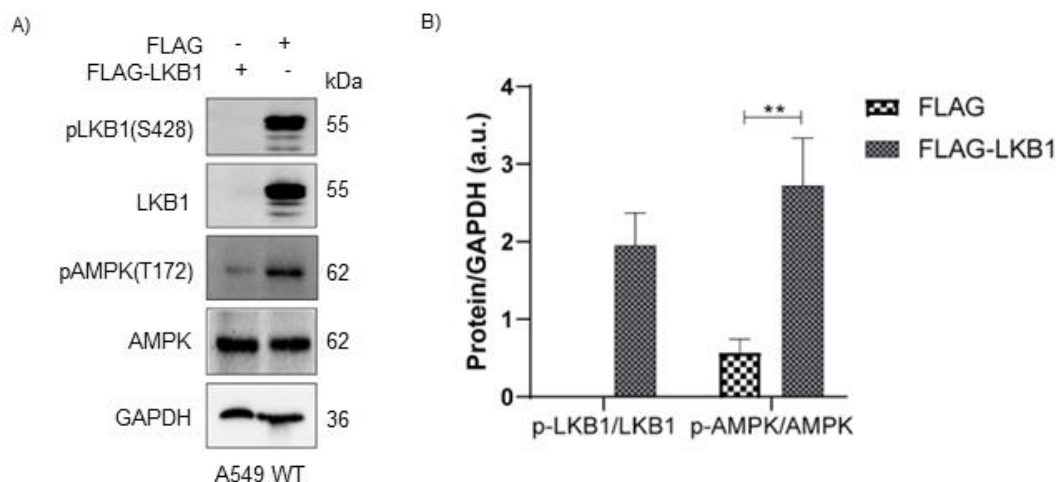
It was also modeled the canonical LKB1 (Figure S4B), and Super LKB1 (Figure S4C) isoforms with AlphaFold software, an artificial intelligence to predict biological structures, to evaluate the differences between the isoforms it was aligned the amino acids structures in PyMOL software. The Super LKB1 presents an additional loop (highlighted in the image), probably due to the new sequence in the Super LKB1, in comparison with canonical LKB1 (Figure S4D).

Finally, we employed TargetP 2.0 software to predict the localization of the isoforms, focusing on the potential mitochondrial transient peptide (mTP). Both the canonical and Super LKB1 isoforms exhibited a higher probability of localization outside the mitochondria, in contrast to the recently documented mitochondrial LKB1 by TAN et al, 2023. Intriguingly, the mitochondrial LKB1 displayed a tenfold higher likelihood of possessing a mitochondrial localization (Figure S4E). Additionally, MULocDeep software concurred in predicting a similar localization for the canonical and Super LKB1 isoforms (Nucleus/Cytoplasm), aligning with the cytoplasmic localization of the mitochondrial LKB1 (Figure S4F).

the alternative exon are highlighted. **(B)** Structural modeling of canonical LKB1 by Alpha Fold software. **(C)** Structural modeling of CRISPR LKB1 isoform by Alpha Fold software. **(D)** Amino acid sequences alignment of the canonical, and the CRISPR LKB1 isoform modeling in the PyMOL software. **(E)** Prediction of protein localization by TargetP 2.0. software **(F)** Prediction of protein localization by MULocDeep software

3.3.2 LKB1 overexpression enhances AMPK phosphorylation at 173 Threonine residue.

According with SHAW et al., 2004a LKB1 interact and activate AMPK, to demonstrate this activation it was constructed a canonical LKB1 vector named pFLAG-LKB1 for LKB1 overexpression (Figure S5) (Figure S5B). It was observed that the A549 WT cells transfected with the pFLAG-LKB1 vector presented a higher AMPK phosphorylation in 172 Threonine compared to the FLAG transfection group (FLAG vs FLAG-LKB1^{**}; ^{**}p<0.01).



Support information Figure 5. LKB1 overexpression in increase the 172 Threonine phosphorylation of AMPK in A549 WT cells. **(A)** Western Blotting of LKB1, pLKB1 (S428), pAMPK (T172), AMPK, and GAPDH in A549 WT cells. The cells were transfected with empty pFLAG vector or pFLAG-LKB1 vector; **(B)** Normalized levels of proteins by GAPDH (a.u). Data are presented as mean \pm standard deviation (SD). Statistical analysis has been performed by T-student's test ^{**}p<0.01. This data is representative of one independent experiment.

After examining the edited cell lines, we initially conducted optical microscopy imaging of the cells 24 hours post-seeding (Figure 1A). Subsequently, it was performed

protein expression analysis on all edited cells to investigate whether Super LKB1 could enhance AMPK activation through phosphorylation at Threonine 172. It was observed elevated molecular weight protein bands corresponding to LKB1 and phospho-LKB1 at Serine 428. All edited clones exhibited increased AMPK phosphorylation at the Threonine 172 residue (c2SL+ vs cWT**, c3SL+ vs cWT**) (Figure 1BC; ** $p < 0.01$). Furthermore, we assessed the localization of LKB1 and phospho-LKB1 (S428) through confocal fluorescence microscopy. In the edited cells, both LKB1 and pLKB1 appeared predominantly localized in the cytoplasm, with some nuclear signal detected in phospho-LKB1. Conversely, WT cells displayed no antibody staining (Figure 1DE).

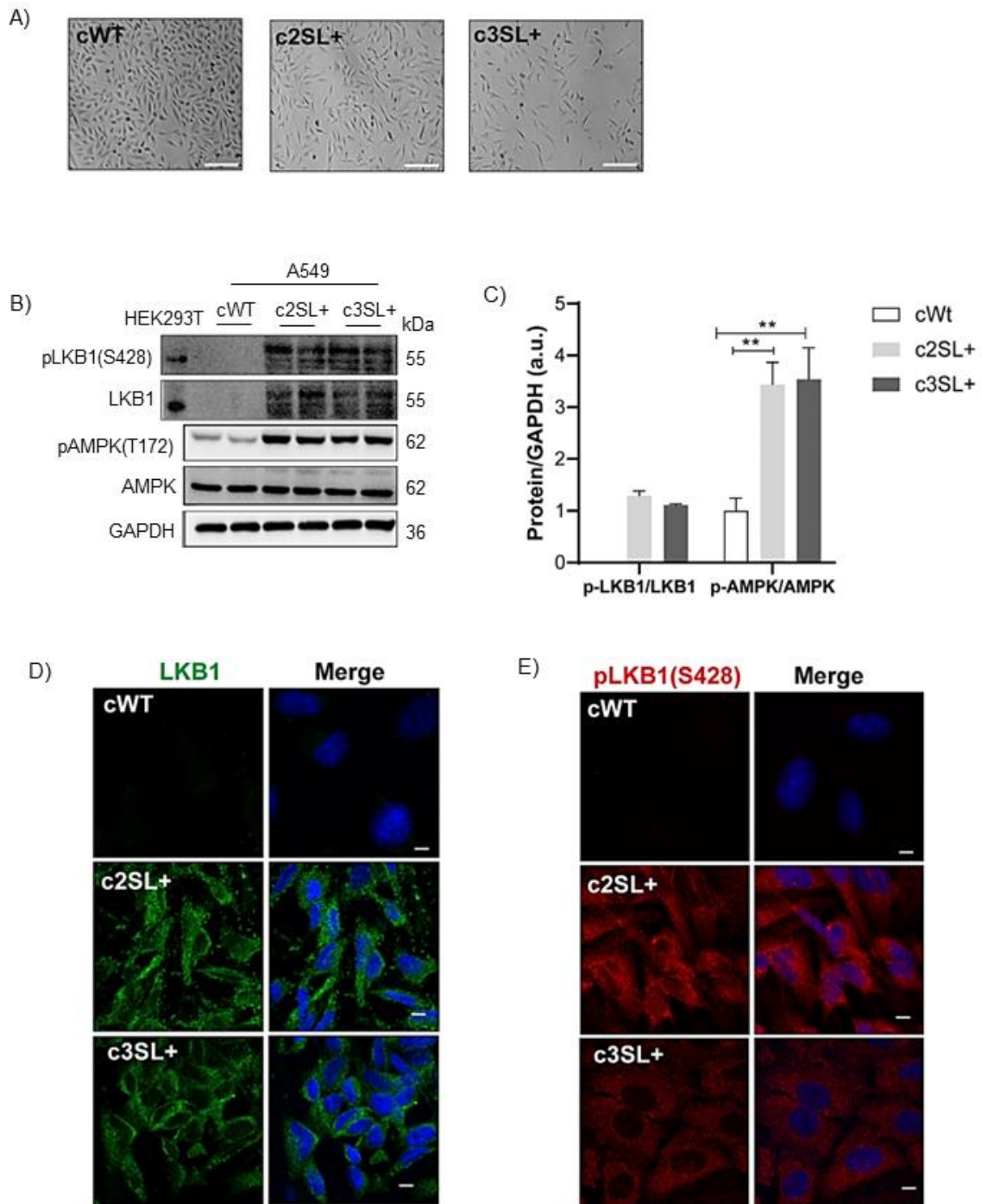
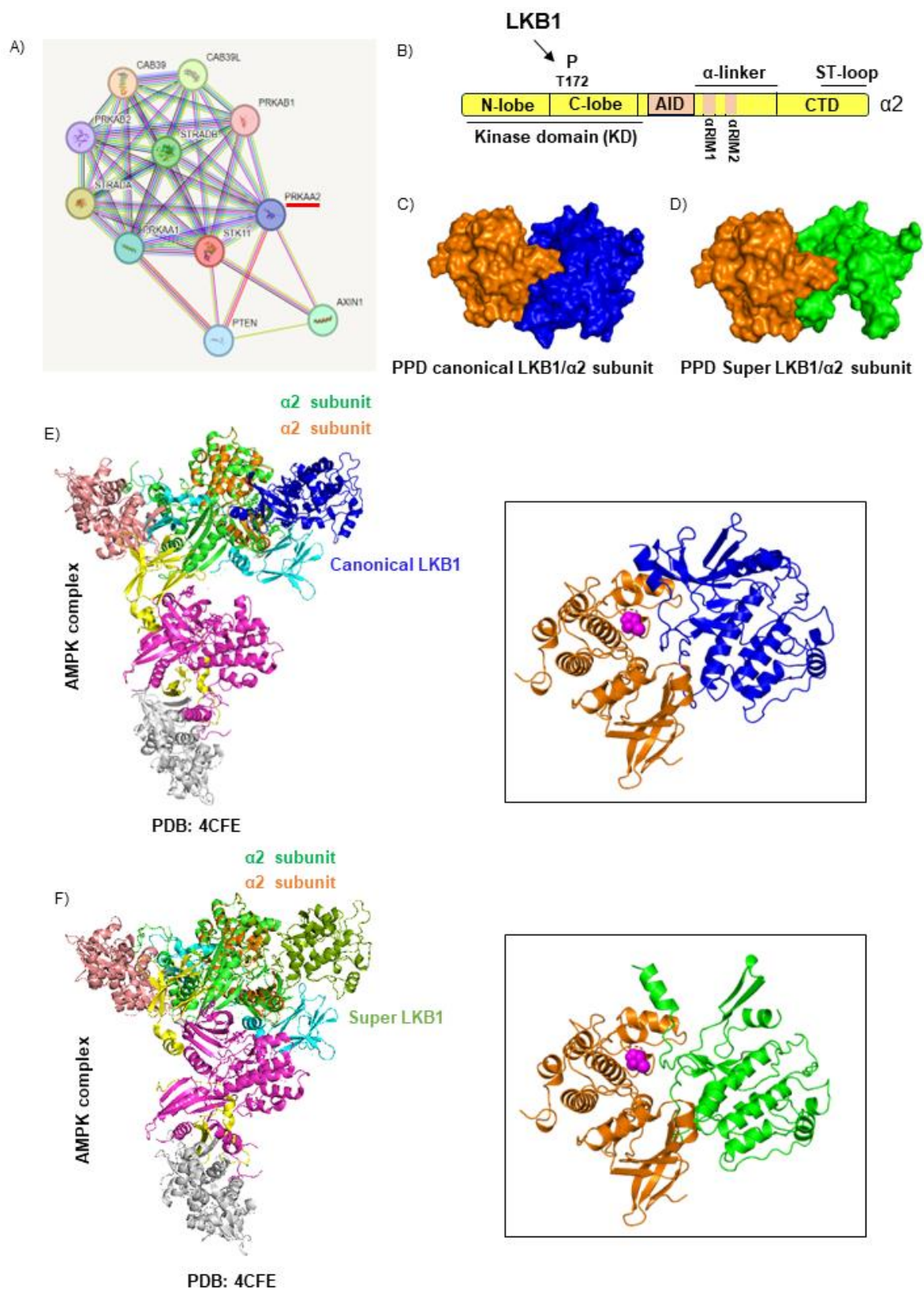


Figure 1. Super LKB1 enhance the AMPK activation through the 172 threonine phosphorylation . (A) Optical microscopy photos of cell lines; (B) Western Blotting of pLKB1 (S428), LKB1, pAMPK (T172), AMPK, and GAPDH in HEK293T used as an LKB1 positive control, cWT, c2SL+, and c3SL+ cells; (C) Normalized levels of proteins by GAPDH (a.u); (D) Immunofluorescence of LKB1 in cWT, c2SL+, and c3SL+ cells; (E) Immunofluorescence of pLKB1 (S428) in cWT, c2SL+, and c3SL+ cells. Data are presented as mean \pm standard deviation (SD). Statistical

analysis has been performed by ANOVA followed by Dunnet's test * $p < 0.05$, ** $p < 0.01$. These data are representative of two independent experiments.

To validate the interaction of the Super LKB1 it was analyzed the protein-protein interaction network by STRING (Figure S5A). As described, LKB1 presents interactions with four AMPK subunits, AMPK is a heterotrimer complex composed of α catalytic subunit, β , and γ regulatory subunits. In the interaction network, the $\alpha 2$ (*PRKAA2*) subunit is highlighted since the 172 Threonine residue in the C-lobe Kinase Domain is phosphorylated by LKB1 (Figure S5B).

To elucidate the potential interactions between the LKB1 isoforms and the AMPK $\alpha 2$ subunit, we initially identified and extract low-confidence regions in the canonical LKB1, Super LKB1, and AMPK $\alpha 2$ subunit proteins through b-factor coloring. These high confident regions were then subjected to protein-protein docking (PPD) using ClusPro. The output files from ClusPro, considering electrostatics and clustering to predict the most plausible interactions, were further analyzed. Among the top 10 structures generated by ClusPro, we aligned the portion of the AMPK $\alpha 2$ subunit docking with the AMPK complex (PDB: 4CFE). This alignment facilitated the identification of dockings that did not overlap with the regulatory subunits of the AMPK complex, as such overlap might pose a physical impediment to interaction. The selected protein-protein dockings were visualized in surface view using PyMOL for both canonical LKB1 (Figure S5A) and the CRISPR LKB1 isoform (Figure S5B) to enhance the clarity of the interaction. Specifically, we presented the docking of canonical LKB1 aligned with the AMPK complex (Figure S5E), and AMPK $\alpha 2$ subunit, highlighting the 172 Threonine residue. Similarly, the docking of Super LKB1 aligned with the AMPK complex was illustrated (Figure S5F), along with the interaction of Super LKB1 with the AMPK $\alpha 2$ subunit, emphasizing the 172 Threonine residue. The interactions between the LKB1 isoforms and the AMPK $\alpha 2$ subunit were found to be closer.



Support information Figure 6. The canonical LKB1, and Super LKB1 interacts similarity with the catalytic AMPK $\alpha 2$ subunit. (A) Protein-protein interaction network (PPI) by String software with highlight in the PRKAA2 the catalytic subunit of AMPK in human samples. (B) Scheme of PRKAA2 ($\alpha 2$ subunit), showing the kinase domain, and the 172-Threonine residue that is phosphorylated by LKB1. (C) Structure alignment of $\alpha 2$ subunit against the AMPK complex. (D) Protein-protein docking of canonical LKB1 and $\alpha 2$ AMPK subunit generated with ClusPro software. (E) Protein-protein docking of CRISPR-LKB1 isoform and $\alpha 2$ AMPK subunit generated with ClusPro software. (F) Structure alignment of Canonical LKB1, and CRISPR-LKB1 isoform in docking with $\alpha 2$ AMPK subunit in the PyMOL software.

3.3.3 Super LKB1 affects the epithelium mesenchymal transition (EMT), survival, and migration of A549 cells.

The EMT is a process in which the cells lose polarity and is associated with regulations in cell-cell adhesion proteins. The mesenchymal morphology of cancer cells is linked to the increase in migration and metastasis (PASTUSHENKO; BLANPAIN, 2019). Since LKB1 participates in cell morphologies contributing to the maintenance of the epithelium morphology, we looked at EMT markers. In SL+ cell lines, the expression of epithelium cadherin (E-cadherin) was higher compared to the WT cell line (c2SL+ vs cWT**, c3SL+ vs cWT**) (Figure 2AB; ** $p < 0.01$). On the other hand, mesenchymal cadherin (N-cadherin) expression was higher in WT cell line (c2SL+ vs cWT**, c3SL+ vs cWT**) (Figure 2AB; ** $p < 0.01$). The migration capacity was measured by scratch assay, after inhibiting the cell cycle with Mytomycin C. A lower rate of scratch closure of edited cells was observed in 24 hours (c2SL+ vs cWT**, c3SL+ vs cWT**) (Figure 2CD; ** $p < 0.01$). The clonogenic and survival potential of cells was determined by colony formation assay and the edited cells presented a reduction in both parameters (Figure 2EFGH). The quantifications used were: colony number (c2SL+ vs cWT***, c3SL+ vs cWT***) (Figure 2F; *** $p < 0.001$). ; colony area (c2SL+ vs cWT**, c3SL+ vs cWT**) (Figure 2G; ** $p < 0.01$), and absorbance of Violet Crystal incorporated in colonies (c2SL+ vs cWT***, c3SL+ vs cWT***) (Figure 2H; *** $p < 0.001$).

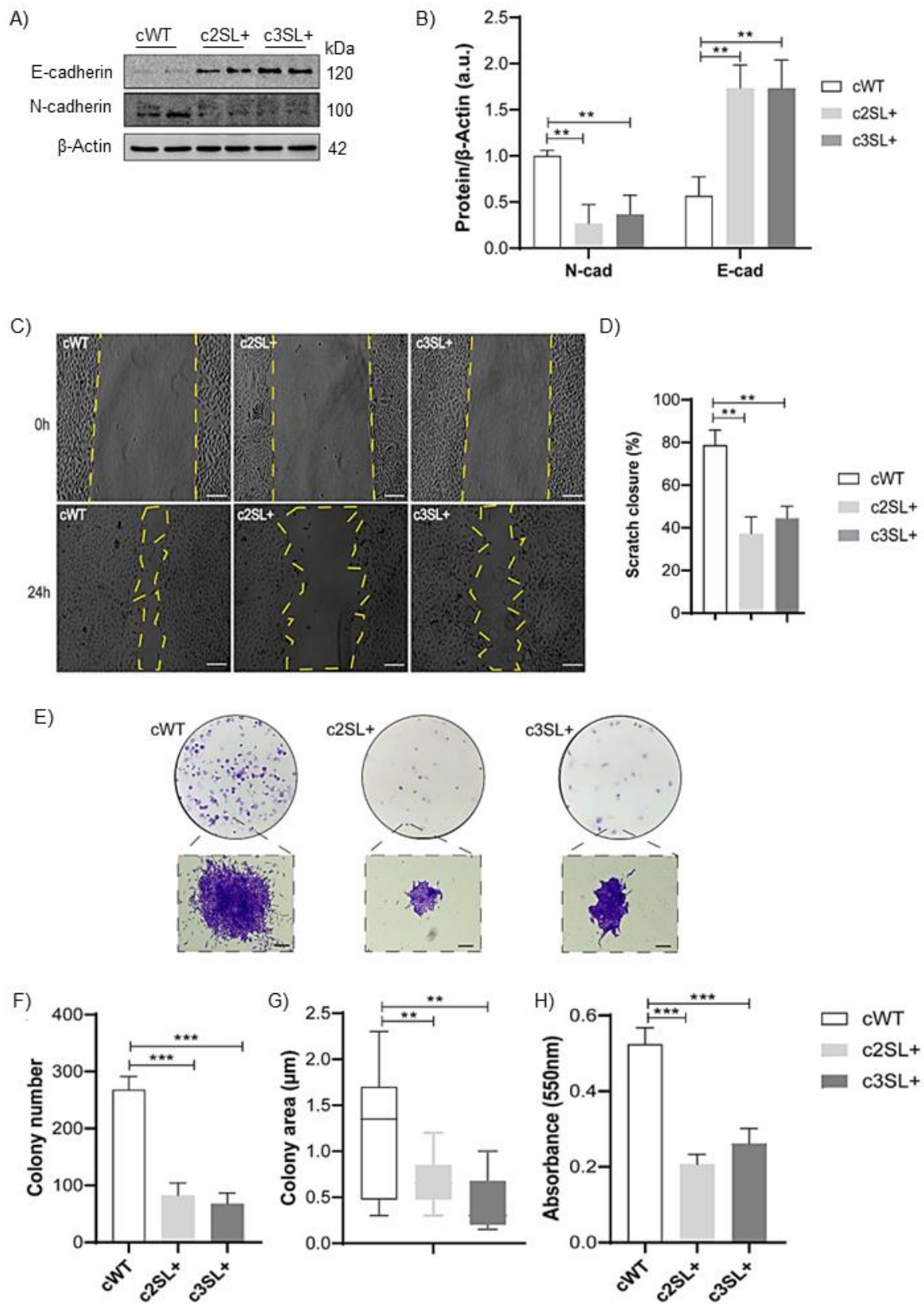


Figure 2. Super LKB1 affects the epithelium mesenchymal transition (EMT), survival, and migration in A549 edited cells. (A) Western Blotting of E-cadherin, N-cadherin, and β -Actin in cWT, c2SL+, and c3SL+ cells; (B) Normalized levels of proteins by β -Actin (a.u); (C) Scratch assay of cWT, c2SL+, and c3SL+ cells treated with 60 μ M of Mytomicin C for 2 hours; (D) Quantification of scratch area after 24 hours of scratch in percentage; (E) Colony formation of cWT, c2SL+, and c3SL+; (F) Quantification of colony number in cWT, c2SL+, and c3SL+; (G) Colony area (μ m) in cWT, c2SL+, and c3SL+; (H) Total absorbance of violet crystal of cWT, c2SL+, and c3SL+ cells colonies. Data are presented as mean \pm standard deviation (SD). Statistical analysis has been performed by ANOVA followed by Dunnet's test * p <0.05, ** p <0.01, *** p <0.001. These data are representative of two independent experiments.

3.3.4 Super LKB1 enhances oxidative metabolism in A549 edited cells.

Since AMPK is a central protein regulating cellular metabolism (GARCIA; SHAW, 2017), it was checked some metabolic parameters of A549 edited cells. The HK2 and LDHA proteins, associated with glycolytic metabolism, were analyzed and the HK2 expression was decreased in SL+ A549 cells compared to WT cells (cWT vs c2SL+*, cWT vs c3SL+**) (Figure 3AB; * p <0.05, ** p <0.01). We also measured the expression of the Mitochondrial Oxidative Phosphorylation System (OXPHOS), which is associated with oxidative metabolism. The A549 edited cells presented a higher expression of the OXPHOS, as highlighted by the complexes 1, referent NADH dehydrogenase [ubiquinone] 1 subcomplex beta subunit 8, (c2SL+ vs cWT*, c3SL+ vs cWT*) (Figure 3CD; * p <0,05), and 5, referent to ATP-synthase 5A (c2SL+ vs cWT*, c3SL+ vs cWT*) (Figure 3CD; * p <0,05). Therefore, in response to the metabolism change, we performed Oroboros analysis as a functional experiment, evaluating the ratio of oxygen consumption of the cells. An increase in O₂ consumption of SL+ cells in comparison with WT cells in basal condition was observed (c2SL+ vs cWT*, c3SL+ vs cWT**) (Figure 3EF, * p <0.05; ** p <0.01) and also the challenge for maximum respiration (FCCP) (c2SL+ vs cWT**, c3SL+ vs cWT***) (Figure 3EF; ** p <0.01, *** p <0.001).

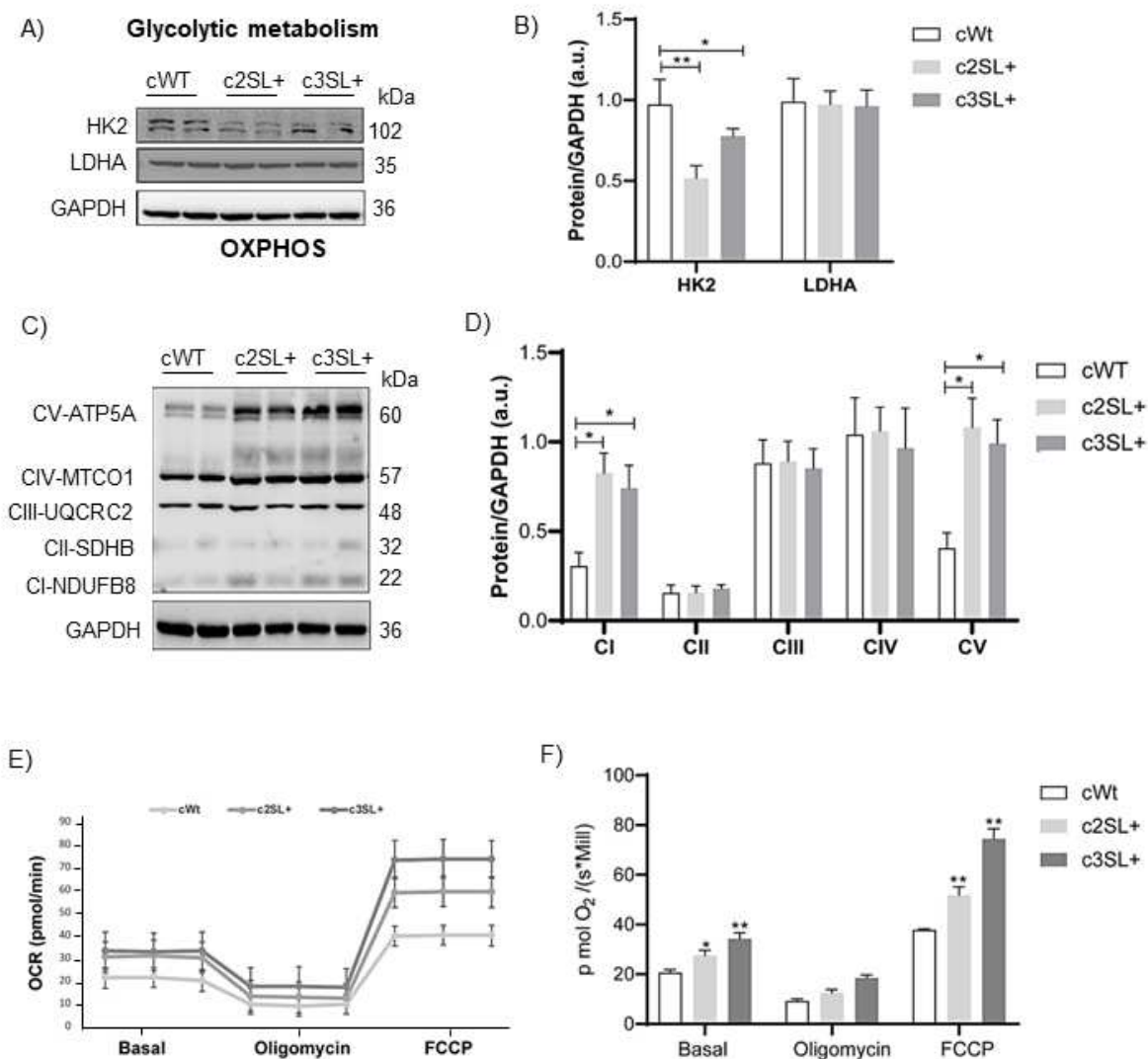


Figure 3. Super LKB1 enhances the oxidative metabolism in A549 edited cells. (A) Western Blotting of HK2, LDHA, and GAPDH in cWT, c2SL+, and c3SL+ cells; (B) Normalized levels of proteins by GAPDH (a.u.); (C) Western Blotting of OXPHOS, and GAPDH in cWT, c2SL+, and c3SL+ cells. (D) Normalized levels of Proteins by GAPDH (a.u.); (E) Oxygen Consumption Rate (OCR) by OROBORUS in cWT, c2SL+, and c3SL+ cells; (F) Comparison levels of O₂ in the cell lines in the basal condition, and after treatments with Oligomycin and FCCP. Data are presented as mean \pm standard deviation (SD). Statistical analysis has been performed by ANOVA followed by Dunnet's test * $p < 0.05$, ** $p < 0.01$. These data are representative of two independent experiments.

3.3.5 The expression of Super LKB1 in edited A549 cells led to the inhibition in mTORC1 and increase of autophagy signaling.

Since AMPK can simultaneously activate the Tuberous Sclerosis Proteins 1/2 (TSC1/2), which forms a protein complex that inhibits the Rheb GTPase, an activator of mTORC1 (KIM et al., 2011b), and ULK1 protein, which is a known activator of autophagy (PUUSTINEN et al., 2020). It was evaluated the mTORC1 and autophagy pathways in cells expressing the Super LKB1 protein. For mTORC1, edited cells presented a reduction in the activation of mTORC1 downstream targets: phospho-S6K2 Serine 423 (cWT vs c2SL+*, cWT vs c3SL+*) (Figure 4AB; *p>0.05) and phospho-S6 Serine 240/244 (cWT vs c2SL+**, cWT vs c3SL+*) (Figure 4AB; *p<0,05, **p<0,01). Since the activation of mTORC1 is important for translation control (LIAO et al., 2021), thus it was performed the SUnSET analysis to evaluate if the LKB1 expression could impact protein synthesis. WT cells incorporated more puromycin in 30 minutes, compared to edited cells, indicating that WT has more protein synthesis than edited cells (cWT vs c2SL+**, cWT vs c3SL+**) (Figure 4CD; **p<0.01). As mTOR and protein synthesis are directly involved with proliferation (LARSSON et al., 2012), a proliferation assay was performed over 72 hours. WT cells presented a higher number of cells compared to edited cells starting from an initial concentration of 1×10^4 cells after 72h (cWT vs c2SL+**, cWT vs c3SL+**) (Figure 4E; **p<0.01).

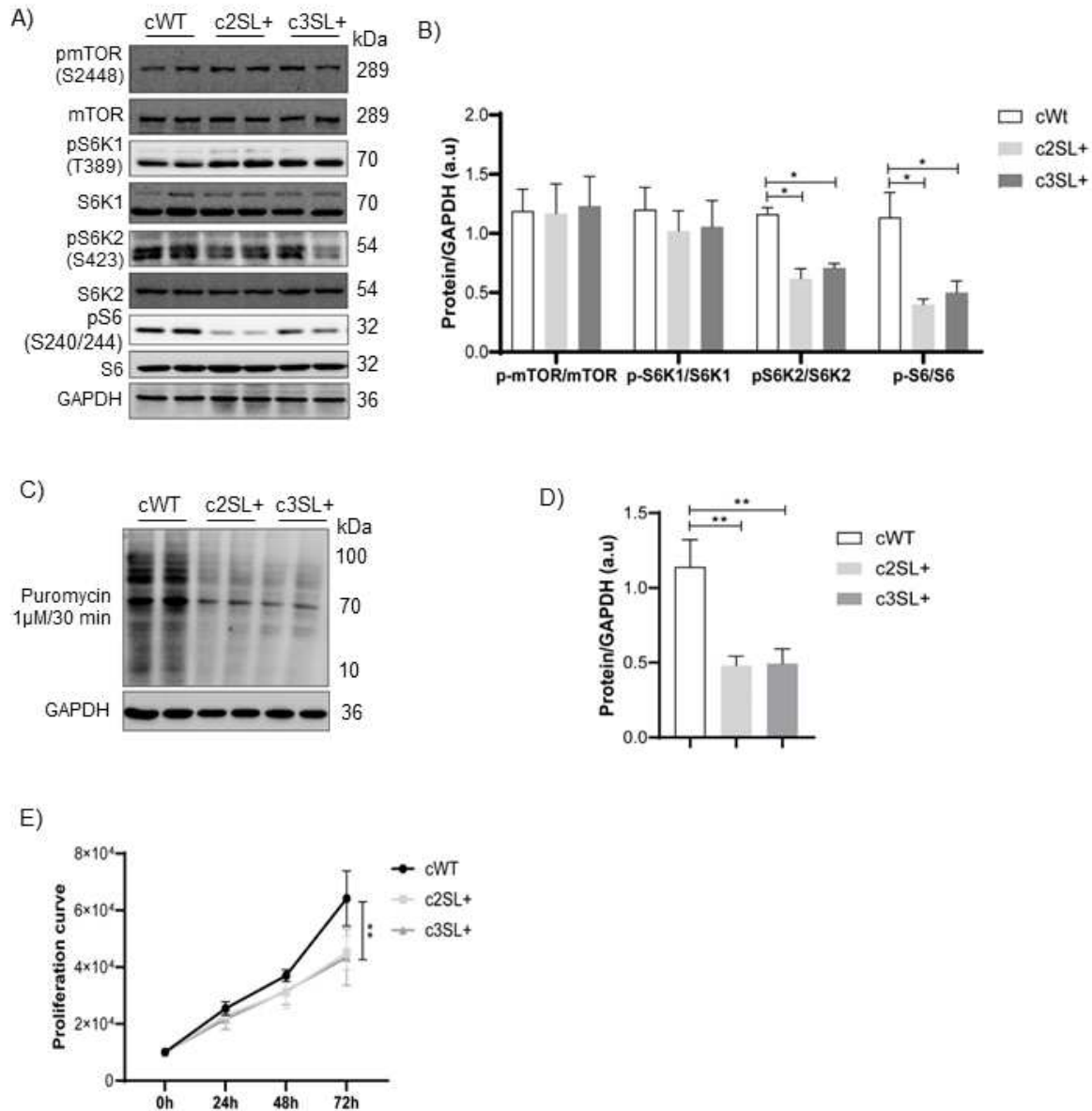


Figure 4. The Super LKB1 inhibits mTORC1 effectors kinases, S6K2 and S6, impacting in translation, and proliferation activity. (A) Western Blotting of pmTOR (S2448), mTOR, pS6K1 (T389), S6K1, pS6K2 (S423), S6K2, pS6 (S240/244), S6, and GAPDH in cWT, c2SL+, and c3SL+ cells; (B) Normalized levels of proteins by GAPDH (a.u.); (C) Surface Sensing of Translation (SUnSET) by Puromycin treatment followed by Western Blotting to detect puromycin labeled amino acids in cWT, c2SL+, and c3SL+ cells; (D) Normalized levels of protein by GAPDH (a.u.); (E) Proliferation curve beginning with 1.10^4 cells, and counting for 72 hours in cWT, c2SL+, and c3SL+ cells. Data are presented as mean \pm standard deviation (SD). Statistical analysis has been performed by ANOVA followed by Dunnet's test * $p<0.05$, ** $p<0.01$. These data are representative of two independent experiments.

Regarding the autophagy pathway, ULK1 activation was observed through the increase in Serine 555 phosphorylation in LKB1 in edited cells (c2SL+ vs cWT*, c3SL+ vs cWT*) (Figure 5AB; * $p < 0.05$). Besides, a reduction in p62 (c2SL+ vs cWT*, c3SL+ vs cWT*) (Figure 5AB; * $p < 0.05$) and an increase in LC3II (c2SL+ vs cWT*, c3SL+ vs cWT*) (Figure 5AB; * $p < 0.05$) was observed in edited cells in comparison to WT cells. These findings are compatible with autophagy activation. We used the pflLC3 plasmid to evaluate if the edited cell present an increase in autophagy flux. Super LKB1+ cells presented more red dots, exhibiting a higher RFP/GFP ratio, indicating more autophagy flux since LC3-RFP is an internal control and LC3-GFP is an autophagy substrate (c2SL+ vs cWT*, c3SL+ vs cWT*) (Figure 5C; * $p < 0.05$).

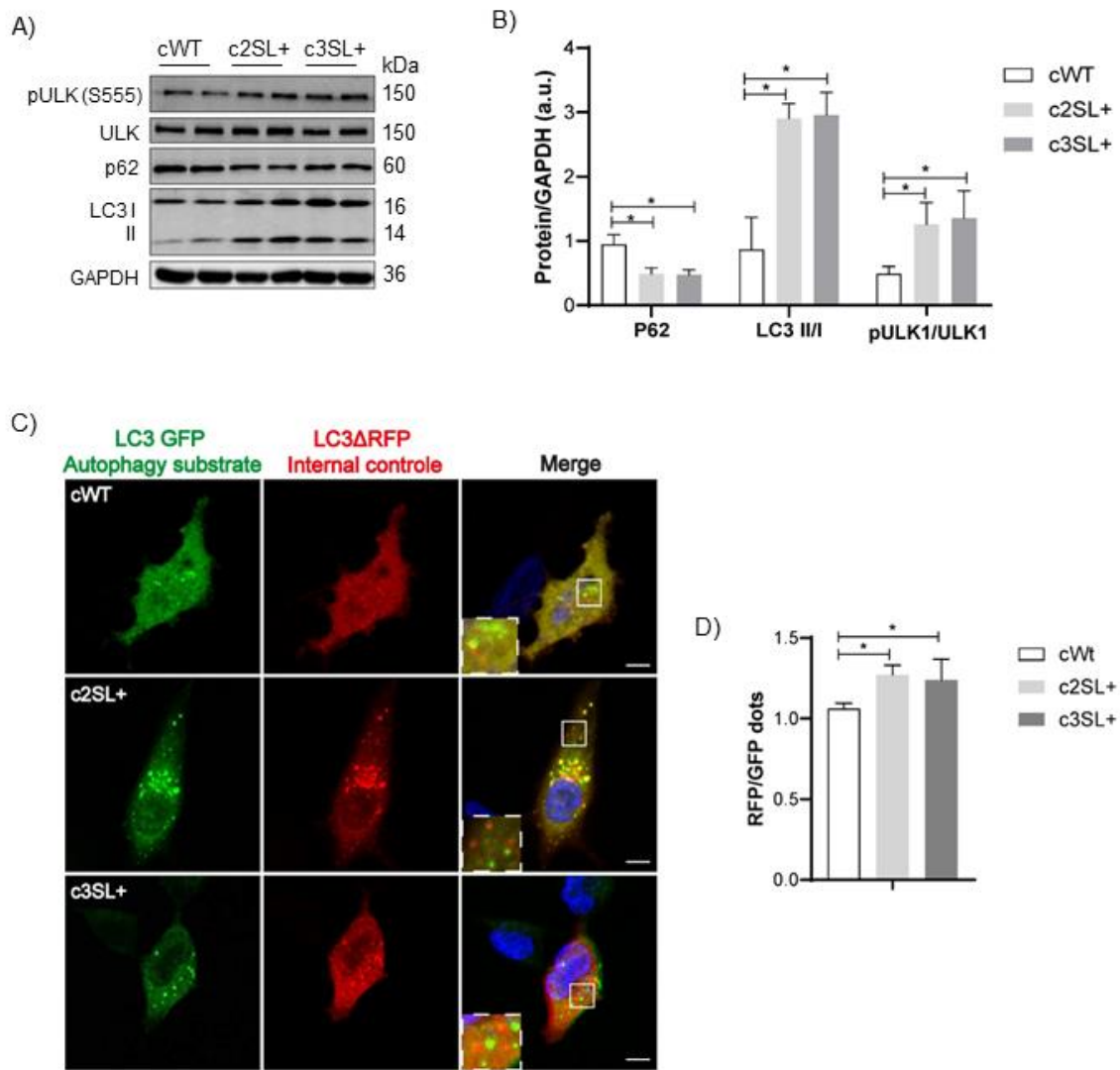
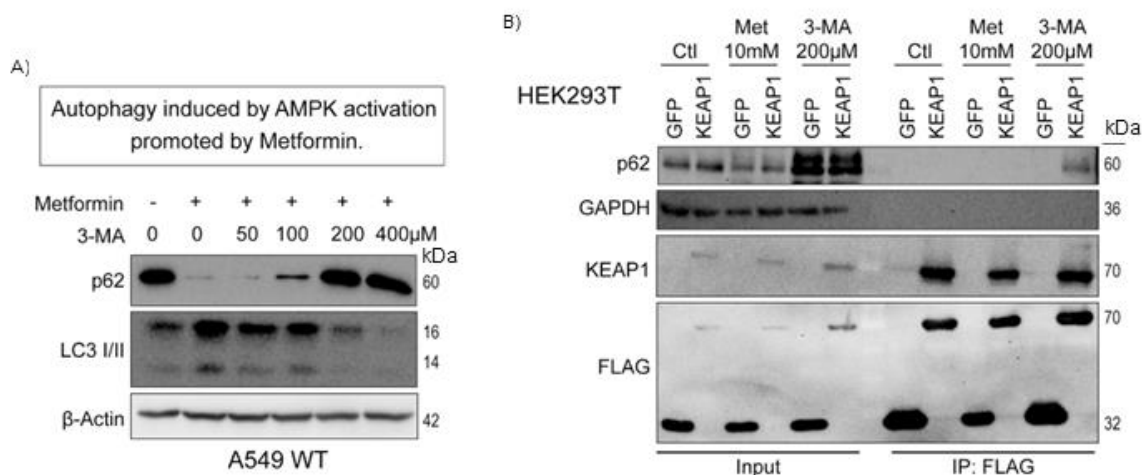


Figure 5. The A549 edited cells has increase in autophagy flux due to Super LKB1 expression. (A) Western Blotting of pULK (S555), ULK, p62, LC3 I/II, and GAPDH in cWT, c2SL+, and c3SL+ cells. (B) Normalized levels of proteins by GAPDH (a.u). (C) Autophagy flux detection with ptfLC3 plasmid being LC3 GFP autophagy substrate, and LC3 RFP internal control in cWT, c2SL+, and c3SL+ cells, the highlighted square evidence the fluorescent dots; (D) Normalized RFP/GFP in cWT, c2SL+, and c3SL+ cells. The higher ratio indicates an increase in autophagy flux. Data are presented as mean \pm standard deviation (SD). Statistical analysis has been performed by ANOVA followed by Dunnet's test * $p < 0.05$. These data are representative of two independent experiments.

3.3.6 The autophagy inhibition leads to p62/KEAP1 interaction, and its interaction can enhance the NRF2 cytoplasmic localization and down regulation the expression of antioxidant enzymes in A549 edited cells.

The activation of autophagy in A549-edited cells seems to be relevant to redox balance, possibly due to the link between autophagy and redox pathways in non-canonical activation of NRF2 (AL-MUBARAK et al., 2021). First, was validated the treatments with metformin for autophagy stimulation through AMPK activation and 3-MA as an autophagy inhibitor. Metformin treatment decreased the p62 protein levels and increased LC3II isoform indicating an increase in autophagy activity (Figure S6A). With the combination of metformin and 3-MA in increasing concentration until 400 μ M, an increase in the p62 protein levels and a decrease in LC3II expression was observed. (Figure S6A). In HEK193T, immunoprecipitation targeting the interaction between p62 and KEAP1 was detected in 3-MA treatment, corroborating the hypothesis that autophagy dysfunction can lead to KEAP1 and p62 interaction (Figure S6B). It is known that KEAP1 can be sequestered in autophagosomes, which are hindered from interacting with lysosomes due to the inhibition of autophagy flux and the heightened activation of mTORC1. (ICHIMURA et al., 2013).



Support information Figure 7. Autophagy inhibition can lead the p62/KEAP1 interaction. (A) Metformin, and 3-MA pharmacological effect validation in autophagy: A549 WT cells were treated in the conditions: control, Metformin 10mM, or Metformin with increasing concentrations of 3-MA until 400 μ M for 72 hours followed by Western Blotting of p62, LC3 I/II, and β -Actin. (B) Immunoprecipitation of HEK293T cells transfected with pFLAG-GFP or pFLAG-KEAP1 in the conditions: control, treated with Metformin 10 mM, and 3-MA 200 μ M for 24 hours, followed by Western Blotting for p62, KEAP1, FLAG, and GAPDH;

Thereby we evaluated the redox balance in A549 edited cells. A decrease in the expression of antioxidant enzymes NQO1 and PRDX3 in Super LKB1+ cells was observed, indicating less redox power (cWT vs c2SL+**, cWT vs c3SL+**) (Figure 6AB; ** $p < 0.01$). Besides, A549 WT cells presented a higher expression of NRF2 associated with lower KEAP1 levels, perhaps it was associated with the non-canonical activation of NRF2 in WT cells. On the other hand, edited cells presented a lower expression of NRF2 associated with a higher KEAP1 expression (cWT vs c2SL+**, cWT vs c3SL+**) (Figure 6AB; ** $p < 0.01$). Immunofluorescence and subcellular fractionation were also done to evaluate the localization of NRF2, once in the nucleus NRF2 is active, and in the cytoplasm NRF2 is degraded by the proteasome (BELLEZZA et al., 2018). In the WT cells, nuclear signaling of NRF2 was detected (cWT vs c2SL+**, cWT vs c3SL+**) (Figure 6CE; ** $p < 0.01$,) and in Super LKB1+ cells more cytoplasmic signaling of NRF2 was found (cWT vs c2SL+*, cWT vs c3SL+*) (Figure 6CE; * $p < 0.05$). These results were corroborated by subcellular fractionation, with a higher expression of NRF2 on cytoplasm fraction in LKB1 edited cells (Figure 6D).

To confirm that LKB1 edited cells presented inhibition of redox control, was measured the mRNA levels of antioxidant enzymes: NQO1 (cWT vs c2SL+**, cWT vs c3SL+**) (Figure 6F; ** $p < 0.01$), SOD1, and SOD2 (cWT vs c2SL+*, cWT vs c3SL+*) (Figure 6F; * $p < 0.05$). Thus, was tested if the edited cells present ROS accumulation due to inhibition of the redox system. Was observed that the edited cells presented higher concentrations of H₂O₂ (c2SL+ vs cWT*) (Figure 6G; * $p < 0.05$). When the cells were treated with metformin, an increase in H₂O₂ concentration in both cell lines were observed (cWT Ctl vs Met* and c2SL+ Ctl vs Met*) (Figure 6G; * $p < 0.05$). Finally, when we treated the cells with 3-MA a decrease of H₂O₂ concentration was observed in the SL+ cells (c2SL+ 3-MA vs Ctl*) (Figure 6G; * $p < 0.05$). The H₂O₂ levels with 3-MA treatment were the same in WT A549 cells (Figure 6G). Thus, the LKB1 edited cells seem to be more susceptible to oxidative damage, which can improve the response to cisplatin through H₂O₂ accumulation.

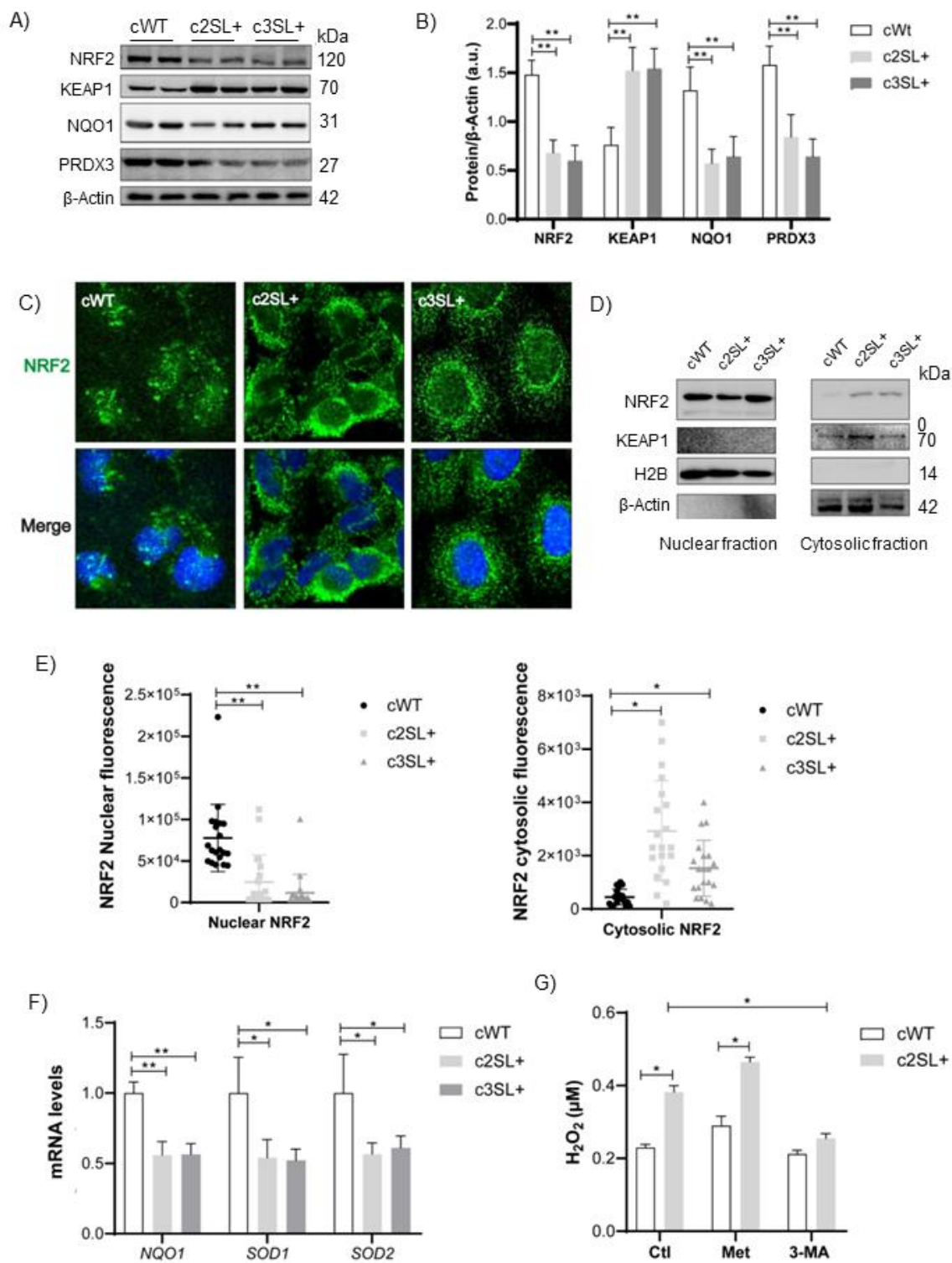


Figure 6. The Super LKB1+ cells presented a cytoplasmatic localization of NRF2, and lower expression of antioxidant enzymes. (A) Western Blotting of NRF2, KEAP1, NQO1, PRDX3, and β -Actin in cWT, c2SL+, and c3SL+ cells; (B) Normalized levels of proteins by β -Actin (a.u.); (C) Immunofluorescence of NRF2 in cWT, c2SL+,

and c3SL+ cells; **(D)** Quantification of nuclear and cytosolic NRF2 localization in cWT, c2SL+, and c3SL+ cells; **(E)** Subcellular fractionation of nucleus and cytosolic, followed by Western Blotting of NRF2, KEAP1, and β -Actin cWT, c2SL+, and c3SL+ cells; **(F)** Relative mRNA expression of NQO1, SOD1, and SOD2 in cWT, c2SL+, and c3SL+ cells; **(G)** Relative H₂O₂ level (μ M) in cWT, and c2SL+ cells in the control condition, and the treatments with Metformin 10 mM, and 3-MA 200 μ M for 72 hours. Data are presented as mean \pm standard deviation (SD). Statistical analysis has been performed by ANOVA followed by Dunnet's test * p <0.05, ** p <0.01. These data are representative of two independent experiments.

3.3.7 Edited cells accumulated more DNA Damage, and had a higher pro apoptotic protein expression.

The oxidative damage in cells can recruit a DNA Damage Response (DDR) for the maintenance of genomic homeostasis (ENDUTKIN; ZHARKOV, [s.d.]). Foci of γ H2AX in the cell nucleus is an example of DDR and can indicate oxidative damage in DNA of cells (LUCZAK; ZHITKOVICH, 2018). In the immunofluorescence of γ H2AX in the LKB1 edited cells, increased number of foci in the nucleus was observed in comparison with WT cells (c2SL+ vs cWT****, c3SL+ vs cWT****) (Figure 7AB; **** p <0.0001). It was also evaluated the apoptosis signaling due to oxidative damage in Super LKB1+ cells. Increased expression of BAK and BAX in this cell (cWT*, c3SL+ vs cWT*) (Figure 7CD; * p <0.05) was detected. The antiapoptotic BCL2 was also increased in Super LKB1+ cells (c2SL+ vs cWT**, c3SL+ vs cWT*) (Figure 7CD; * p <0.05, and ** p <0.001). Perhaps these findings could be a related to autophagy, since autophagy induces antiapoptotic signaling (KANG et al., 2011).

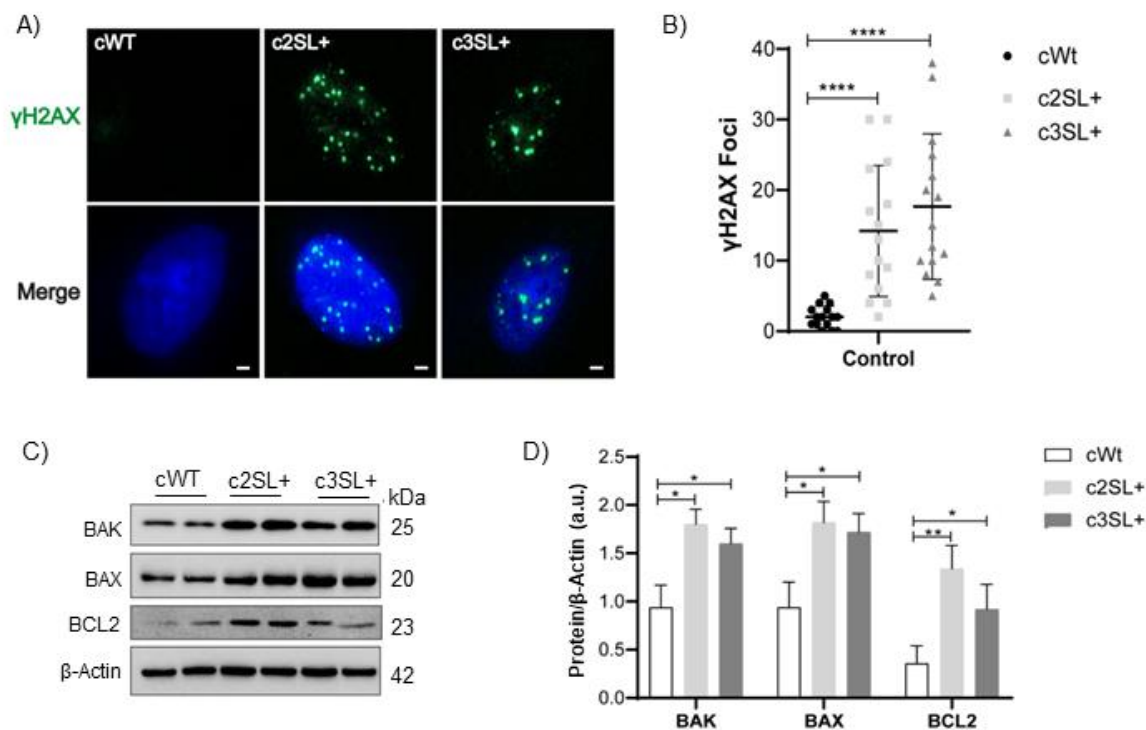


Figure 7. Edited cells accumulated more DNA damage, and higher pro apoptotic protein expression. (A) Immunofluorescence of γ H2AX in cWT, c2SL+, and c3SL+ cells; **(B)** Quantification of γ H2AX foci in the nucleus of cWT, c2SL+, and c3SL+ cells; **(C)** Western Blotting of BAK, BAX, BCL2, and β -Actin in cWT, c2SL+, and c3SL+ cells; **(D)** Normalized protein level by β -Actin (a.u). Data are presented as mean \pm standard deviation (SD). Statistical analysis has been performed by ANOVA followed by Dunnet's test * $p < 0.05$, ** $p < 0.01$, **** $p < 0.0001$. These data are representative of two independent experiments.

3.3.8 The A549 edited cells exhibited increased oxidative damage, rendering them more susceptible to cisplatin. The combined inhibition of autophagy by 3-MA and cisplatin resulted in reduced H₂O₂ generation and rescued cell viability.

Since cisplatin can induce ROS (KLEIH et al., 2019), and we demonstrated the oxidative damage in Super LKB1 cells, the edited cells were challenged with cisplatin. First, the IC₅₀ of cisplatin in the cell lines was determined, the WT cells presented a higher IC₅₀: 10 μ M compared to the edited cells, which presented among half of the IC₅₀: c2SL+: 5.5 μ M, c3SL+: 6 μ M (Figure 8A and 8B). To evaluate the oxidative damage after the cisplatin treatment, we quantified the γ H2AX in the nucleus of cells. In the LKB1 edited

cells, more γ H2AX foci was detected in comparison to WT cells (c2SL+ vs cWT****, c3SL+ vs cWT****) (Figure 8CD; **** $p < 0.0001$). The c2SL+ presented higher H₂O₂ amounts in comparison to WT cells and the combination of metformin with cisplatin increased H₂O₂ in both cells. On the other hand, the treatment with 3-MA and cisplatin decreased H₂O₂ in c2SL+. In the scenario, the cellular viability, the combination of metformin with cisplatin decreased the viability (cWT Cis/Met vs Cis***) (Figure 8F; *** $p < 0.001$) in the c2SL+ the combination of metformin with cisplatin also decreases the viability (c2SL+ Cis/Met vs Cis**) (Figure 8F; ** $p < 0.001$). Finally, when the cells were treated with the combination of 3-MA with cisplatin, a rescue of viability was observed in both cell lines (cWT Cis/3-MA vs Cis*) (Figure 8F; * $p < 0.05$), (c2SL+ Cis/3MA vs Cis**), (Figure 8F; ** $p < 0.01$). Thereby, autophagy activation seems to improve cisplatin response by H₂O₂ accumulation, and autophagy inhibition seems to inhibit cisplatin efficiency by H₂O₂ clearance, even in the presence of cisplatin treatment in A549 cells.

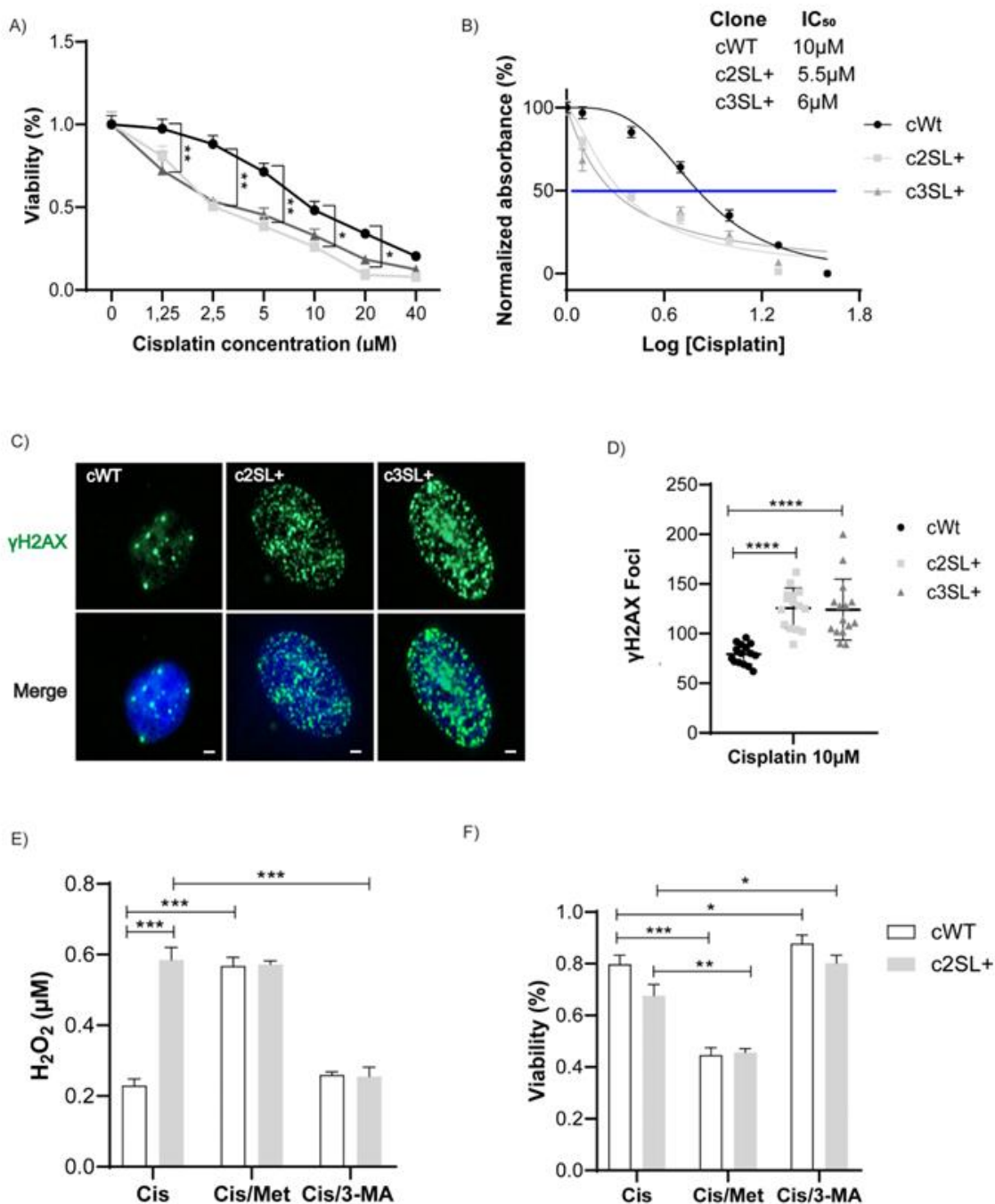


Figure 8. ROS accumulated in edited cells improves cisplatin response. (A) cWT, c2SL+, and c3SL+ cells treated with several concentrations of cisplatin for 72 hours followed by MTT to determine cell viability; (B) IC₅₀ determination using PRISM Software; (C) Immunofluorescence of γ H2AX in cWT, c2SL+, and c3SL+ cells treated with 10 μ M of cisplatin; (D) Quantification of γ H2AX foci in the nucleus in cWT, c2SL+, and c3SL+ cells; (E) H₂O₂ levels (μ M) in cWT, and c2SL+ cells in the control condition, and the treatments with Cisplatin, and combination with Metformin 10 mM (Cis/Met), and 3-MA 200 μ M (Cis/3MA) for 72 hours. (F) MTT viability in cWT, and c2SL+ cells

in the control condition, and the treatments with Cisplatin, and combination with Metformin 10 mM (Cis/Met), and 3-MA 200 μ M (Cis/3MA) for 72 hours. Data are presented as mean \pm standard deviation (SD). Statistical analysis has been performed by ANOVA followed by Dunnet's test * $p < 0.05$, ** $p < 0.01$, *** $p < 0.001$. These data are representative of two independent experiments.

DISCUSSION

The generation of INDELS by NHEJ with the CRISPR/Cas9 system as a strategy to rescue functional proteins was already in use. The MIN et al., 2019 targeted the Dystrophin gene, that frequently afflicted with mutations in the 50-exon linked to Duchenne Muscular Dystrophy (DMD), was targeted. This mutation often resulted in a non-sense sequence in subsequent exons and deletions in mRNA transcripts. The approach involved editing regions preceding the 50-exon mutation using CRISPR/Cas9. Specifically, the strategy aimed to reframe the exon by introducing a +1 insertion in the DNA sequence, thereby generating a functional DMD transcript. Additionally, exon skipping of the mutated exon was induced by directing the editing locus between acceptor and donor sites for splicing. The MIN et al., 2019, and CHEMELLO et al., 2021 using this strategy got to promote the improvement the quality of skeletal muscle tissue of models.

The mutated mRNA transcripts by CRISPR/Cas9 edition can retain function, TULADHAR et al., 2019 showed that in HAP1 cells with *TOP1* frameshift induced by CRISPR retains catalytic activity. Besides that, they generated specifically the Super LKB1 in MIA cells, as a higher molecular weight isoform of LKB1. However, it is worth noting that functional data for Super LKB1 were not provided in their study. In the cell lines described here, was detected the presence of the alternative exon (131 nt), the +1 adenine insertion by CRISPR, and the (Q37*, c.109C>T) in A549 cells on the first LKB1 exon in the A549 edited cells (Figure S3).

SHACKELFORD; SHAW, 2009 reviewed the role of LKB1 as an activator of AMPK, emphasizing its influence on the phosphorylation of the 172 Threonine residue of AMPK and its interconnected pathways in metabolism and proliferation. In the manuscript, as described by SHACKELFORD and SHAW, we demonstrated that overexpression of canonical LKB1 increased the phosphorylation in Threonine 172 residue of AMPK in A549

WT cells (Figure S5). The edited cells with expression of the new LKB1 isoform also activated AMPK, similar to the canonical LKB1 (Figure 1), increasing the activation of 172 Threonine phosphorylation of AMPK (Figure 1).

HANAHAN; WEINBERG, 2011 delineated several malignant cancer characteristics, including the deregulation of cellular energetics, evasion of growth suppressors, and activation of invasion and metastasis. These characteristics formed the basis for analyzing the suppressor activity of Super LKB1 in A549 cells. LI; ZHANG, 2016 established a connection between the increase in glucose uptake by malignant cancer cells, emphasizing aerobic glycolysis, also known as the Warburg effect. They highlighted the crucial role of HK2 expression in this process and its significance in tumor progression.

In a study by FANG et al., 2019 it was demonstrated that inhibiting GSK3 β in HCC and Hep3B cells led to a reduction in glucose uptake and HK2 expression. This inhibition resulted in an increase in AMPK activation through the phosphorylation of the 172 Threonine residue, subsequently promoting the inhibition of mTORC1 and S6K1. Additionally, cells with GSK3 β inhibition exhibited reduced clonogenic and migration activities, underscoring the tumor-suppressive potential of AMPK in malignant cancer cells.

In our manuscript, the A549 cells edited that express the Super LKB1 exhibited lower clonogenic and migration potential (Figure 2CE). Furthermore, there was a reduction in HK2 (Figure 3A) and mTORC1 expression (Figure 4A) and an increase in oxygen consumption (Figure 3F), mirroring the findings described by FANG regarding AMPK activation.

The interplay between mTORC1 and autophagy was investigated by KIM et al., 2011b. Using HEK293 cells, they demonstrated that AMPK interacts with ULK, inducing autophagy through Serine 555 phosphorylation. However, mTORC1 can disrupt this interaction through the phosphorylation of ULK1 at Serine 757. Additionally, KARABIYIK et al., 2021 revealed that in HeLa cells overexpressing LKB1, AMPK-mediated ULK activation is crucial for autophagy flux and LC3II expression.

Our findings align with these studies, due to mTORC1 inhibition and increased phosphorylation of ULK1 at Serine 555 by AMPK, promoting autophagy (Figure 5). This supports the observations put forth by KIM and KARABIYIK.

LKB1/AMPK signaling is intricately connected to NRF2 and the regulation of oxidative stress. SID et al., 2014 reported that in HCC cells, the AMPK activator Acadesine/AICA riboside (AICAr) led to NRF2 activation and increased expression of antioxidant enzymes. While these findings underscore the association between LKB1/AMPK and NRF2, other pathways influencing cellular redox balance have emerged. (BARTOLINI et al., 2018) highlighted the impact of mTORC1-mediated p62 phosphorylation at Serine 349 within the KIR domain. According to (DODSON; ZHANG, 2017a) this phosphorylation is prominent in cells with highly activated mTORC1 and low autophagy flux. It enhances p62 affinity for KEAP1, prompting NRF2 translocation to the nucleus and upregulating the expression of antioxidant enzymes in a non-canonical NRF2 activation pathway

Our study validated the interaction between p62 and KEAP1 in HEK293T cells treated with 3-MA (Figure S7). Additionally, in A549 WT cells characterized by elevated mTORC1 levels and low autophagy flux, we observed higher NRF2 levels (Figure 6A) and increased antioxidant enzyme expression. In contrast, cells expressing Super LKB1, with lower mTORC1 and heightened autophagy flux, displayed lower NRF2 levels (Figure 6A) and reduced antioxidant enzyme expression.

Thus, the cisplatin was more effective in Super LKB1+ cells (Figure 8), suggesting that the lack of LKB1 and the high NRF2 activation in A549 WT can promote resistance to oxidative damage by cisplatin. We hypothesize that the downregulation of NQO1, PRDX3, SOD1, and SOD2 ultimately leads to the accumulation of ROS levels. This hypothesis aligns with the findings of PAN; CHEN; HU, 2022, who treated T24 cells with cisplatin, detecting reactive oxygen species (ROS) through DCF staining and observing an intensification of apoptosis.

Our results indicate that, under cisplatin treatment, cells with Super LKB1 expression exhibit an increased concentration of H₂O₂ compared to WT cells (Figure 8), supporting the notion that the downregulation of antioxidant enzymes in A549 cells may

contribute to elevated ROS levels, potentially influencing cellular responses to cisplatin-induced oxidative stress.

We described the hypothesis of potential role of Super LKB1 signaling in A549 cells related with metabolism, mTORC1 activity, autophagy, and redox homeostasis. This schematic outlines a plausible mechanism underlying the response to cisplatin treatment in A549 NSCLC cells, both cWT and Super LKB1+ cell variants.

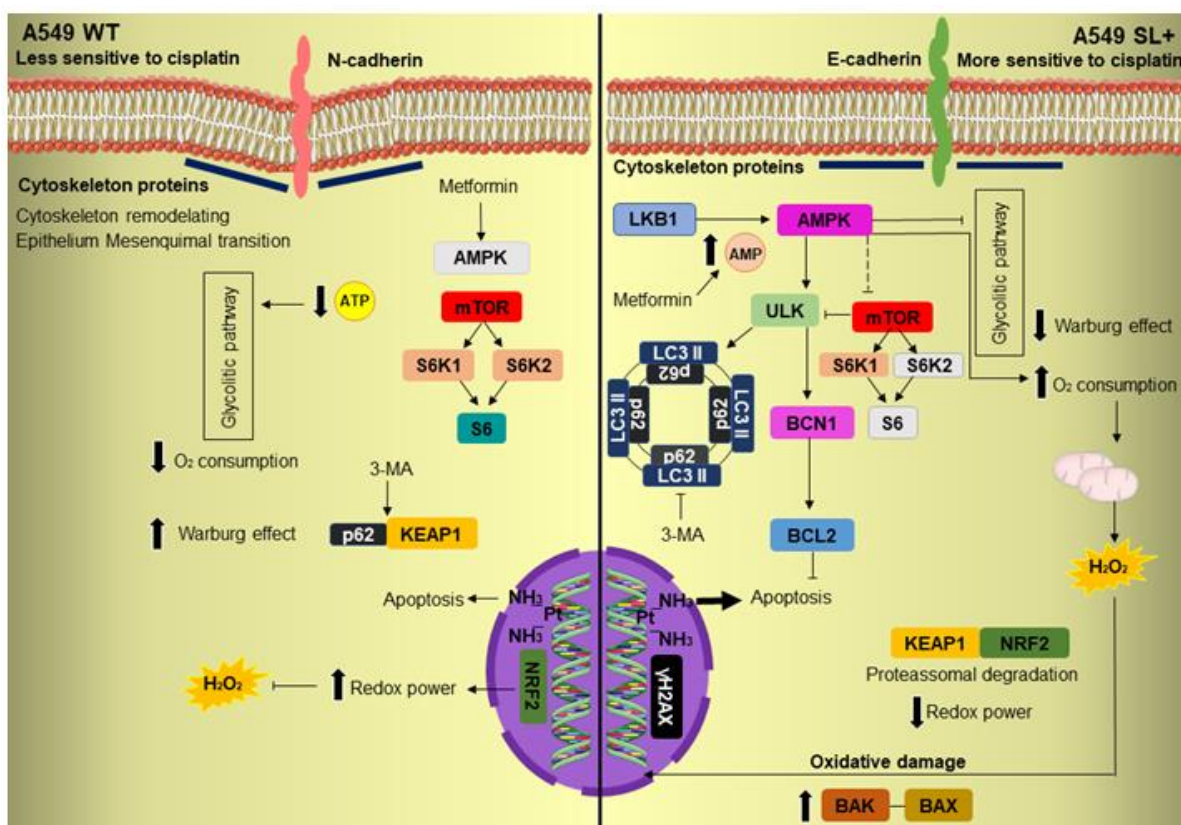


Figure 9. The hypothesis of potential role of Super LKB1 signaling in A549 in cisplatin treatment. A possible mechanism of LKB1/AMPK signaling in A549 cells based on data presented in the manuscript, comparing the cells that present A549 WT (LKB1 KO), and the A549 edited cells (Super LKB1) described here. In A549 WT cells we have a lower AMPK activation leading to an increase in mTORC1 signaling, and less autophagy flux. In this scenario p62 can interact with KEAP1, promoting non-canonical activation of NRF2. The enhanced aerobic glycolytic metabolism can also contribute to the generation of NADPH by the pentose phosphate pathway and improve the expression of antioxidant enzymes, besides that the LKB1 lack can contribute to the EMT process, increased migration, and survival. Thus, in A549 WT cells, the activation of redox pathways such as NRF2 that contributes to the diminished apoptosis signaling under cisplatin treatment. The Super LKB1 cells had increased activation of AMPK

and increased autophagy flux. On the other hand, Super LKB1+ cells present decreased of mTORC1 pathway. In this scenario, the interaction between p62 and KEAP1 was compromised, leading to NRF2 proteasomal degradation. Increased O₂ consumption and oxidative metabolism can also contribute to oxidative damage in the edited cells, leading to cisplatin induced apoptosis in edited cells. Finally, the Super LKB1 expression contributed to epithelium phenotype, reducing migration and survival in the edited cells.

3.4 CONCLUSIONS

In this study, we generated a functional higher molecular weight LKB1 isoform by CRISPR-Cas9. The A549 WT cell line presented increased redox activation in comparison to edited cells, which could be associated with the fact that the A549 WT cells are less sensitive to cisplatin. We explored a possible mechanism of LKB1/AMPK signaling that contributes to cisplatin, finding metabolic, mTORC1, and autophagy regulations. These pathways can be related to redox balance and NRF2 activation by the non-canonical activation of NRF2. Thus, the Super LKB1+ cells accumulate more oxidative damage that possibly contributes to a better response to cisplatin treatment in comparison to WT cells. The pharmacological combination of metformin, an autophagy inducer, with cisplatin seems to contribute to the increase of H₂O₂ in WT cells. The combination of 3-MA, an autophagy inhibitor, with cisplatin seems to rescue the viability of Super LKB1+ cells. This study characterizes the effects of a novel LKB1 isoform generated by CRISPR/Cas9 in A549 and its impact on metabolic targets and cellular pathways. This research may contribute to future therapeutic strategies for enhancing cisplatin treatment in lung cancer presenting mutation in LKB1 gene .

3.5 ACKNOWLEDGMENTS

We thank Dr. Igor Luchini Baptista for granting the 3-MA reagent, LABDIME, and INFABIC from UNICAMP for granting the use of fluorescence microscopy and Real-Time PCR instruments.

3.6 FUNDING INFORMATION

This study was supported by the São Paulo Research Foundation (FAPESP), grant numbers 2018/14818-9 (F.M.S), and fellowship 2020/13660-2 (M.B.S).

3.7 CONFLICT OF INTEREST

The authors declare no conflict of interest.

4. CONCLUSÕES DO TRABALHO

Até o momento, consoante aos dados apresentados neste trabalho, foi possível concluir que:

- 1) Os clones gerados por NHEJ através do sistema CRISPR/Cas9 apresentaram a expressão de uma nova isoforma de LKB1, chamada de “Super LKB1”
- 2) A nova proteína LKB1 gerada no trabalho apresentou maior peso molecular em comparação com a isoforma canônica, contudo, se mostrou efetiva em ativar seu alvo, a proteína AMPK, e parecer exercer de forma eficaz as regulações esperados de supressão tumoral,.
- 3) Foi explorado a interação de KEAP1 com p62 na ativação de NRF2 e expressão de enzimas antioxidantes.
- 4) A autofagia foi apontada como uma via importante no processo de indução à apoptose por cisplatina na linhagem A549.
- 5) As células com expressão da Super LKB1 mostraram níveis mais elevados de H_2O_2 em comparação com as células não editadas em condições basais, o que pode ter ocasionado danos oxidativos, devido ao aumento $\gamma H2AX$.
- 6) O tratamento combinado de cisplatina com metformina se mostrou mais eficiente do que o tratamento isolado com cisplatina nas células A549 do tipo selvagens, entretanto, nas células editadas em LKB1 a combinação de cisplatina com metformina não se mostrou mais efetiva do que o tratamento isolado com cisplatina.
- 7) A utilização de 3-MA conseguiu reverter os níveis basais de H_2O_2 dos clones com expressão da super LKB1, o que repercutiu em uma maior viabilidade dos clones quando co tratados com cisplatina e 3-MA.

Este estudo evidencia a utilidade do sistema CRISPR/Cas9 como uma ferramenta promissora para gerar novas isoformas de proteínas, avaliando os efeitos da expressão do novo construto na célula-alvo da patologia estudada, o que pode torná-lo uma ferramenta importante no campo da medicina personalizada.

5. REFERÊNCIAS

- AL-MUBARAK, B. R. et al. Non-canonical Keap1-independent activation of Nrf2 in astrocytes by mild oxidative stress. **Redox biology**, v. 47, p. 102158, 2021.
- AMIN, S.; LUX, A.; O'CALLAGHAN, F. The journey of metformin from glycaemic control to mTOR inhibition and the suppression of tumour growth. **British journal of clinical pharmacology**, v. 85, n. 1, p. 37–46, jan. 2019.
- BARTOLINI, D. et al. Nrf2-p62 autophagy pathway and its response to oxidative stress in hepatocellular carcinoma. **Translational research : the journal of laboratory and clinical medicine**, v. 193, p. 54–71, 2018.
- BELLEZZA, I. et al. Nrf2-Keap1 signaling in oxidative and reductive stress. **Biochimica et biophysica acta. Molecular cell research**, v. 1865, n. 5, p. 721–733, maio 2018.
- BHARATH, L. P. et al. Metformin Enhances Autophagy and Normalizes Mitochondrial Function to Alleviate Aging-Associated Inflammation. **Cell metabolism**, v. 32, n. 1, p. 44- 55.e6, 2020.
- BOLDINOVA, E. O. et al. Translesion activity of PrimPol on DNA with cisplatin and DNA-protein cross-links. **Scientific reports**, v. 11, n. 1, p. 17588, 2021.
- BOTT, M. J. et al. Initial results of pulmonary resection after neoadjuvant nivolumab in patients with resectable non-small cell lung cancer. **The Journal of thoracic and cardiovascular surgery**, v. 158, n. 1, p. 269–276, 2019.
- CANCER GENOME ATLAS RESEARCH NETWORK. Comprehensive molecular profiling of lung adenocarcinoma. **Nature**, v. 511, n. 7511, p. 543–50, 31 jul. 2014.
- CHEMELLO, F. et al. Precise correction of Duchenne muscular dystrophy exon deletion mutations by base and prime editing. **Science advances**, v. 7, n. 18, 2021.
- CICCARESE, F.; ZULATO, E.; INDRACCOLO, S. LKB1/AMPK Pathway and Drug Response in Cancer: A Therapeutic Perspective. **Oxidative medicine and cellular longevity**, v. 2019, p. 8730816, 2019a.
- CICCARESE, F.; ZULATO, E.; INDRACCOLO, S. LKB1/AMPK Pathway and Drug Response in Cancer: A Therapeutic Perspective. **Oxidative medicine and cellular longevity**, v. 2019, p. 8730816, 2019b.
- CRIBBS, A. P.; PERERA, S. M. W. Science and Bioethics of CRISPR-Cas9 Gene Editing: An Analysis Towards Separating Facts and Fiction. **The Yale journal of biology and medicine**, v. 90, n. 4, p. 625–634, 2017.
- CRUZ-BERMÚDEZ, A. et al. Cisplatin resistance involves a metabolic reprogramming through ROS and PGC-1 α in NSCLC which can be overcome by OXPHOS inhibition. **Free radical biology & medicine**, v. 135, p. 167–181, 2019.
- CUI, Q. et al. Modulating ROS to overcome multidrug resistance in cancer. **Drug resistance updates : reviews and commentaries in antimicrobial and anticancer chemotherapy**, v. 41, p. 1–25, 2018.
- DENG, Z. et al. ALS-FTLD-linked mutations of SQSTM1/p62 disrupt selective autophagy and NFE2L2/NRF2 anti-oxidative stress pathway. **Autophagy**, v. 16, n. 5, p. 917–931, 2020.

DODSON, M.; ZHANG, D. D. Non-canonical activation of NRF2: New insights and its relevance to disease. **Current pathobiology reports**, v. 5, n. 2, p. 171–176, jun. 2017a.

DODSON, M.; ZHANG, D. D. Non-canonical activation of NRF2: New insights and its relevance to disease. **Current pathobiology reports**, v. 5, n. 2, p. 171–176, jun. 2017b.

DONG, Y. et al. Inhibition of autophagy by 3-MA promotes hypoxia-induced apoptosis in human colorectal cancer cells. **European review for medical and pharmacological sciences**, v. 23, n. 3, p. 1047–1054, fev. 2019.

ENDUTKIN, A. V; ZHARKOV, D. O. [GO System, a DNA Repair Pathway to Cope with Oxidative Damage]. **Molekuliarnaia biologii**, v. 55, n. 2, p. 223–242, [s.d.].

FANG, G. et al. Inhibition of GSK-3 β activity suppresses HCC malignant phenotype by inhibiting glycolysis via activating AMPK/mTOR signaling. **Cancer letters**, v. 463, p. 11–26, 28 out. 2019.

FAUBERT, B. et al. AMPK is a negative regulator of the Warburg effect and suppresses tumor growth in vivo. **Cell metabolism**, v. 17, n. 1, p. 113–24, 8 jan. 2013.

FRITH, M. C. et al. Pseudo-messenger RNA: phantoms of the transcriptome. **PLoS genetics**, v. 2, n. 4, p. e23, abr. 2006.

GALLUZZI, L. et al. Molecular mechanisms of cisplatin resistance. **Oncogene**, v. 31, n. 15, p. 1869–83, 12 abr. 2012.

GARCIA, D.; SHAW, R. J. AMPK: Mechanisms of Cellular Energy Sensing and Restoration of Metabolic Balance. **Molecular cell**, v. 66, n. 6, p. 789–800, 15 jun. 2017.

GHOSH, S. Cisplatin: The first metal based anticancer drug. **Bioorganic chemistry**, v. 88, p. 102925, 2019.

GÖTZE, H.; BRÄHLER, E. [Cancer in the family--burden of relatives?]. **Psychotherapie, Psychosomatik, medizinische Psychologie**, v. 62, n. 5, p. 155–6, maio 2012.

GREENLEE, R. T. et al. Cancer statistics, 2001. **CA: a cancer journal for clinicians**, v. 51, n. 1, p. 15–36, [s.d.].

GU, L. et al. [The application of needle video-assisted thoracoscopic biopsy in pathologic diagnosis and staging for advanced lung cancer]. **Zhonghua jie he he hu xi za zhi = Zhonghua jiehe he huxi zazhi = Chinese journal of tuberculosis and respiratory diseases**, v. 26, n. 7, p. 396–9, jul. 2003.

HANAHAN, D.; WEINBERG, R. A. Hallmarks of cancer: the next generation. **Cell**, v. 144, n. 5, p. 646–74, 4 mar. 2011.

HSIEH LI, S.-M. et al. Metformin causes cancer cell death through downregulation of p53-dependent differentiated embryo chondrocyte 1. **Journal of biomedical science**, v. 25, n. 1, p. 81, 15 nov. 2018a.

HSIEH LI, S.-M. et al. Metformin causes cancer cell death through downregulation of p53-dependent differentiated embryo chondrocyte 1. **Journal of biomedical science**, v. 25, n. 1, p. 81, 15 nov. 2018b.

ICHIMURA, Y. et al. Phosphorylation of p62 activates the Keap1-Nrf2 pathway during selective autophagy. **Molecular cell**, v. 51, n. 5, p. 618–31, 12 set. 2013.

- JAIN, A. et al. p62/SQSTM1 is a target gene for transcription factor NRF2 and creates a positive feedback loop by inducing antioxidant response element-driven gene transcription. **The Journal of biological chemistry**, v. 285, n. 29, p. 22576–91, 16 jul. 2010.
- JÖGI, A. et al. Cancer cell differentiation heterogeneity and aggressive behavior in solid tumors. **Upsala journal of medical sciences**, v. 117, n. 2, p. 217–24, maio 2012.
- KANG, R. et al. The Beclin 1 network regulates autophagy and apoptosis. **Cell death and differentiation**, v. 18, n. 4, p. 571–80, abr. 2011.
- KARABIYIK, C. et al. Glucose starvation induces autophagy via ULK1-mediated activation of PIKfyve in an AMPK-dependent manner. **Developmental cell**, v. 56, n. 13, p. 1961- 1975.e5, 2021.
- KE, R. et al. Mechanisms of AMPK in the maintenance of ATP balance during energy metabolism. **Cell biology international**, v. 42, n. 4, p. 384–392, abr. 2018.
- KIM, J. et al. AMPK and mTOR regulate autophagy through direct phosphorylation of Ulk1. **Nature cell biology**, v. 13, n. 2, p. 132–41, fev. 2011a.
- KIM, J. et al. AMPK and mTOR regulate autophagy through direct phosphorylation of Ulk1. **Nature cell biology**, v. 13, n. 2, p. 132–41, fev. 2011b.
- KIM, S. J.; KIM, H. S.; SEO, Y. R. Understanding of ROS-Inducing Strategy in Anticancer Therapy. **Oxidative medicine and cellular longevity**, v. 2019, p. 5381692, 2019.
- KLEIH, M. et al. Direct impact of cisplatin on mitochondria induces ROS production that dictates cell fate of ovarian cancer cells. **Cell death & disease**, v. 10, n. 11, p. 851, 2019.
- KOLAK, A. et al. Primary and secondary prevention of breast cancer. **Annals of agricultural and environmental medicine : AAEM**, v. 24, n. 4, p. 549–553, 23 dez. 2017.
- LARSSON, O. et al. Distinct perturbation of the translome by the antidiabetic drug metformin. **Proceedings of the National Academy of Sciences of the United States of America**, v. 109, n. 23, p. 8977–82, 5 jun. 2012.
- LEE, M. B. et al. Defining the impact of mutation accumulation on replicative lifespan in yeast using cancer-associated mutator phenotypes. **Proceedings of the National Academy of Sciences of the United States of America**, v. 116, n. 8, p. 3062–3071, 2019.
- LENTSCH, E. et al. CRISPR/Cas9-Mediated Knock-Out of KrasG12D Mutated Pancreatic Cancer Cell Lines. **International journal of molecular sciences**, v. 20, n. 22, 14 nov. 2019.
- LI, N. et al. Role of the LKB1/AMPK pathway in tumor invasion and metastasis of cancer cells (Review). **Oncology reports**, v. 34, n. 6, p. 2821–6, dez. 2015.
- LI, N. et al. ALKBH5 regulates anti-PD-1 therapy response by modulating lactate and suppressive immune cell accumulation in tumor microenvironment. **Proceedings of the National Academy of Sciences of the United States of America**, v. 117, n. 33, p. 20159–20170, 2020.
- LI, Z.; ZHANG, H. Reprogramming of glucose, fatty acid and amino acid metabolism for cancer progression. **Cellular and molecular life sciences : CMLS**, v. 73, n. 2, p. 377–92, jan. 2016.

LIAO, H. et al. GPR39 promotes cardiac hypertrophy by regulating the AMPK-mTOR pathway and protein synthesis. **Cell biology international**, v. 45, n. 6, p. 1211–1219, jun. 2021.

LIN, S. et al. Enhanced homology-directed human genome engineering by controlled timing of CRISPR/Cas9 delivery. **eLife**, v. 3, p. e04766, 15 dez. 2014.

LUCZAK, M. W.; ZHITKOVICH, A. Monoubiquitinated γ -H2AX: Abundant product and specific biomarker for non-apoptotic DNA double-strand breaks. **Toxicology and applied pharmacology**, v. 355, p. 238–246, 2018.

LYKKE-ANDERSEN, S.; JENSEN, T. H. Nonsense-mediated mRNA decay: an intricate machinery that shapes transcriptomes. **Nature reviews. Molecular cell biology**, v. 16, n. 11, p. 665–77, nov. 2015.

MANCINI, M. C. S. et al. Knockout of NRF2 triggers prostate cancer cells death through ROS modulation and sensitizes to cisplatin. **Journal of cellular biochemistry**, 3 out. 2022.

MASUDA, K. et al. Characterization of the STK11 splicing variant as a normal splicing isomer in a patient with Peutz-Jeghers syndrome harboring genomic deletion of the STK11 gene. **Human genome variation**, v. 3, p. 16002, 2016.

MCLAUGHLIN, M. et al. Inflammatory microenvironment remodelling by tumour cells after radiotherapy. **Nature reviews. Cancer**, v. 20, n. 4, p. 203–217, 2020.

MIHAYLOVA, M. M.; SHAW, R. J. The AMPK signalling pathway coordinates cell growth, autophagy and metabolism. **Nature cell biology**, v. 13, n. 9, p. 1016–23, 2 set. 2011.

MIN, Y.-L. et al. CRISPR-Cas9 corrects Duchenne muscular dystrophy exon 44 deletion mutations in mice and human cells. **Science advances**, v. 5, n. 3, p. eaav4324, mar. 2019.

MOLONEY, J. N.; COTTER, T. G. ROS signalling in the biology of cancer. **Seminars in cell & developmental biology**, v. 80, p. 50–64, 2018.

MORELLI, A. P. et al. Metformin impairs cisplatin resistance effects in A549 lung cancer cells through mTOR signaling and other metabolic pathways. **International journal of oncology**, v. 58, n. 6, 2021.

MOSS, J. L. et al. Rural-urban differences in health-related quality of life: patterns for cancer survivors compared to other older adults. **Quality of life research : an international journal of quality of life aspects of treatment, care and rehabilitation**, v. 30, n. 4, p. 1131–1143, abr. 2021.

NDEMBE, G. et al. LKB1: Can We Target an Hidden Target? Focus on NSCLC. **Frontiers in oncology**, v. 12, p. 889826, 2022.

PAN, X.; CHEN, G.; HU, W. Piperlongumine increases the sensitivity of bladder cancer to cisplatin by mitochondrial ROS. **Journal of clinical laboratory analysis**, v. 36, n. 6, p. e24452, jun. 2022.

PANIERI, E.; SASO, L. Inhibition of the NRF2/KEAP1 Axis: A Promising Therapeutic Strategy to Alter Redox Balance of Cancer Cells. **Antioxidants & redox signaling**, v. 34, n. 18, p. 1428–1483, 2021.

PAPA, L.; MANFREDI, G.; GERMAIN, D. SOD1, an unexpected novel target for cancer therapy. **Genes & cancer**, v. 5, n. 1–2, p. 15–21, abr. 2014.

- PAPILLON-CAVANAGH, S. et al. STK11 and KEAP1 mutations as prognostic biomarkers in an observational real-world lung adenocarcinoma cohort. **ESMO open**, v. 5, n. 2, abr. 2020.
- PASTUSHENKO, I.; BLANPAIN, C. EMT Transition States during Tumor Progression and Metastasis. **Trends in cell biology**, v. 29, n. 3, p. 212–226, 2019.
- PODHORECKA, M.; IBANEZ, B.; DMOSZYŃSKA, A. Metformin - its potential anti-cancer and anti-aging effects. **Postepy higieny i medycyny doświadczalnej (Online)**, v. 71, n. 0, p. 170–175, 2 mar. 2017.
- PUUSTINEN, P. et al. DNA-dependent protein kinase regulates lysosomal AMP-dependent protein kinase activation and autophagy. **Autophagy**, v. 16, n. 10, p. 1871–1888, 2020.
- QUINN, B. J. et al. Repositioning metformin for cancer prevention and treatment. **Trends in Endocrinology & Metabolism**, v. 24, n. 9, p. 469–480, set. 2013.
- RAMASAMY, P. et al. PRDX3 is associated with metastasis and poor survival in uveal melanoma. **Journal of clinical pathology**, v. 73, n. 7, p. 408–412, jul. 2020.
- RIVAS-DOMÍNGUEZ, A. et al. The Role of DNA Damage Response in Dysbiosis-Induced Colorectal Cancer. **Cells**, v. 10, n. 8, 2021.
- SFAKIANOS, A. P. et al. The mTOR-S6 kinase pathway promotes stress granule assembly. **Cell death and differentiation**, v. 25, n. 10, p. 1766–1780, 2018.
- SHACKELFORD, D. B.; SHAW, R. J. The LKB1-AMPK pathway: metabolism and growth control in tumour suppression. **Nature reviews. Cancer**, v. 9, n. 8, p. 563–75, 2009.
- SHAW, R. J. et al. The tumor suppressor LKB1 kinase directly activates AMP-activated kinase and regulates apoptosis in response to energy stress. **Proceedings of the National Academy of Sciences of the United States of America**, v. 101, n. 10, p. 3329–35, 9 mar. 2004a.
- SHAW, R. J. et al. The tumor suppressor LKB1 kinase directly activates AMP-activated kinase and regulates apoptosis in response to energy stress. **Proceedings of the National Academy of Sciences of the United States of America**, v. 101, n. 10, p. 3329–35, 9 mar. 2004b.
- SHIVRAM, H. et al. Controlling and enhancing CRISPR systems. **Nature chemical biology**, v. 17, n. 1, p. 10–19, 2021.
- SID, B. et al. AICAR induces Nrf2 activation by an AMPK-independent mechanism in hepatocarcinoma cells. **Biochemical pharmacology**, v. 91, n. 2, p. 168–80, 15 set. 2014.
- SILVA-ISLAS, C. A.; MALDONADO, P. D. Canonical and non-canonical mechanisms of Nrf2 activation. **Pharmacological research**, v. 134, p. 92–99, 2018.
- SIVA, N. et al. Genome-editing approaches and applications: a brief review on CRISPR technology and its role in cancer. **3 Biotech**, v. 11, n. 3, p. 146, mar. 2021.
- SMITHEY, D. et al. Sub-shot-noise correlation of total photon number using macroscopic twin pulses of light. **Physical review letters**, v. 69, n. 18, p. 2650–2653, 2 nov. 1992.

- SONG, Y. et al. TWIST2 inhibits EMT and induces oxidative stress in lung cancer cells by regulating the FGF21-mediated AMPK/mTOR pathway. **Experimental cell research**, v. 405, n. 1, p. 112661, 2021.
- TAN, I. et al. Identification of a novel mitochondria-localized LKB1 variant required for the regulation of the oxidative stress response. **The Journal of biological chemistry**, v. 299, n. 7, p. 104906, jul. 2023.
- THANDRA, K. C. et al. Epidemiology of lung cancer. **Contemporary oncology (Poznan, Poland)**, v. 25, n. 1, p. 45–52, 2021.
- TULADHAR, R. et al. CRISPR-Cas9-based mutagenesis frequently provokes on-target mRNA misregulation. **Nature communications**, v. 10, n. 1, p. 4056, 2019.
- WANG, Y. et al. Liver Kinase B1 (LKB1) Regulates Proliferation and Apoptosis of Non-Small Cell Lung Cancer A549 Cells via Targeting ERK Signaling Pathway. **Cancer management and research**, v. 13, p. 65–74, 2021.
- WEISS, R. A. Viruses, cancer and AIDS. **FEMS immunology and medical microbiology**, v. 26, n. 3–4, p. 227–32, dez. 1999.
- WU, Y.-W. et al. Autophagy regulates vinorelbine sensitivity due to continued Keap1-mediated ROS generation in lung adenocarcinoma cells. **Cell death discovery**, v. 4, p. 33, 2018.
- XU, Z. et al. Targeting PI3K/AKT/mTOR-mediated autophagy for tumor therapy. **Applied microbiology and biotechnology**, v. 104, n. 2, p. 575–587, jan. 2020.
- YU, W. et al. Cisplatin generates oxidative stress which is accompanied by rapid shifts in central carbon metabolism. **Scientific reports**, v. 8, n. 1, p. 4306, 2018.
- YUDHANI, R. D. et al. Metformin Modulates Cyclin D1 and P53 Expression to Inhibit Cell Proliferation and to Induce Apoptosis in Cervical Cancer Cell Lines. **Asian Pacific journal of cancer prevention : APJCP**, v. 20, n. 6, p. 1667–1673, 1 jun. 2019.
- ZHANG, F.; WEN, Y.; GUO, X. CRISPR/Cas9 for genome editing: progress, implications and challenges. **Human molecular genetics**, v. 23, n. R1, p. R40–6, 15 set. 2014.
- ZHANG, K. et al. LKB1 deficiency promotes proliferation and invasion of glioblastoma through activation of mTOR and focal adhesion kinase signaling pathways. **American journal of cancer research**, v. 9, n. 8, p. 1650–1663, 2019a.
- ZHANG, Z.-G. et al. KDM5B promotes breast cancer cell proliferation and migration via AMPK-mediated lipid metabolism reprogramming. **Experimental cell research**, v. 379, n. 2, p. 182–190, 2019b.
- ZHAO, R.-X.; XU, Z.-X. Targeting the LKB1 tumor suppressor. **Current drug targets**, v. 15, n. 1, p. 32–52, jan. 2014.
- ZUO, J. et al. TNF- α -mediated upregulation of SOD-2 contributes to cell proliferation and cisplatin resistance in esophageal squamous cell carcinoma. **Oncology reports**, v. 42, n. 4, p. 1497–1506, out. 2019.

6. ANEXOS

1. Primeira página de: PAVAN, ISADORA CAROLINA BETIM ; BASEI, FERNANDA LUISA **SEVERINO, MATHEUS BRANDEMARTE** ; ROSA E SILVA, IVAN ; ISSAYAMA, LUIDY AZUO ; MANCINI, MARIANA CAMARGO SILVA ; GÓIS, MARIANA MARCELA ; DA SILVA, LUIZ GUILHERME SALVINO ; BEZERRA, ROSANGELA MARIA NEVES ; SIMABUCO, FERNANDO OREIRA ; KOBARG, JÖRG . NEK6 Regulates Redox Balance and DNA Damage Response in U-145 Prostate Cancer Cells. *Cells JCR*, v. 12, p. 256, 2023.
2. Primeira página de: MUÑOZ, VITOR ROSETTO ; BOTEZELLI, JOSÉ DIEGO ; GASPAR, RAFAEL ALAIS ; DA ROCHA, ALISSON L. ; VIEIRA, RENAN FUDOLI LINS ; CRISOL, BARBARA MOREIRA ; BRAGA, RENATA ROSSETO ; **SEVERINO, MATHEUS BRANDEMARTE** ; NAKANDAKARI, SUSANA CASTELO BRANCO RAMOS ; ANTUNES, GABRIEL CALHEIROS ; BRUNETTO, SÉRGIO Q. ; RAMOS, CELSO D. ; VELLOSO, LÍCIO AUGUSTO ; SIMABUCO, FERNANDO MOREIRA ; DE MOURA, LEANDRO PEREIRA ; DA SILVA, ADELINO SANCHEZ RAMOS ; ROPELLE, EDUARDO ROCHETE ; CINTRA, DENNYS ESPER ; PAULI, JOSÉ RODRIGO . Effects of short-term endurance and strength exercise in the molecular regulation of skeletal muscle in hyperinsulinemic and hyperglycemic Slc2a4+/- mice. *CELLULAR AND MOLECULAR LIFE SCIENCES JCR*, v. 80, p. 122, 2023.
3. Primeira página de: MANCINI, MARIANA C. S. ; MORELLI, ANA P. ; **SEVERINO, MATHEUS B.** ; PAVAN, ISADORA C. B. ; ZAMBALDE, ÉRIKA P. ; GÓIS, MARIANA M. ; SILVA, LUIZ G. S. DA ; QUINTERO'RUIZ, NATHALIA ; ROMEIRO, CAIO F. ; DOS SANTOS, DANIEL F. G. ; BEZERRA, ROSÂNGELA M. N. ; SIMABUCO, FERNANDO M. . Knockout of NRF2 triggers prostate cancer cells death through ROS modulation and sensitizes to cisplatin. *JOURNAL OF CELLULAR BIOCHEMISTRY JCR*, v. 123, p. 2079-2092, 2022.
4. Primeira página de: PONTE, LUIS GUSTAVO SABOIA ; PAVAN, ISADORA CAROLINA BETIM ; MANCINI, MARIANA CAMARGO SILVA ; DA SILVA, LUIZ GUILHERME SALVINO ; MORELLI, ANA PAULA ; **SEVERINO, MATHEUS BRANDEMARTE** ; BEZERRA, ROSANGELA MARIA NEVES ; SIMABUCO, FERNANDO MOREIRA . The Hallmarks of Flavonoids in Cancer. *MOLECULES JCR*, v. 26, p. 2029, 2021.
5. Primeira página de: MORELLI, ANA PAULA ; TORTELLI, THARCÍSIO CITRÂNGULO ; MANCINI, MARIANA CAMARGO SILVA ; PAVAN, ISADORA CAROLINA BETIM ; SILVA, LUIZ GUILHERME SALVINO ; **SEVERINO, MATHEUS BRANDEMARTE** ; GRANATO, DANIELA CAMPOS ; PESTANA, NATHALIE FORTES ; PONTE, LUIS GUSTAVO SABOIA ; PERUCA, GUILHERME FRANCISCO ; PAULETTI, BIANCA ALVES ; DOS SANTOS, DANIEL FRANCISCO GUIMARÃES ; DE MOURA, LEANDRO PEREIRA ; BEZERRA, ROSÂNGELA MARIA NEVES ; LEME, ADRIANA FRANCO PAES ; CHAMMAS, ROGER ; SIMABUCO, FERNANDO MOREIRA . STAT3 contributes to cisplatin resistance, modulating EMT markers, and the mTOR signaling in lung adenocarcinoma. *NEOPLASIA JCR*, v. 23, p. 1048-1058, 2021.
6. Primeira página de: MUÑOZ, VITOR R. ; GASPAR, RAFAEL C. ; **SEVERINO, MATHEUS B.** ; MACÊDO, ANA P. A. ; SIMABUCO, FERNANDO M. ; ROPELLE, EDUARDO R. ; CINTRA, DENNYS E. ; DA SILVA, ADELINO S. R. ; KIM, YOUNG-BUM ; PAULI, JOSÉ RODRIGO . Exercise Counterbalances Rho/ROCK2 Signaling Impairment in the Skeletal Muscle and Ameliorates Insulin Sensitivity in Obese Mice. *Frontiers in Immunology JCR*, v. 12, p. 2441, 2021.

7. Primeira página de: ESTECA, MARCOS V. ; **SEVERINO, MATHEUS B.** ; SILVESTRE, JOÃO G. ; PALMEIRA DOS SANTOS, GUSTAVO ; TAMBORLIN, LETÍCIA ; LUCHESSI, AUGUSTO D. ; MORISCOT, ANSELMO S. ; GUSTAFSSON, ÅSA B. ; BAPTISTA, IGOR L. . Loss of Parkin Results in Altered Muscle Stem Cell Differentiation during Regeneration. INTERNATIONAL JOURNAL OF MOLECULAR SCIENCES **JCR**, v. 21, p. 8007-8007, 2020.

Article

NEK6 Regulates Redox Balance and DNA Damage Response in DU-145 Prostate Cancer Cells

Isadora Carolina Betim Pavan ^{1,2}, Fernanda Luisa Basei ¹ , Matheus Brandemarte Severino ² , Ivan Rosa e Silva ¹ , Luidy Kazuo Issayama ¹, Mariana Camargo Silva Mancini ², Mariana Marcela Góis ² , Luiz Guilherme Salvino da Silva ², Rosângela Maria Neves Bezerra ², Fernando Moreira Simabuco ^{2,3}  and Jörg Kobarg ^{1,*} 

¹ Laboratory of Signal Mechanisms, School of Pharmaceutical Sciences (FCF), University of Campinas (UNICAMP), Campinas 13083-871, Brazil

² Multidisciplinary Laboratory of Food and Health, School of Applied Sciences (FCA), University of Campinas (UNICAMP), Limeira 13484-350, Brazil

³ Department of Biochemistry, Federal University of São Paulo, São Paulo 04044-020, Brazil

* Correspondence: jorgkoba@unicamp.br; Tel: +55-19-3521-8143

Abstract: NEK6 is a central kinase in developing castration-resistant prostate cancer (CRPC). However, the pathways regulated by NEK6 in CRPC are still unclear. Cancer cells have high reactive oxygen species (ROS) levels and easily adapt to this circumstance and avoid cell death by increasing antioxidant defenses. We knocked out the NEK6 gene and evaluated the redox state and DNA damage response in DU-145 cells. The knockout of NEK6 decreases the clonogenic capacity, proliferation, cell viability, and mitochondrial activity. Targeting the NEK6 gene increases the level of intracellular ROS; decreases the expression of antioxidant defenses (SOD1, SOD2, and PRDX3); increases JNK phosphorylation, a stress-responsive kinase; and increases DNA damage markers (p-ATM and γ H2AX). The exogenous overexpression of NEK6 also increases the expression of these same antioxidant defenses and decreases γ H2AX. The depletion of NEK6 also induces cell death by apoptosis and reduces the antiapoptotic Bcl-2 protein. NEK6-lacking cells have more sensitivity to cisplatin. Additionally, NEK6 regulates the nuclear localization of NF- κ B2, suggesting NEK6 may regulate NF- κ B2 activity. Therefore, NEK6 alters the redox balance, regulates the expression of antioxidant proteins and DNA damage, and its absence induces the death of DU-145 cells. NEK6 inhibition may be a new strategy for CRPC therapy.

Keywords: NEK6; CRISPR/Cas9; ROS; DDR; apoptosis



check for updates

Citation: Pavan, I.C.B.; Basei, F.L.; Severino, M.B.; Rosa e Silva, I.; Issayama, L.K.; Mancini, M.C.S.; Góis, M.M.; da Silva, L.G.S.; Bezerra, R.M.N.; Simabuco, F.M.; et al. NEK6 Regulates Redox Balance and DNA Damage Response in DU-145 Prostate Cancer Cells. *Cells* 2023, 12, 256. <https://doi.org/10.3390/cells12020256>

Academic Editor: Michitaka Ozaki

Received: 9 November 2022

Revised: 8 December 2022

Accepted: 22 December 2022

Published: 7 January 2023



Copyright: © 2023 by the authors. Licensee MDPI, Basel, Switzerland. This article is an open access article distributed under the terms and conditions of the Creative Commons Attribution (CC BY) license (<https://creativecommons.org/licenses/by/4.0/>).

1. Introduction

Prostate cancer is the second most frequent cancer diagnosis in men and the fifth leading cause of death worldwide [1]. Androgen deprivation therapy is the standard treatment for prostate cancer. Unfortunately, although nearly all patients respond to treatment, most of these individuals will eventually progress to a fatal stage of the disease called castration-resistant prostate cancer (CRPC) [2].

NIMA (Never In Mitosis, gene A)-related kinase-6 (NEK6) belongs to a protein kinase superfamily composed of 11 members of NIMA-related kinases [3]. Although NEK proteins are poorly studied, they are known to be involved in cell cycle regulation [4], primary cilium function [5–7], and DNA damage response [8]. Additionally, a few recent studies have emerged exploring the relationship between NEKs and mitochondrial activity [9,10] and also emphasized the family of NEKs as biomarkers of several types of cancer [11].

NEK6 is a 313 amino acid serine/threonine kinase encoded in humans by the NEK6 gene located at chromosome 9 [9,10]. Regarding its known functions, NEK6 participates in mitotic spindle kinetochore fiber formation, metaphase-anaphase transition, cytokinesis, and the checkpoint [8]. NEK6 is also involved in liver, breast, colorectal, gastric, and

ORIGINAL ARTICLE



Effects of short-term endurance and strength exercise in the molecular regulation of skeletal muscle in hyperinsulinemic and hyperglycemic *Slc2a4*^{+/-} mice

Vitor Rosetto Muñoz¹ · José Diego Botezelli¹ · Rafael Calais Gaspar¹ · Alisson L. da Rocha¹ · Renan Fudoli Lins Vieira¹ · Barbara Moreira Crisol¹ · Renata Rosseto Braga¹ · Matheus Brandemarte Severino² · Susana Castelo Branco Ramos Nakandakari³ · Gabriel Calheiros Antunes¹ · Sérgio Q. Brunetto⁴ · Celso D. Ramos^{4,5} · Lício Augusto Velloso^{6,7} · Fernando Moreira Simabuco² · Leandro Pereira de Moura^{1,6} · Adelino Sanchez Ramos da Silva⁸ · Eduardo Rochete Ropelle^{1,6,9} · Dennys Esper Cintra^{3,6} · José Rodrigo Pauli^{1,6,9}

Received: 5 November 2022 / Revised: 8 March 2023 / Accepted: 28 March 2023 / Published online: 13 April 2023
© The Author(s), under exclusive licence to Springer Nature Switzerland AG 2023

Abstract

Objective Intriguingly, hyperinsulinemia, and hyperglycemia can predispose insulin resistance, obesity, and type 2 diabetes, leading to metabolic disturbances. Conversely, physical exercise stimulates skeletal muscle glucose uptake, improving whole-body glucose homeostasis. Therefore, we investigated the impact of short-term physical activity in a mouse model (*Slc2a4*^{+/-}) that spontaneously develops hyperinsulinemia and hyperglycemia even when fed on a chow diet.

Methods *Slc2a4*^{+/-} mice were used, that performed 5 days of endurance or strength exercise training. Further analysis included physiological tests (GTT and ITT), skeletal muscle glucose uptake, skeletal muscle RNA-sequencing, mitochondrial function, and experiments with C2C12 cell line.

Results When *Slc2a4*^{+/-} mice were submitted to the endurance or strength training protocol, improvements were observed in the skeletal muscle glucose uptake and glucose metabolism, associated with broad transcriptomic modulation, that was, in part, related to mitochondrial adaptations. The endurance training, but not the strength protocol, was effective in improving skeletal muscle mitochondrial activity and unfolded protein response markers (UPRmt). Moreover, experiments with C2C12 cells indicated that insulin or glucose levels could contribute to these mitochondrial adaptations in skeletal muscle.

Conclusions Both short-term exercise protocols were efficient in whole-body glucose homeostasis and insulin resistance. While endurance exercise plays an important role in transcriptome and mitochondrial activity, strength exercise mostly affects post-translational mechanisms and protein synthesis in skeletal muscle. Thus, the performance of both types of physical exercise proved to be a very effective way to mitigate the impacts of hyperglycemia and hyperinsulinemia in the *Slc2a4*^{+/-} mouse model.

Keywords Physical exercise · Hyperinsulinemia · Mitochondrial adaptations · Skeletal muscle

Introduction

Hyperinsulinemia may precede body fat gain, insulin resistance, and type 2 diabetes (T2D) development [1–3]. The molecular mechanisms connecting hyperinsulinemia to metabolic diseases and body fat gain have not yet been fully elucidated. Moreover, defects in skeletal muscle insulin signaling are observed much earlier than the onset of T2D in people with genetic risk [4]. In humans, skeletal muscle is the primary tissue involved in peripheral insulin resistance, contributing to insulin secretion by β -cells, insulin circulating levels, insulin resistance, and inflammation, factors

Vitor Rosetto Muñoz and José Diego Botezelli have contributed equally to this work.

✉ Vitor Rosetto Muñoz
vitor.munoz93@gmail.com

✉ José Rodrigo Pauli
rodrigopaulifca@gmail.com

Extended author information available on the last page of the article

Knockout of NRF2 triggers prostate cancer cells death through ROS modulation and sensitizes to cisplatin

Mariana C. S. Mancini¹ | Ana P. Morelli¹ | Matheus B. Severino¹ |
 Isadora C. B. Pavan^{1,2} | Érika P. Zambalde¹ | Mariana M. Góis¹ |
 Luiz G. S. da Silva¹ | Nathalia Quintero-Ruiz¹ | Caio F. Romeiro¹ |
 Daniel F. G. dos Santos Jr.¹ | Rosângela M. N. Bezerra¹ |
 Fernando M. Simabuco^{1,3}

¹Multidisciplinary Laboratory of Food and Health (LabMAS), School of Applied Sciences (FCA), University of Campinas (UNICAMP), Limeira, São Paulo, Brazil

²Laboratory of Signal Mechanisms, School of Pharmaceutical Sciences (FCF), University of Campinas (UNICAMP), Campinas, São Paulo, Brazil

³Department of Biochemistry, Federal University of São Paulo, São Paulo, São Paulo, Brazil

Correspondence

Fernando M. Simabuco, Multidisciplinary Laboratory of Food and Health (LabMAS), School of Applied Sciences (FCA), University of Campinas (UNICAMP), R. Pedro Zaccaria, 1300, Jardim São Paulo, CEP 13484-350, Limeira, São Paulo, Brazil.
 Email: simabuco@gmail.com

Funding information

Fundação de Amparo à Pesquisa do Estado de São Paulo, Grant/Award Numbers: 2016/06457-0, 2018/14818-9

Abstract

Prostate cancer (PCa) represents the second most common cancer in men and affects millions worldwide. Chemotherapy is a common treatment for PCa but the development of resistance is often a problem during therapy. NRF2 (nuclear factor erythroid 2-related factor 2) is one of the major transcription factors regulating antioxidant enzymes and is also involved with drug efflux and detoxification. Cancer cells submitted to chemotherapy often promote NRF2 activation to benefit themselves with the cytoprotective response. Here, we found that DU145 and PC3 PCa cell lines have different responses regarding NRF2 activation, when subjected to arsenite-induced stress, even in the presence of MG132, a proteasome inhibitor. We also observed that only in PC3 cells treated with arsenite, NRF2 was able to translocate to the nucleus. To better understand the role of NRF2 in promoting chemoresistance, we performed CRISPR knockout of NRF2 (NKO) in DU145 and PC3 cells. The effectiveness of the knockout was confirmed through the downregulation of NRF2 targets ($p < 0.0001$). PC3 NKO cells exhibited higher levels of reactive oxygen species (ROS) compared to wild-type cells ($p < 0.0001$), while this alteration was not observed in DU145 NKO cells. Despite no modulation in ROS content, a lower IC50 value ($p < 0.05$) for cisplatin was observed in DU145 NKO cells, suggesting that the knockout sensitized the cells to the treatment. Besides, the treatment of DU145 NKO with cisplatin led cells to apoptosis as observed by the increased levels of PARP1 cleavage ($p < 0.05$), possibly triggered by increased DNA damage. Reduced levels of KU70 and phospho-CHK2 ($p < 0.05$) were also detected. The data presented here support that NRF2 is a mediator of oncogenesis and could be a potential target to sensitize PCa cells to chemotherapy, reinforcing the importance of knowing the specific genetic and biochemical characteristics of the cancer cells for a more effective approach against cancer.

Original Research

STAT3 contributes to cisplatin resistance, modulating EMT markers, and the mTOR signaling in lung adenocarcinoma ^{☆,☆☆}

Ana Paula Morelli ^a; Tharcísio Citrângulo Tortelli Jr ^b;
Mariana Camargo Silva Mancini ^b;
Isadora Carolina Betim Pavan ^{a,c};
Luiz Guilherme Salvino Silva ^a;
Matheus Brandemarte Severino ^a;
Daniela Campos Granato ^d; Nathalie Fortes Pestana ^a;
Luis Gustavo Saboia Ponte ^a;
Guilherme Francisco Peruca ^a; Bianca Alves Pauletti ^d;
Daniel Francisco Guimarães dos Santos Jr ^a;
Leandro Pereira de Moura ^a;
Rosângela Maria Neves Bezerra ^a;
Adriana Franco Paes Leme ^d; Roger Chammas ^b;
Fernando Moreira Simabuco ^{a,e}

^aMultidisciplinary Laboratory of Food and Health, School of Applied Sciences, State University of Campinas, Limeira, SP, Brazil

^bCentro de Investigação Translacional em Oncologia, Departamento de Radiologia e Oncologia, Faculdade de Medicina da Universidade de São Paulo and Instituto do Câncer do Estado de São Paulo, São Paulo, SP, Brazil

^cLaboratory of Signaling Mechanisms, School of Pharmaceutical Sciences, State University of Campinas, Campinas, SP, Brazil

^dLaboratório Nacional de Biotecnologia (LNBio), Centro Nacional de Pesquisa em Energia e Materiais (CNPEM), Campinas, Brazil

^eExercise Cell Biology Laboratory, School of Applied Sciences, State University of Campinas, Limeira, SP, Brazil

Abstract

Lung cancer is the second leading cause of cancer death worldwide and is strongly associated with cisplatin resistance. The transcription factor signal transducer and activator of transcription 3 (STAT3) is constitutively activated in cancer cells and coordinates critical cellular processes as survival, self-renewal, and inflammation. In several types of cancer, STAT3 controls the development, immunogenicity, and malignant behavior of tumor cells while it dictates the responsiveness to radio- and chemotherapy. It is known that STAT3 phosphorylation at Ser727 by mechanistic target of rapamycin (mTOR) is necessary for its maximal activation, but the crosstalk between STAT3 and mTOR signaling in cisplatin resistance remains elusive. In this study, using a proteomic approach, we revealed important targets and signaling pathways altered in cisplatin-resistant A549 lung adenocarcinoma cells. STAT3 had increased expression in a resistance context, which can be associated with a poor prognosis. STAT3 knockout (SKO) resulted in a decreased mesenchymal phenotype in A549 cells, observed by clonogenic potential and by the expression of epithelial-mesenchymal transition markers. Importantly, SKO cells did not acquire the mTOR pathway overactivation induced by cisplatin resistance. Consistently, SKO cells were more responsive to mTOR inhibition by rapamycin and presented impairment of the feedback activation loop in Akt. Therefore, rapamycin was even more potent in inhibiting the clonogenic potential in SKO cells and sensitized to cisplatin treatment. Mechanistically, STAT3 partially coordinated the cisplatin resistance phenotype via the mTOR pathway in non-small cell lung cancer. Thus, our findings reveal important targets and highlight the significance of the crosstalk between STAT3 and mTOR signaling in cisplatin resistance. The synergic inhibition of STAT3 and mTOR potentially unveil a potential mechanism of synthetic lethality to be explored for human lung cancer treatment.

Neoplasia (2021) 23, 1048–1058

Keywords: Lung cancer, Cisplatin, Proteomics, STAT3, mTOR, Rapamycin



Exercise Counterbalances Rho/ROCK2 Signaling Impairment in the Skeletal Muscle and Ameliorates Insulin Sensitivity in Obese Mice

Vitor R. Muñoz¹, Rafael C. Gaspar¹, Matheus B. Severino², Ana P. A. Macêdo¹, Fernando M. Simabuco², Eduardo R. Ropelle¹, Dennys E. Cintra³, Adelino S. R. da Silva^{4,5}, Young-Bum Kim^{6*} and José Rodrigo Pauli^{1*}

OPEN ACCESS

Edited by:

Dunfang Zhang,
National Institute of Dental and
Craniofacial Research (NIDCR),
United States

Reviewed by:

Peter Zanvit,
National Institutes of Health (NIH),
United States
Zuoqin Chen,
National Institutes of Health (NIH),
United States

*Correspondence:

José Rodrigo Pauli
rodrigopauli@uol.com.br
Young-Bum Kim
ykim2@bidmc.harvard.edu

Specialty section:

This article was submitted to
Inflammation,
a section of the journal
Frontiers in Immunology

Received: 28 April 2021

Accepted: 07 June 2021

Published: 21 June 2021

Citation:

Muñoz VR, Gaspar RC, Severino MB,
Macêdo APA, Simabuco FM,
Ropelle ER, Cintra DE, da Silva ASR,
Kim Y-B and Pauli JR (2021) Exercise
Counterbalances Rho/ROCK2
Signaling Impairment in the Skeletal
Muscle and Ameliorates Insulin
Sensitivity in Obese Mice.
Front. Immunol. 12:702025.
doi: 10.3389/fimmu.2021.702025

¹Laboratory of Molecular Biology of Exercise, University of Campinas (UNICAMP), Limeira, Brazil, ²Multidisciplinary Laboratory of Food and Health, School of Applied Sciences, State University of Campinas, Limeira, Brazil, ³Laboratory of Nutritional Genomics, University of Campinas (UNICAMP), Limeira, Brazil, ⁴Postgraduate Program in Rehabilitation and Functional Performance, Ribeirão Preto Medical School, University of São Paulo (USP), Ribeirão Preto, Brazil, ⁵School of Physical Education and Sport of Ribeirão Preto, University of São Paulo (USP), Ribeirão Preto, Brazil, ⁶Division of Endocrinology, Diabetes and Metabolism, Beth Israel Deaconess Medical Center and Harvard Medical School, Boston, MA, United States

Physical exercise is considered a fundamental strategy in improving insulin sensitivity and glucose uptake in skeletal muscle. However, the molecular mechanisms underlying this regulation, primarily on skeletal muscle glucose uptake, are not fully understood. Recent evidence has shown that Rho-kinase (ROCK) isoforms play a pivotal role in regulating skeletal muscle glucose uptake and systemic glucose homeostasis. The current study evaluated the effect of physical exercise on ROCK2 signaling in skeletal muscle of insulin-resistant obese animals. Physiological (ITT) and molecular analysis (immunoblotting, and RT-qPCR) were performed. The contents of RhoA and ROCK2 protein were decreased in skeletal muscle of obese mice compared to control mice but were restored to normal levels in response to physical exercise. The exercised animals also showed higher phosphorylation of insulin receptor substrate 1 (IRS1 Serine 632/635) and protein kinase B (Akt) in the skeletal muscle. However, phosphatase and tensin homolog (PTEN) and protein-tyrosine phosphatase-1B (PTP-1B), both inhibitory regulators for insulin action, were increased in obesity but decreased after exercise. The impact of ROCK2 action on muscle insulin signaling is further underscored by the fact that impaired IRS1 and Akt phosphorylation caused by palmitate in C2C12 myotubes was entirely restored by ROCK2 overexpression. These results suggest that the exercise-induced upregulation of RhoA-ROCK2 signaling in skeletal muscle is associated with increased systemic insulin sensitivity in obese mice and further implicate that muscle ROCK2 could be a potential target for treating obesity-linked metabolic disorders.

Keywords: obesity, insulin sensitivity, exercise, Rho-kinase (ROCK), skeletal muscle

Review

The Hallmarks of Flavonoids in Cancer

Luis Gustavo Saboia Ponte ^{1,†}, Isadora Carolina Betim Pavan ^{1,2,†}, Mariana Camargo Silva Mancini ¹,
Luiz Guilherme Salvino da Silva ¹, Ana Paula Morelli ¹ , Matheus Brandemarte Severino ¹,
Rosângela Maria Neves Bezerra ¹ and Fernando Moreira Simabuco ^{1,*} 

- ¹ Multidisciplinary Laboratory of Food and Health (LabMAS), School of Applied Sciences (FCA), University of Campinas (UNICAMP), Limeira, São Paulo 13484-350, Brazil; lg_saboia@hotmail.com (L.G.S.P.); isadora.bpavan@gmail.com (I.C.B.P.); marianamancini5@gmail.com (M.C.S.M.); luizsalvino@yahoo.com.br (L.G.S.d.S.); apm.morelli@gmail.com (A.P.M.); matheusbr.severino@gmail.com (M.B.S.); rosangelabezerra02@hotmail.com (R.M.N.B.)
- ² Laboratory of Signal Mechanisms (LMS), School of Pharmaceutical Sciences (FCF), University of Campinas (UNICAMP), Campinas, São Paulo 13083-871, Brazil
- * Correspondence: simabuco@gmail.com
- † These authors contributed equally.

Abstract: Flavonoids represent an important group of bioactive compounds derived from plant-based foods and beverages with known biological activity in cells. From the modulation of inflammation to the inhibition of cell proliferation, flavonoids have been described as important therapeutic adjuvants against several diseases, including diabetes, arteriosclerosis, neurological disorders, and cancer. Cancer is a complex and multifactor disease that has been studied for years however, its prevention is still one of the best known and efficient factors impacting the epidemiology of the disease. In the molecular and cellular context, some of the mechanisms underlying the oncogenesis and the progression of the disease are understood, known as the hallmarks of cancer. In this text, we review important molecular signaling pathways, including inflammation, immunity, redox metabolism, cell growth, autophagy, apoptosis, and cell cycle, and analyze the known mechanisms of action of flavonoids in cancer. The current literature provides enough evidence supporting that flavonoids may be important adjuvants in cancer therapy, highlighting the importance of healthy and balanced diets to prevent the onset and progression of the disease.

Keywords: flavonoids; cancer; cell signaling



Citation: Ponte, L.G.S.; Pavan, I.C.B.; Mancini, M.C.S.; da Silva, L.G.S.; Morelli, A.P.; Severino, M.B.; Bezerra, R.M.N.; Simabuco, F.M. The Hallmarks of Flavonoids in Cancer. *Molecules* **2021**, *26*, 2029. <https://doi.org/10.3390/molecules26072029>

Academic Editor: Francesca Giampieri

Received: 27 February 2021
Accepted: 30 March 2021
Published: 2 April 2021

Publisher's Note: MDPI stays neutral with regard to jurisdictional claims in published maps and institutional affiliations.



Copyright © 2021 by the authors. Licensee MDPI, Basel, Switzerland. This article is an open access article distributed under the terms and conditions of the Creative Commons Attribution (CC BY) license (<https://creativecommons.org/licenses/by/4.0/>).

1. Introduction

Flavonoids represent the largest group of polyphenols found in plant-based foods, including fruits, vegetables, grains, and herbs, as well as in beverages such as tea, wine, and juices [1]. In plants, flavonoids play the role of secondary metabolites, acting as protectors against biotic and abiotic threats, particularly in the defense against ultraviolet radiation and pathogen action. Additionally, they also actively participate in odor, flavor, and color determination in several species [2,3]. The concentration of flavonoids in food is related to several factors, including the variety of the phylum, order, family, and/or species of the plant, as well as the characteristics related to plantings, such as the type of soil, the climatic conditions of the region and the level of maturation of the food. Flavonoids' concentration and composition also vary depending on the different parts of the plant. Leaves and the peels of fruits are commonly rich sources of flavonoids due to increased susceptibility to stress [4–6].

These compounds are composed of fifteen carbon atoms in their chemical structure (Table 1), presenting two benzene rings (A and B) connected through a heterocyclic ring containing oxygen (C). Flavonoids can be subdivided into flavones, isoflavones, flavanones, flavonols, anthocyanidins, and flavans. These classes differ from one another according

Article

Loss of Parkin Results in Altered Muscle Stem Cell Differentiation during Regeneration

Marcos V. Esteca ¹ , Matheus B. Severino ¹ , João G. Silvestre ² ,
 Gustavo Palmeira dos Santos ¹, Leticia Tamborlin ^{3,4} , Augusto D. Luchessi ^{3,4},
 Anselmo S. Moriscot ², Åsa B. Gustafsson ⁵ and Igor L. Baptista ^{1,*} 

¹ Laboratory of Cell and Tissue Biology, School of Applied Sciences, University of Campinas, 13484-350 Limeira, Brazil; marcos.esteca@gmail.com (M.V.E.); matheusbr.severino@gmail.com (M.B.S.); gustavopalmeira7@gmail.com (G.P.d.S.)

² Department of Anatomy, Institute of Biomedical Sciences, University of São Paulo, 05508-900 São Paulo, Brazil; jgsilvestre@gmail.com (J.G.S.); moriscotanselmo@gmail.com (A.S.M.)

³ Laboratory of Biotechnology, School of Applied Sciences, University of Campinas, 13484-350 Limeira, Brazil; leticia_tamborlin@hotmail.com (L.T.); augusto.luchessi@gmail.com (A.D.L.)

⁴ Institute of Biosciences, São Paulo State University, 13506-900 Rio Claro, Brazil

⁵ Skaggs School of Pharmacy and Pharmacological Sciences, University of California San Diego, La Jolla, CA 92093-0021, USA; abgustafsson@health.ucsd.edu

* Correspondence: igorbapt@unicamp.br

† Current Address: School of Applied Sciences, University of Campinas, Rua Pedro Zaccaria, 1300, 13484-350 Limeira, Brazil.

Received: 24 September 2020; Accepted: 24 October 2020; Published: 28 October 2020



Abstract: The high capacity of the skeletal muscle to regenerate is due to the presence of muscle stem cells (MuSCs, or satellite cells). The E3 ubiquitin ligase Parkin is a key regulator of mitophagy and is recruited to mitochondria during differentiation of mouse myoblast cell line. However, the function of mitophagy during regeneration has not been investigated *in vivo*. Here, we have utilized Parkin deficient (Parkin^{-/-}) mice to investigate the role of Parkin in skeletal muscle regeneration. We found a persistent deficiency in skeletal muscle regeneration in Parkin^{-/-} mice after cardiotoxin (CTX) injury with increased area of fibrosis and decreased cross-sectional area (CSA) of myofibres post-injury. There was also a significant modulation of MuSCs differentiation and mitophagic markers, with altered mitochondrial proteins during skeletal muscle regeneration in Parkin^{-/-} mice. Our data suggest that Parkin-mediated mitophagy plays a key role in skeletal muscle regeneration and is necessary for MuSCs differentiation.

Keywords: satellite cells; differentiation; mitochondria; mitophagy

1. Introduction

Skeletal muscle has high capacity to regenerate after injury because of the presence of MuSCs, also known as satellite cells, between the basal membrane and the sarcolemma [1]. In a healthy adult skeletal muscle, MuSCs remain in their quiescent state due to expression of paired-box transcription factor 7 (Pax7) [2]. This transcription factor has been reported to be critical for maintaining the pool of MuSCs [1,2]. Muscle injury leads to activation of MuSCs and upregulation of various cell cycle factors to initiate proliferation [3]. The activation of MuSCs, also called myoblasts at this stage, is the first step in the repair process and occurs during the inflammatory phase, within 1–3 days post-injury (dpi). After the inflammatory phase, the regenerative phase is initiated with a portion of the MuSCs differentiating into myocytes [4]. Fusion of myoblasts results in formation of multinucleated myotubes. The differentiation process is characterized by the upregulation of Myogenin, which is one